

**FINAL PROJECT**

**SLOPE STABILITY ANALYSIS BY USING GEOTEXTILE  
REINFORCEMENT AND CONSIDERING OF  
GROUNDWATER LEVEL VARIANCE**

**(A CASE STUDY AT EMBANKMENT STA 3+550 OF  
CIBITUNG - CILINCING TOLL CONSTRUCTION PROJECT)**

**Submitted to Universitas Islam Indonesia Yogyakarta to Fulfil the  
Requirements for Bachelor's Degree in Civil Engineering**



**Tegar Bangkit Pangestu**

**17 511 256**

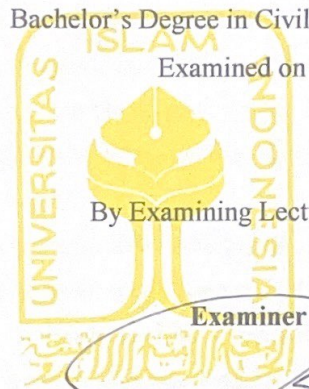
**CIVIL ENGINEERING STUDY PROGRAM  
FACULTY OF CIVIL ENGINEERING AND PLANNING  
UNIVERSITAS ISLAM INDONESIA  
YOGYAKARTA**

**2023**

**FINAL PROJECT**  
**SLOPE STABILITY ANALYSIS BY USING GEOTEXTILE**  
**REINFORCEMENT AND CONSIDERING OF GROUNDWATER**  
**LEVEL VARIANCE**

Arranged by  
**Tegar Bangkit Pangestu**  
**17511256**


Submitted to Universitas Islam Indonesia Yogyakarta to Fulfil the Requirements for a  
Bachelor's Degree in Civil Engineering



Supervisor

  
Muhammad Rifqi A., S.T., M.Eng  
NIK: 135111101

Examiner I

  
Hanindya Kusuma Artati, S.T., M.T.  
NIK: 045110407

Examiner II

  
Anisa Nur Amalina, S.T., M.Eng.  
NIK: 21511130

Validated,

Head of Civil Engineering Department

  
Ir. Yunalla Muntafi, S.T., M.T., Ph.D.  
NIK: 095110101



## PREFACE

*Assalamualaikum wr. wb.*

*Alhamdulillah* thank God for all the blessings of Allah SWT. With the permission from Allah SWT, the author could finish this Final Project Proposal with title *Slope Stability Analysis By Using Geotextile Reinforcement and Considering Groundwater Level Variance*. Shalawat and greetings to our beloved prophet, Prophet Muhammad SAW. This Final Project Proposal is one of the requirements in completing undergraduate studies at the Civil Engineering Program, Faculty of Civil Engineering and Planning, Islamic University of Indonesia, Yogyakarta.

There are many obstacles for the author when making this Final Project Proposal but thanks to the support, and encouragement from various parties for the author, this Final Project Proposal can be finished. The author expresses appreciate and gratitude towards:

1. Mr. Muhammad Rifqi Abdurrozak S.T., M.Eng as the supervising lecturer which has given many support, guidance, and advice for the author so the author can finish this Final Project Proposal.
2. Mrs. Hanindya Kusuma Artati S.T., M.T. and Miss Anisa Nur Amalina, S.T., M.Eng. as Examiner Lecturer.
3. Ir. Yunalia Muntafi, S.T., M.T., Ph.D. as Head of Program Study Civil Engineering in Islamic University of Indonesia.
4. Both author's parents Mr. Gatot Daryanto and Mrs. Maryati and also all my brothers. Without their support, sacrifice, guidance and love the author can't finish this Final Project Proposal.
5. The author's best friends Alen, Zulian, Verdy, Naufal, Ammar, Ayoda who always give support to the author.
6. The author's internship friends Alfian, Arief, and Tara who always give support to the author.
7. The author friends from Civil Engineering International Program (IP) 2017.

8. The author's friends from Civil Engineering 2017 students who always give support to the author.

The author is fully aware that this Final Project is far from perfect, caused by the lack of experience and knowledge from the author. The author hope that this Final Project can benefit and help other academic writer and serve as reliable reference for the sake of knowledge.

Amen.

*Wassalamualaikum Wr. Wb.*

Yogyakarta, 28 February 2023



Tegar Bangkit Pangestu

(17 511 256)



## PLAGIARISM FREE STATEMENT

The author solemnly declare that the Final Project which the author have compiled as one of the requirements for completing the Undergraduate program at the Civil Engineering Study Program, University of Islam Indonesia is author's own work. As for certain parts of the writing of the Final Project that author quote from the work of other people, the source has clearly written in accordance with the norms, rules, and ethics of writing scientific papers. If in the future it is found that in whole or in part there is plagiarism in certain parts, the authors prepared to accept sanctions, including revocation of the academic degree that the authors hold in accordance with applicable laws.

Yogyakarta, 28 February 2023

ement,  
  
Tegar Bangkit Pangestu  
(17 511 256)

## TABLE OF CONTENT

TITLE	i
VALIDITY SHEET	ii
PREFACE	iii
PLAGIARISM FREE STATEMENT	v
TABLE OF CONTENT	vii
TABLE LIST	ix
FIGURE LIST	xiii
ATTACHMENT LIST	xiv
NOTATION LIST	xv
ABSTRACT	xvii
CHAPTER I PRELIMINARY	1
1.1 Background	1
1.2 Problem Statement	3
1.3 Research Purposes	3
1.4 Benefits of Research	3
1.5 Research Limits	3
CHAPTER II LITERATURE REVIEW	5
2.1 Slope Stability	5
2.2 Slope Stability Analysis With Geotextile Reinforcement	6
2.3 Slope Stability Analysis Without Geotextile Reinforcement	7
2.4 Influence of Groundwater Level on Slope Stability	8
2.5 Comparison of Previous Search	8
CHAPTER III THEORETICAL BASIS	11
3.1 Soil	11

3.1.1	Soil Classification System	11
3.1.2	Parameters and Soil Shear Strength	15
3.1.3	Lateral Soil Stress	16
3.1.4	Soil Compaction	17
3.1.5	Elasticity Modulus and Poisson Number	18
3.2	Slope	19
3.2.1	Cause of Embankment	21
3.2.2	Slope Stability Analysis	23
3.2.3	Theory of Slope Stability Analysis	23
3.2.4	Circle Landslide Field	25
3.2.5	Slice Method	25
3.3	Geotextile	26
3.3.1.	Geotextile Mechanical Properties	27
3.3.2	Geotextile Function	28
3.3.3	Soil-Geotextile Interaction	29
3.4	Plaxis	29
CHAPTER IV RESEARCH METHODS		34
4.1	General Review	34
4.2	Research Data	34
4.3	Data Analysis Method	35
4.4	Research Stage	35
4.5	Loading	35
4.5.1	Vehicle Loading	35
4.5.2	Earthquake Load	36
4.6	Plaxis Modeling	37
4.6.1	Soil Parameter	37
4.6.2	Geotextile	38

4.7	Plaxis Program Operation	39
4.7.1	Plaxis Input	39
4.7.2	Plaxis Calculation	44
4.7.3	Plaxis Output	45
4.8	Research Flowchart	45
CHAPTER V ANALYSIS AND DISCUSSION		47
5.1	Analysis Overview	47
5.2	Existing Embankment	48
5.2.1	Analysis Using Plaxis Program	48
5.3	Slice Calculation Method (Fellinius)	55
5.4	Slope Reinforcement With Geotextile	60
5.4.1	Geotextile Calculation Data	60
5.4.2	External Stability	61
5.4.3	Internal Stability	67
5.4.4	Soil-Geotextile Tensile Force Check	69
5.5	Slope Modelling With Geotextile Reinforcement	76
5.6	Results of Slope Modeling with Geotextile Reinforcement in Groundwater Level Variations	83
5.7	Discussion	86
CHAPTER VI CONCLUSION AND SUGGESTION		91
6.1	Conclusion	91
6.2	Suggestion	91
BIBLIOGRAPHY		93
ATTACHMENT		96



## TABLE LIST

Table 2.1 Comparison of Previous Research with Future Research	9
Table 3.1 Classification System of USCS soil	14
Table 3.2 Classification System of AASHTO Soil	15
Table 3.3 Approximate Value of Soil Elasticity Modulus	20
Table 3.4 Approximate Value of Soil Poisson's Number	21
Table 4.1 Traffic Load Parameter Data	36
Table 4.2 Parameter of Data Soil Construction Period	37
Table 4.3 Parameter Data of Soil Post Construction	38
Table 4.4 Parameter Data Woven Geotextile UW-250	39
Table 5.1 Existing Embankment Coordinates	52
Table 5.2 Recapitulation of Calculations Using the Fellenisius Method	63
Table 5.3 Coefficient of Soil Bearing Capacity	65
Table 5.4 Recapitulation of Geotextile Length Requirements	72
Table 5.5 Slope Coordinates	76
Table 5.6 Recapitulation of Plaxis 8.6 Analysis Result with Variations in the Groundwater Level	89
Table 5.7 Recapitulation Result of Analysis and Calculation with Plaxis 8.6	90

## FIGURE LIST

Figure 1.1 Cibitung – Cilincing Tollroad Locations	2
Figure 3.1 Mohr and Coulomb failure criteria	16
Figure 3.2 Mohr Circle	17
Figure 3.3 The Riverbed Deepens Due to Excavation or Erosion	23
Figure 3.4 The force that Acting on the Slice	28
Figure 3.5 Differences in grain movement mechanism	30
Figure 3.6 Position of Nodal Point and Stress Point on Earth Element	32
Figure 3.7 Position of Nodal Points and Stress Points on Geotextile Elements	33
Figure 3.8 Distribution of Nodal Points and Stress Points in Interfacial Elements	34
Figure 4.1 Earthquake Zoning Map	37
Figure 4.2 Square Box of Create/open Project	40
Figure 4.3 Tab Project from the General Setting Window	40
Figure 4.4 Tab Dimension from General Setting Window	41
Figure 4.5 Tab General Sheet from Material Sets Window	42
Figure 4.6 Tab Parameters from Material Sets Window	43
Figure 4.7 Finite Element Network (Meshing)	43
Figure 4.8 First Stress on Geometry	44
Figure 4.9 Calculations Window with Tab General Sheet	44
Figure 4.10 Selection of Curve Points Under Review	45
Figure 4.11 Flowchart of Final Project	46
Figure 5. 1 Geometry of the Existing Condition of the Initial Soil Slope.	48
Figure 5. 2 Modelling of Existing Embankment on Plaxis 8.6	49
Figure 5. 3 Meshing on Existing Embankment	50
Figure 5. 4 Initial Stresses on Existing Embankments	50
Figure 5. 5 Deformed Mesh of Existing Embankment Due to Traffic Structure Load	51

Figure 5. 6 Deformed Mesh of Existing Embankment Due to Traffic and Earthquake Load	51
Figure 5. 7 Total Displacement of Existing Embankment Due to Traffic Structure Load	52
Figure 5. 8 Total Displacement of Existing Embankment Duet to Traffic and Earthquake Load	52
Figure 5. 9 Direction Movement of Embankment Due to Traffic Structure Load	52
Figure 5. 10 Direction Movement of Embankment Due to Traffic and Earthquake Load	53
Figure 5. 11 Potential Landslides of Embankment Due to Traffic Structure Load	53
Figure 5. 12 Potential Landslide of Embankment Due to Traffic Load and Earthquake Load	53
Figure 5. 13 Effective Stresses of Existing Embankment Due to Traffic and Earthquake Load	54
Figure 5. 14 Effective Stresses of Existing Slope Embankment Due to Traffic Structure Load	54
Figure 5. 15 SF Curve of Existing Embankment	55
Figure 5. 16 Stability Analysis Sta. 3+550 with the Fellenius Method	55
Figure 5. 17 Forces Acting on Slope Pile	62
Figure 5. 18 Soil-Geotextile Friction Transfer	70
Figure 5. 19 Modeling of Reinforced 12.5m Soil Embankment Slope	72
Figure 5. 20 Meshing on Reinforced 12.5m Soil Embankment Slope	72
Figure 5. 21 Initial Soil Stress On The Slope Of 12.5m Embankment With Reinforcement	73
Figure 5. 22 Deformed Mesh 12.5m Slope Embankment Due to Traffic Loads	73
Figure 5. 23 Deformed Mesh Slope 12.5m Embankment Due to Traffic and Earthquake Loads	73
Figure 5. 24 Total Displacement of 12.5m Embankment Slope Due to Traffic Load	74

Figure 5. 25 Total Displacement of 12.5m Embankment Slope Due to Traffic Load and Earthquake Load	74
Figure 5. 26 Direction of Movement of 12.5m Earth Piled Slope Due to Traffic Load	75
Figure 5. 27 Direction of Movement of 12.5m Earth Piled Slope Due to Traffic and Earthquake Load	75
Figure 5. 28 Potential for Landslide of 12.5m Embankment Slope Due to Traffic Load	76
Figure 5. 29 Potential for Landslide of 12.5m Embankment Slope Due to Traffic and Earthquake Load	76
Figure 5. 30 Effective Stresses 12.5m Embankment Slope Due to Traffic Loads	77
Figure 5. 31 Effective Stresses 12.5m Embankment Slope Due to Traffic and Earthquake Loads	77
Figure 5. 32 SF Curve Slope 12.5m Soil	78
Figure 5. 33 Deformed Mesh on Slopes with Geotextile Reinforcement Due Own Loaded at a Groundwater Level of 6 Meter	78
Figure 5. 34 Deformed Mesh on Slopes with Geotextile Reinforcement Due Traffic and Earthquake Load at a Groundwater Level of 6 Meter	79
Figure 5. 35 Landslide Potential Area on Own Loaded Geotextile at a Groundwater Level of 6 Meter	79
Figure 5. 36 Landslide Potential Areas on Reinforced Geotextile Slopes with Vehicle and Earthquake Loads at a Groundwater Level of 6 Meters	80
Figure 5. 37 Deformed Mesh on Slopes with Geotextile Reinforcement Due Own Loaded at a Groundwater Level of 4 Meter	80
Figure 5. 38 Deformed Mesh on Slopes with Geotextile Reinforcement Due to Traffic and Earthquake Load at a Groundwater Level of 4 Meter	81
Figure 5. 39 Landslide Potential Area on Own Loaded Geotextile at a Groundwater Level of 4 Meter	81
Figure 5. 40 Landslide Potential Areas on Reinforced Geotextile Slopes with Vehicle and Earthquake Loads at a Groundwater Level of 4 Meters	82
Figure 5. 41 Deformed Mesh on Slopes with Geotextile Reinforcement Due to	

Own Loaded at a Groundwater Level of 3 Meter	82
Figure 5. 42 Deformed Mesh on Slopes with Geotextile Reinforcement Due to Traffic and Earthquake Load at a Groundwater Level of 3 Meter	83
Figure 5. 43 Landslide Potential Area on Own Loaded Geotextile at Groundwater Level of 3 Meter	83
Figure 5. 44 Landslide Potential Areas on Reinforced Geotextile Slopes with Vehicle and Earthquake Loads at Groundwater Level of 3 Meter	84
Figure 5. 45 Deformed Mesh on Slopes with Geotextile Reinforcement Due to Own Loaded at a Groundwater Level of 0 Meter	84
Figure 5. 46 Deformed Mesh on Geotextile Slopes with Earthquake Loads at a Groundwater Level of 0 Meter	84
Figure 5. 47 Landslide Potential Area on Own Loaded Geotextile at a Groundwater Level of 0 Meter	85
Figure 5. 48 Landslide Potential Areas on Reinforced Geotextile Slopes with Vehicle and Earthquake Loads at a Groundwater Level of 0 Meter	85



## ATTACHMENT LIST

Attachment 1 Cross Section Geometry	90
Attachment 2 Soil Sample Lab Test Data	91
Attachment 3 SPT data at Sta 3+550	92
Attachment 4 Data of Technical Specifications Geotextile Woven	93



## NOTATIONS AND ABBREVIATION LIST

m = Meters

mm = Millimetre

Sta = Station

Cu = Undrained shear strength

$\tau$  = Shear stresses (kN/m<sup>2</sup>)

$\sigma$  = Normal stresses (kN/m<sup>2</sup>)

$\gamma$  = Soil volume weight (kN/m<sup>3</sup>)

$\gamma_{sat}$  = Saturated soil volume weight

SF = Safety factor

Sc = Consolidation settlement (m)

Cc = Soil compression index

kN = Kilo newton

Mpa = Megapascal

% = Percent

L = Length of the geotextile

$\tau_f$  = Soil shear strength

m<sup>2</sup> = Square metre

c = Cohesion (kN/m<sup>2</sup>)

$\phi$  = Inner friction angle (°)

e = Modulus young

k = Permeability coefficient

$g$  = Shear modulus

$\sigma$  = Normal stresses

$u$  = Pore water pressure (kN/m<sup>2</sup>)

$R$  = The radius of the landslide circle

$n$  = number of slices

$W_i$  = weight of the  $n$ -th soil slice

$N_i$  = the resultant of the effective normal force acting along the base of the slice

$\theta_i$  = defined angle

$a_i$  = the length of the arch of the circle at the  $n$ -th intersection (m)

$\alpha$  = shear angle  $\sigma_v$  = vertical soil pressure (kN/m<sup>2</sup>)

$\sigma_{ult}$  = permit bearing strength (kN/m<sup>2</sup>)

$T_a$  = allowable tensile strength

$K_a$  = active soil coefficient

$\sigma_{hc}$  = horizontal soil pressure (kN/m<sup>2</sup>)

$S_v$  = vertical distance between geotextile layers (m).

$T_{all}$  = tensile strength of geotextile permit (kN/m<sup>2</sup>).

$H$  = the thickness of the soil layer (m)

$q$  = load distribution (kN/m<sup>2</sup>)

$L_o$  = geotextile overlapping length (m).

## ABSTRACT

To improve accessibility and capacity for traffic in the industrial sector, which is helpful in raising productivity, the Cibitung-Cilincing toll road was developed in Bekasi City. This last project's analysis aims to compare the slope's safety factor before and after it has been strengthened using geotextiles.

The method used on the existing slope is by using the plaxis 8.6 program and to find the safety value of the slope with the Slice Method (Fellenius). On the slopes reinforced with geotextiles, the analysis was carried out using the plaxis 8.6 program and groundwater table variations were also taken into account in the design with variation of 6 meter, 4 meter, 3 meter, and 0 meter.

The safe value for the 12.5m embankment was obtained when the original soil was 1.1138 for traffic structure load and 1.1131 for traffic and earthquake load. Geotextiles were then used to strengthen the 12.5m embankment. The reinforced 12.5 m embankment's analysis with reinforcement produced a higher safety number than was necessary of 1.3 that are 1.3983 for traffic structure load and 1.3322 for traffic and earthquake load.. For a groundwater level of 6 meters, the slope safety figure for self-loading is 1.3297, with vehicle loads and earthquakes being 1.3280. For a groundwater level of 4 meters, the slope safety figure with self-load is 1.3263, and with vehicle loads and earthquakes is 1.3252. At a groundwater level of 3 meters, the slope safety figure with self-loading is 1.3210, and with vehicle loads and earthquake loads is 1.3033. At a groundwater level of 0 meters, the slope safety figure with self-loading is 1.0970, and with vehicle loads and earthquake loads is 1.0891. Thus, all slope safety values meet the requirements  $> 1.3$  except the 0 meter groundwater level that below 1.3 but above 1.0 which means have a doubtful stability condition. Based on the analysis above, slopes with geotextile reinforcement are able to withstand landslides up to a groundwater level of 3 meters from the surface of the slope.

**Keywords:** Embankment, Safety Factor, Geotextile, Groundwater level, Plaxis 8.6.

# **CHAPTER I**

## **PRELIMINARY**

### **1.1 Background**

Indonesia is one of the countries that is intensively carrying out development in all sectors such as the transportation sector. Transportation in Indonesia has an important role in economic development, therefore development in the transportation sector is being intensively carried out in order to achieve national development goals. One of the centers of the economy in Indonesia is on the island of Java, most of its turnover is in big cities on the island of Java. Bekasi City is one of the cities in the province of West Java which is the main destination in terms of economy and industry.

The Cibitung-Cilincing Toll Road was constructed with the intention of improving road accessibility and capability for serving industrial traffic area, which is helpful for boosting economic productivity and enhancing community welfare. The government's responsibility to implement the 2015–2020 Medium-Term Development Program (RPJMN), one of which is the development of road infrastructure to backed the national economic growth strategy, includes the construction of the Cibitung–Cilincing toll road. The stretch of the Cibitung-Cilincing Toll Road, which connects the JORR II toll road to the Cimanggis-Cilincing Toll Road and the JORR I east toll road, is 34 km long.







**Figure 1. 1 Cibitung – Cilincing Tollroad Locations**

(Source: PT CTP Tollways, 2020)

In construction, especially in road construction, slope slides are often encountered, which mostly occur during the rainy season. This occurs due to an increase in pore water on the slopes which results in a decrease in soil shear strength and internal shear angle. Factors that affect slope stability can produce shear stresses throughout the soil mass, and a movement will occur unless the shear resistance at any failure surface which may occur is greater than the acting shear stress.

One of the strengthening efforts in minimizing the occurrence of landslides can be done by installing geotextiles. Geotextile is a flexible structure, does not have a big risk in the event of deformation, and is easy to carry out its work. So in this final project, the author tries to use geotextiles as an alternative to slope reinforcement on the Cibitung – Cilincing Sta 3+550 toll road.

## **1.2 Problem Statement**

Based on the background described above, the research problem can be formulated, while specifically in this research it is formulated as follows:

1. What is the safety factor for the existing slope?
2. What is the slope safety factor with alternative geotextile reinforcement?
3. How is the influence of groundwater level in the existing slopes and also in the variations on the safety factor of slopes that have been reinforced with geotextiles and also with and without earthquake?

## **1.3 Research Purposes**

The main purpose of this final project is as follows:

1. knowing the value of the original slope factor of safety,
2. knowing the value of the slope safety factor with geotextile reinforcement, and
3. determine the effect of variations in ground water level on the safety factor of slopes reinforced with geotextiles.

## **1.4 Benefits of Research**

The benefits of this results analysis are as follows:

1. Expanding knowledge, especially in the field of geotechnical and geotextile technology development.
2. Increase knowledge about slope stability using the Plaxis program
3. As a reference for students or other researchers to conduct similar research.
4. As a reference in planning the same field as the landslide that occurred on the Cibitung - Cilincing sta 3+550 toll road.

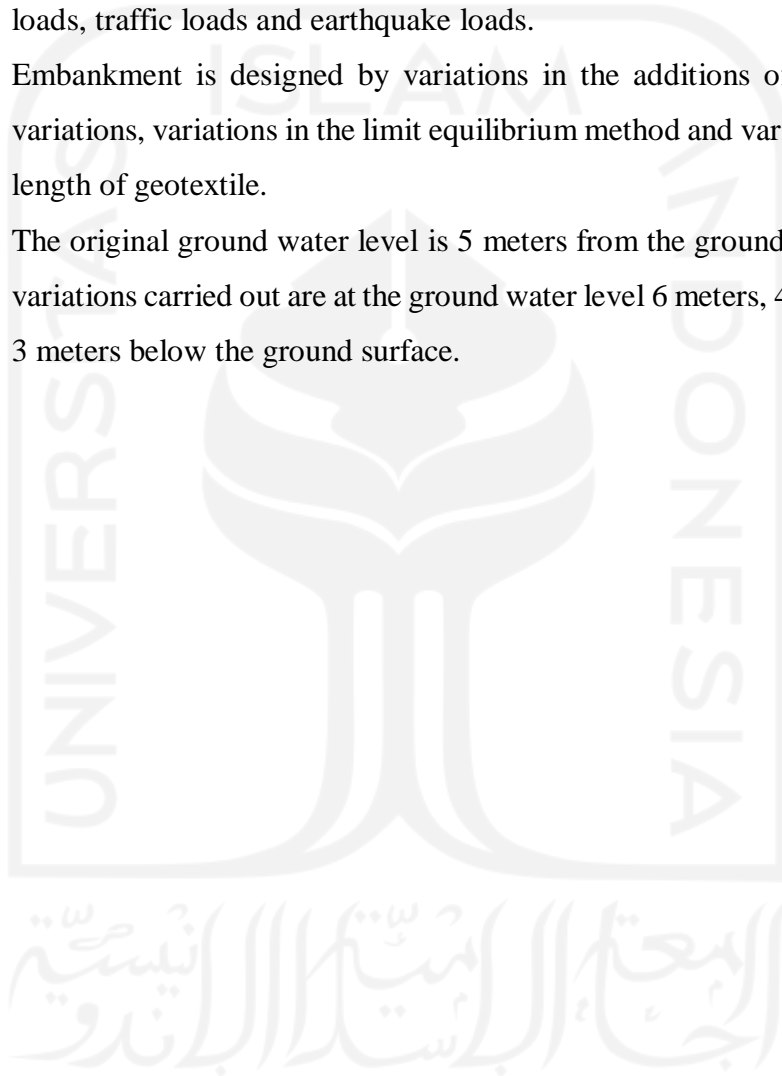
## **1.5 Research Limits**

The limitations of the research problem can be seen in the following description.

1. The research location is on an embankment in the Cibitung – Cilincing Toll

Construction Project Section 1 Sta 3+550.

2. Geosynthetic soil reinforcement using woven geotextiles.
3. Slope stability analysis was carried out using the Plaxis software.
4. Existing slope analysis using Plaxis software.
5. Loads imposed on the subgrade are due to embankment, rigid pavement loads, traffic loads and earthquake loads.
6. Embankment is designed by variations in the additions of traps, load variations, variations in the limit equilibrium method and variations in the length of geotextile.
7. The original ground water level is 5 meters from the ground surface, the variations carried out are at the ground water level 6 meters, 4 meters, and 3 meters below the ground surface.



## **CHAPTER II**

### **LITERATURE REVIEW**

#### **2.1 Slope Stability**

Soil stabilization is the process of improving the load bearing capacity and engineering properties of subgrade soil to support pavements and structures. This work examined the stabilization of two soil samples (lateritic and clay) using geotextile as reinforcement. Geotechnical test were carried out to determine Particle size analysis, Atterberg Limit test, moisture content, specific gravity, Compaction test and California Bearing Ratio test (Ogundare, D.A., 2019)

Wibowo (2016) in his research on the effect of extreme conditions on internal and external stability of retaining walls aims to analyze the internal and external stability of retaining walls due to extreme loads using Plaxis 8.6, by modeling slopes with extreme loads. This is to determine the stress that occurs in the retaining wall when it receives loads and in extreme slope conditions, so as to get an overview of the internal and external stability conditions of the retaining wall under these conditions. Based on the analysis of the internal stability of the retaining wall and seen from the stresses that occur, the wall can still withstand these stresses to extreme conditions but for external stability the retaining wall is unable to withstand shear forces, overturning forces and the stability of the collapse of the bearing capacity of the soil.

In Wardana (2011) conducted research by making slope simulations using the Stable 2004 program by analyzing variations in slope geometry as well as different terraces and soil properties. For analysis, the terraces are divided into 4 groups, namely T1, T2, T3 and T4 which have 1 to 4 terraces. The slope without terraces is called T0, the slope of the slope moves from 1:1, 1:2 and 1:3 with different soil types (clay, sand and clay-sand variations). The results of the analysis of groundwater level rise cause a decrease in slope stability, for slopes with a slope



of 1:1, 1:2 and 1:3 the safety value increases with increasing the core from T1-T4, the greatest safety score is obtained from T4. Sand slope with a slope of 1:1, the increase in safety value with T1 terracing is very visible, while for types T2, T3 and T4 it is not much different. Sand slopes with a slope of 1:2 and 1:3 terracing T1- T4 on average provide a very small increase in safety.

#### 1. Protection

Geosynthetic material is used as a layer to lower local stress and avoid or delay surface or layer damage.

In addition to their technical advantages, using geotextiles for soil reinforcement can drastically cut costs and be more efficient than other approaches. The time it takes to build an embankment can be shortened by installing a geosynthetic layer, which can decrease the number of embankment stages.

Kafikanda (2019) conducted a case study utilizing the Balikpapan-Samarinda Toll Road Sta.1+975 to analyze slope stability using geotextiles and the GEOSLOPE tool. This study's objective was to calculate the safety factor on slopes using geotextile reinforcement. The safety factor (SF) from the analysis using the SLOPE/W program was 1.159 1.5, and the safety factor (SF) from the Fellenius method and manual calculations on the original condition of the embankment soil was 0.95 1.5 (unsafe), so it needs to be strengthened, according to the conclusions drawn from this study. From the results of the analysis using SLOPE/W, the comparison between the SF values in the embankment soil reinforced with geotextile reinforcement SF values on slopes produced by reinforced geotextiles without earthquake stresses are 2.303 and SF values with changes in geotextile length per zone are 1.681. Then in zones 3 and 2 it produces an SF value of 2.128 and with an earthquake load in zones 3 and 2 it produces an SF value of 1.511. so, from the results of the software calculations, it can be seen that the results are safe.

Arsy (2018) On the Solo - Kertasono STA 4+175 Toll Road project, research

was done on the analysis of embankment stability in road construction with geotextile reinforcement. The purpose of this study was to determine the results of the analysis of the stability of the embankment on the road body without using geotextiles, using geotextile reinforcement, the relationship between the length of the geotextile and the safety number, the relationship between the vertical distance between the geotextiles and the safe number and the relationship between the slope angle and the safe number. The conclusions obtained from this study include the results of the analysis of the stability of the road embankment without using reinforcement with the Fellenius method by manual calculation, the safety factor value is 1.786. While the results of the analysis of the stability of the road embankment using geotextile reinforcement with the Fellenius method manually calculated the first, second and third length variations with the geotextile length of 10m, 13m and 15m, namely 2.339, 2.347 and 2.375. The results of the analysis of the stability of the road embankment using geotextile reinforcement using the Fellenius method manually calculated the variation of the vertical distance between the first, second and third geotextiles with  $S_v$  of 0.3m, 0.4m and 0.6m, namely 2.646, 2.347 and 2.059. Then the results of the analysis of the stability of the road embankment using geotextile reinforcement with the Fellenius method manually calculated on the variation of the first, second and third slope angles with angles of  $19^\circ$ ,  $25^\circ$ , and  $29^\circ$  namely 2.440, 2.347 and 2.355. So that the longer the geotextile used, the denser or smaller the vertical distance of the geotextile, and the smaller the slope angle, the greater the value of the resulting safety factor.

## **2.2 Slope Stability Analysis Without Geotextile Reinforcement**

Hediyanto (2018) research was done on the Code River Bank about slope stability analysis using cantilever and sheetpile wall reinforcement. With the help of the Geoslope/w program and the Sigma/w program, this study seeks to determine the safety factor (SF) of the existing slope, cantilever reinforcement, and sheet pile reinforcement, as well as the movement of the soil in the two variations of the reinforcement during an earthquake and in the absence of an earthquake. According to the study's findings, the existing slope's safety factor

(SF) was 1.118 due to the earthquake's magnitude of 0.565 and its own weight. Due to its own weight and the 1.789 earthquake, the cantilever-reinforced slope's safety factor (SF) is 2.639. Due to its own weight and the 1.846 earthquake, the cantilever sheet pile reinforced slope's safety factor (SF) is 2.726. From the planning of the two variations of the reinforcement, the safety factor (SF)  $> 1.5$  means the slope is stable. The largest results obtained from the ground movement of cantilever reinforcement during non-earthquake in the A-A sections of 0.7, the B-B sections of 1.01m and the C-C sections of 0.1m. The biggest result of sheet pile reinforcement soil movement during non-earthquake in the A-A section is 0.44, the B-B section is 1.03m and the C-C section is 0.088m.

### **2.3 Influence of Groundwater Level on Slope Stability**

According Hariyadi (2016) in his research on the stability of embankment slopes, the parameters used are the shear angle in unit weight, cohesion and soil density. Based on the results of the analysis using the Fellenius method, the value of the safety factor is included in the stable slope. The purpose of this study is to determine the value of the embankment slope stability to the slope stability, so that it can determine whether or not a slope is stable which is displayed in the form of the value of the safety factor. The stages of the slope stability analysis process are carried out using the Fellenius method, which in the analysis process uses Slide and Phase2 software. From the data obtained from each slope, for the value of slope stability with an average FK value above 1.4, it can be concluded that the FK value of the slope stability value is said to be in a safe or stable condition. The distance from the ground water table to the base plane of the slide can affect the stability of a slope, the farther the distance from the ground water table to the bottom plane of the slide and the closer the groundwater table to the slope surface, the smaller the value of the safety factor.

### **2.4 Comparison of Previous Search**

The difference between the author's research and previous research can be seen in Table 2.1 below.

**Table 2.2 Comparison of Previous Research with Future Research**

<b>Research</b>	<b>Niroumand (2012)</b>	<b>Ogundare, D.A. (2019)</b>	<b>Kafikanda (2019)</b>	<b>Arsy (2018)</b>	<b>Hediyanto (2018)</b>
<b>Title</b>	The Role of Geosynthetics in Slope Stability	Utilization of Geotextile For Soil Stabilization	Slope Stability Analysis Using Geotextiles with the GEOSLOPE Program in a Case Study on the Balikpapan – Samarinda Toll Road Sta. 1+975.	Analysis of Embankment Stability in Road Body Construction with Geotextile Reinforcement Using the Fellenius Method on the Solo – Kertasono Toll Road Project STA 4+175.	Slope Stability Analysis with Cantilever Wall Reinforcement and Sheetpile on the Code River Bank.
<b>Research Purposes</b>	The paper observed the performance of geosynthetics in slope reinforcement.	The study investigated the application of non-woven geotextile to subgrade material as a form of reinforcement to road construction.	Knowing the value of the factor of safety on the slopes given geotextile reinforcement with the GEOSLOPE program	Knowing the results of the analysis of the stability of the embankment on the road body without using geotextiles, with reinforcement, the relationship between the length of the geotextile and the safety number.	Knowing the safety factor (SF) of the existing slope, cantilever reinforcement and sheet pile reinforcement using the Geoslope/W program.

<b>Research</b>	<b>Niroumand (2012)</b>	<b>Ogundare, D.A (2019)</b>	<b>Kafikanda (2019)</b>	<b>Arsy (2018)</b>	<b>Hediyanto (2018)</b>
Method	By installed the Geotextile in the slope stabilization	Testing the soil stabilization by using geotextile to see the difference and utilization	Analysis using Geoslope software for slope stability and manual calculations.	The analysis uses manual calculations with the Fellenius method and the safety factor with the GEOSLOPE program.	Analysis using Geoslope program for slope stability with cantilever reinforcement and Sheet pile.
Result	Geotextile has been used successfully in numerous occasions to stabilized steep slope in residual soil and weathered rock. Geotextile was used as tensile reinforcement and filter to stabilized slopes or embankments.	Geotextile reinforced soils present better performance than traditional soil under dynamic loadings. It is non-biodegradable, durable and also increases the ultimate service life of the pavement. It should, therefore be used to enhance the performance of a subgrade material in a pavement system	The safety factor in the analysis results using the Slope/W program is reinforced with geotextiles and an earthquake load of 2.303 is added.	The results of the analysis of road stability using reinforcement with the Fellenius method by manual calculation obtained a value (SF) of 1.786.	The safety factor (SF) of the slope with Sheet pile reinforcement due to its own weight is 2.726 and due to earthquake loads is 1.846.

## **CHAPTER III**

### **THEORETICAL BASIS**

#### **3.1 Soil**

Above the bedrock, soil is composed of mineral, organic matter, and relatively loose deposits. Carbonates, organic debris, or oxides that have been deposited between the grains may be the reason of the comparatively weak connections between the grains. There may be water, air, or both in the area between the particles.

The process of weathering rocks or other geological processes that occur near the earth's surface forms soil. The formation of soil from its parent rock can be a physical or chemical process. The process of physical soil formation that changes rock into smaller particles, occurs due to the influence of erosion, wind, water, ice, humans, or the destruction of soil particles due to changes in temperature or weather. The particles may be spherical, jagged or in some form in between. Generally, weathering due to chemical processes can occur under the influence of oxygen, carbon dioxide, water (especially those containing acids or alkalis) and other chemical processes. If the results of weathering are still in place, for example, then this soil is called residual soil and if the soil changes its place, it is called transported soil (Hardiyatmo, 2006).

##### **3.1.1 Soil Classification System**

is a methodical division of soil types with similar characteristics into groups and subgroups according to their intended usage. Purpose of the soil classification system is to inform people about the traits and physical qualities of the soil. Due to the enormous range of soil characteristics and behavior, classification methods often group soils into broad categories based on their shared physical characteristics. Its also helpful for a more thorough examination of the condition of the soil and the requirement for testing to ascertain its technical features, such as compaction traits, soil strength, density, and so on.

There are two soil classification systems that are generally used as a result of the development of the existing classification system. The system is a soil classification system based on USCS (Unified Soil Classification System) and a classification system based on AASHTO (American Association of State Highway and Transportation Official)

1. Soil classification based on USCS

In the USCS system (Table 3.1), a soil is classified as a coarse-grained soil (gravel and sand) if less than 50% passes the number 200 sieve and as a fine-grained soil (silt or clay) if more than 50% passes the number 200 sieve.

2. AASTHO System Classification

The AASHTO soil classification system was first introduced by Hoentogler and Terzaghi, which was eventually adopted by the Bureau Of Public Roads. The classification of this system is based on the criteria of grain size and plasticity. So in classifying soil requires testing of sieve analysis and Atterberg limits. This system that can be seen In table 3.2 divides the soil into 8 groups which are named from A-1 to A-8. A-8 is a group of organic soils that are unstable as a road structure layer material, so the last revision by AASHTO was ignored.



**Table 3.5 Classification System of USCS soil**

First Division			Group Symbol	Type Names
Coarse grained soil 50% or more passes sieve no. 200 (0.075mm)	Gravel 50% or more of the coarse fraction retained by the sieve no. 4 (4.75mm)	Clean gravel (little or no fine grain)	GW	Finely graded gravel and a mixture of sand-gravel, a little or does not contain fine granules
			GP	Poorly graded gravel and sand-gravel mixture, little or does not contain fine granules
		Gravel has a lot of granular content	GM	Silty gravel, gravel-sand-clay mixture
		fine	GC	Clay gravel, gravel-sand-clay mixture
	Sand more than 50% of the coarse fraction passes sieve no. 4 (4.75mm)	Clean gravel (little or no fine grain)	SW	Good grade sand, gravel sand, little or no contains fine granules
			SP	Poorly graded sand, gravel sand, little or no contains fine granules
		Gravel has a lot of granular content	SM	Silty sand, sand-silt mix
		fine	SC	Loamy sand, sand-clay mixture
Fine grained soil 50% or more pass sieve no. 200 (0.075mm)	Liquid limit silt and clay 50% or less		ML	Inorganic silt and very fine sand, rock powder or silty or loamy fine sand
			CL	Inorganic clay with low to moderate plasticity, gravel clay, sandy loam, silty loam
			OL	Organic silt and organic silt clay with low plasticity
	Liquid limit silt and clay > 50%		MH	Inorganic silt or fine sand, elastic silt
			CH	Lempung tak organik dengan plastisitas tinggi
			OH	Organic clay with medium to high plasticity
Soil with high organic content			P <sub>t</sub>	Peat and other soils with high organic content

Source: Hardiyatmo (2010)

**Table 3.6 Classification System of AASHTO Soil**

General Classification	Granular material ( < 35% pass filter no.200)						silty-clay soils ( < 35% pass filter no.200)				
Group Classification	A-1		A-3	A-2				A-4	A-5	A-6	A-7
	A-1-a	A-1-b		A-2-4	A-2-5	A-2-6	A-2-7				A-7-5/ A-7-6
Filter analysis (% passed)											
2,00 mm (no.10)	50 max	-	-	-	-	-	-	-	-	-	-
0,425 mm (no.40)	30 max	50 max	51 min	-	-	-	-	-	-	-	-
0,075 mm (no.200)	15 max	25 max	10 max	35 max	35 max	35 max	35 max	36 min	36 min	36 min	36 min
The nature of the fraction that passes the filter no.4											
Liquid Limit (LL)				40 max	41 min	40 max	41 min	40 max	41 min	40 max	41 min
plastic index (PI)	6 max		Np	10 max	10 max	11 min	11 min	10 max	10 max	11 min	11 min
Group index (G)	0		0	0			4 max	8 max	12 max	16 max	2- max
The main type of material in general	Crushed stone, gravel and sand		Soft Sand	Silty or loamy gravel and sand				Kerikil berlanau atau berlempung dan pasir		loamy soil	
General rating as base soil	Very good - good						Medium - bad				
Notes:											
Group of A-7 divided into A-7-5 and A-7-6 depends on the plastic limit (PL)											
For PL > 30, the classification is A-7-5											
For PL < 30, classification A-7-6											
Np = nonplastic											

Source: Hardiyatmo (2010)

### 3.1.2 Soil Shear Strength

A lump of earth can consist of two or three parts. In dry soil, the soil only consists of two parts, namely soil grains and air pores. In saturated soil there are also two parts, namely the solid or granular part and pore water. In an unsaturated state, the soil consists of three parts, namely the solid part (granules), air pores, and pore water. (Hardiyatmo, 2010). Mohr and Coulomb failure criteria is on Figure 3.1

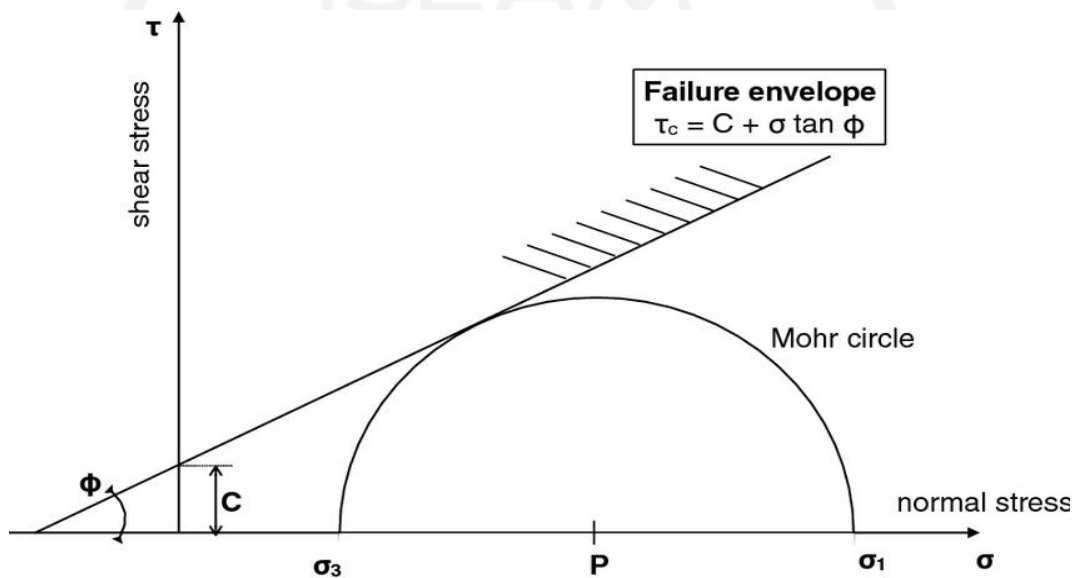


**Figure 3. 1 Mohr and Coulomb failure criteria.**

With,

$c'$  = Effective soil cohesion ( $\text{kN/m}^2$ )

$\sigma'$  Effective normal stress ( $\text{kN/m}^2$ )

$u$  = Water pores pressure ( $\text{kN/m}^2$ )

$\phi'$  = effective angle of friction in soil (degree)

The effective stress '1 and '3 at the point of failure can be used to express the soil's shear strength. Mohr's circle is a semicircle with coordinates ( $\tau$ ) and ( $\sigma'$ ) shown in Figure 3.2

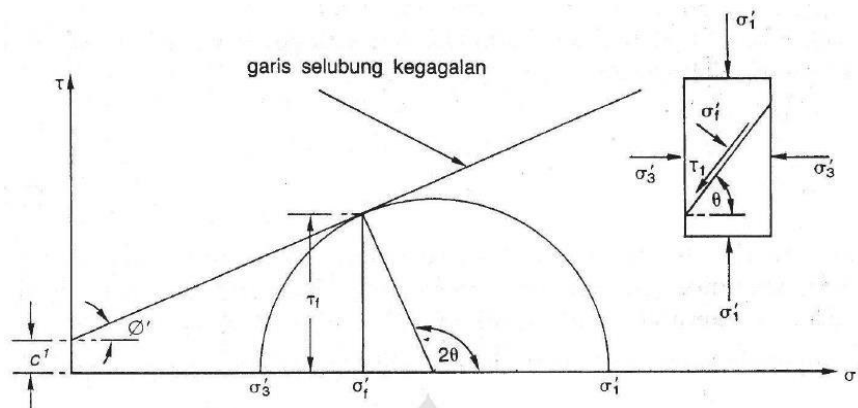


**Figure 3. 2 Mohr Circle**

(Source: Hardiyatmo, 2010)

From the Mohr circle we know:

$\sigma_1'$  = Effective major principal stress (kN/m<sup>2</sup>)

$\sigma_3'$  = Effective minor principal stress (kN/m<sup>2</sup>)

$\theta$  = Collapse Angle (degree)

$C'$  = Cohesion (kN/m<sup>2</sup>)

$\phi$  = Angle of friction in effective

Shear stress ( $\tau'f$ ) = effective shear stress at the time of failure

Normal stress ( $\sigma'f$ ) = effective normal stress at failure.

From the Mohr circle, the relationship between these parameters can be expressed in Equation 3.1 until 3.3 below:

$$\tau'f = (\sigma_1' - \sigma_3') \sin 2\theta \quad (3.1)$$

$$\sigma'f = (\sigma_1' + \sigma_3')/2 + (\sigma_1' - \sigma_3') \cos 2\theta \quad (3.2)$$

$$\sin \phi = \frac{(\sigma_1' - \sigma_3')/2}{(\sigma_1' + \sigma_3')/2} \quad (3.3)$$

### 3.1.3 Lateral Soil Stress

Lateral soil stress is the force generated by the impact of the soil behind the retaining structure. The amount of lateral stress is strongly influenced by changes in the location (displacement) of the retaining wall and soil properties. According to (Rankine, 1857) analysis of lateral soil stress is reviewed under conditions of plastic equilibrium, is when the soil mass at the right conditions will collapse. This condition of plastic equilibrium can only be achieved if there is sufficient

deformation in the soil mass. The magnitude and distribution of earth pressure are functions of displacement and strain.

According to Terzaghi (1923) in Hardiyatmo (1992), provides the principle of effective stress acting on a lump of soil. The principle of effective stress only applies to fully saturated soils, namely:

1. the total normal stress ( $\sigma$ ) on a plane in the soil mass, i.e. the stress due to the total weight of the soil including water in the pore space, per unit area in a perpendicular direction,
2. pore water pressure ( $u$ ) which is also known as neutral pressure or pore water pressure which acts equally in all directions, namely the water pressure that fills the voids between the solid grains, and
3. The effective normal stress ( $\sigma'$ ) on a plane in the soil mass, i.e. the stress resulting from the weight of the soil grains per unit area.

#### 3.1.4 Soil Compaction

According to Hardiyatmo (2010), soil, apart from functioning as a support for building foundations, is also used as embankment material such as embankments, dams, and roads. If the soil in the field requires improvement to support the building above it, or the soil will be used as backfill material, compaction is often carried out. The purposes of soil compaction include the following:

1. Increase the shear strength of the soil.
2. Reduces compressibility.
3. Reduces permeability.
4. Reduces the changes of volumes due the result of the changes of the water content, and so on.

This goal can be achieved by selecting the soil from the backfill, the method of compaction, the selection of the compactor machine, and the appropriate number of passes. The level of soil density is measured from the value of dry volume weight ( $\rho_d$ ). The dry volume weight does not change with the increase in water content. Thus, the soil that has been compacted in the field, and then changes in water

content (eg by rain), then the dry volume weight remains unchanged, as long as the total volume of the soil remains the same. This is because the density or dry volume weight is expressed by  $d = W_s/V$ , if the grain weight ( $W_s$ ) and total volume ( $V$ ) are fixed, then  $d$  is also constant.

Granular soil is considered the easiest to handle for field work. This material can provide high shear strength with little change in volume after compaction. High granular soil permeability can be beneficial or detrimental.

### 3.1.5 Elasticity Modulus and Poisson Ratio

Generally, the modulus of elasticity ( $E$ ) is determined from a triaxial test under undrained conditions, and the value of  $E$  is determined from an approximation of the slope of the stress-strain curve taken at half of the ultimate axial load. Poisson's number ( $\nu$ ) can be calculated from measurements of axial compression strain and lateral strain during the triaxial test. The value of  $\nu$  is difficult to obtain in the laboratory, some researchers have proposed the magnitude of the modulus of elasticity correlated with the undrained shear strength ( $s_u$  or  $\tau_u$ ) to estimate the magnitude of settlement in clay soils. Each researcher produces a different correlation between the values of  $E$  and  $s_u$ . For example, Bjerrum (1964) in Hardiyatmo (1994) has observed the value of  $E$  between 250 to 500  $s_u$ . Subsequent research, Bjerrum (1972) in Hardiyatmo (1994) has shown the value of  $E$  between 500 to 1500  $s_u$ .

For granular soils such as sand, the modulus of elasticity can be determined from the triaxial test. The value of the modulus of elasticity ( $E$ ) is known to be proportional to  $(\sigma_0)^n$ , where  $\sigma_0$  is the hydrostatic confinement pressure and the value of  $n$  is close to 0.5. The values of the elastic modulus ( $E$ ) and Poisson's number ( $\nu$ ) estimates for various soil types according to Bowles (1977) in Hardiyatmo (1994) can be seen in Table 3.3 and Table 3.4.

**Table 3.7 Approximate Value of Soil Elasticity Modulus**

Soil Type	E (kN/m <sup>2</sup> )
Clay:	
Very Soft	300 – 3000
Soft	2000 – 4000
Medium	4500 – 9000
Hard	7000 – 20000
Grained	30000 – 42500
Sand:	
Silted	5000 – 20000
Uncompact	10000 – 25000
Compact	50000 – 100000
Sand and gravel:	
Compact	80000 – 200000
Uncompact	50000 – 140000
Silt	2000 – 20000
Loess	15000 – 60000
Rock	140000 – 1400000

Source: Hardiyatmo (1994)

**Table 3.8 Approximate Value of Soil Poisson's Ratio**

Soil Type	$\nu$
Saturated Clay	0.40 – 0.50
Unsaturated Clay	0.10 – 0.50
Grained Clay	0.20 – 0.30
Silt	0.30 – 0.35
Compact Sand	0.20 – 0.40
Rough Sand ( $e = 0.4 - 0.7$ )	0.15
Soft Sand ( $e = 0.4 - 0.7$ )	0.25
Rock	0.10 – 0.40
Loess	0.10 – 0.30

### 3.2 Slope

Slope is a land surface condition where the soil has a different elevation from one area to another and forms a certain slope. Based on the origin of its formation, slopes are divided into two types, namely slopes formed by nature and slopes formed by human activities.



1. Natural Slope

Natural slopes that have been stable for several years may suddenly collapse due to topographic changes, groundwater flow, earthquakes, loss of shear strength, stress changes and weathering. Hardiyatmo (2012) states that predicting the stability of natural slopes may be well done, only if the area under study is an old landslide zone that has been studied previously, which may have changed its condition by human activities, such as excavation at the foot of the slope. By knowing the existence of old landslide fields on natural slopes, the slopes will be easier to understand and predict their behavior.

2. Artificial Slope

Man-made slopes generally consist of embankment structures and excavations, which are widely used in buildings, roads, river embankments, dam slopes and others (Hardiyatmo, 2006).

- a. Excavation

The purpose of the excavation slope design is to determine the height and slope of the slope which is economical and stable. The design of the depth and slope of the excavation will be influenced by geological conditions, material properties in place, groundwater position, seepage pressure and others (Hardiyatmo, 2012).

- b. Embankment

Embankments are generally built using compacted soil. Such embankments are for example highway embankments, railroad embankments, backfill, embankment dams and embankments. The technical properties of the materials used in the embankment are highly dependent on the material properties of the pick-up location (eg: grain distribution, density, shear strength and so on). Embankment stability analysis is generally easier than natural and excavated slope stability analysis. This is because the embankment material is a relatively homogeneous soil with known mechanical properties from laboratory tests (Hardiyatmo, 2012).

### 3.2.1 Cause of Embankment

Many factors such as geological and hydrological conditions, topography, climate and weather changes can affect slope stability resulting in landslides. Natural causes of landslides, for example weathering, heavy rain or rain that is not so heavy but prolonged, the presence of soft layers and others. Other causes related to human activities, for example excavation at the foot of the slope, construction on the surface of the slope and others (Hardiyatmo, 2012). The following will explain further the causes of slope failure mentioned above.

#### 1. Addition of load, excavation and erosion of the toe of the slope

Many avalanches are caused by excavation of slopes for the construction of roads, railways, housing, excavations of riverbeds (sand or stones are taken) and landslides also often occur in excavations where soil is taken. Heavy buildings erected at the top of slopes can also cause landslides.

Landslides on clayey slopes are often caused by erosion or excavation of soil at the foot of the slope due to river flow (Figure 3.3). Erosion of the riverbed at the foot of the slope causes the slope to become larger and the slope height to increase, as a result the slope becomes unstable. Under certain conditions, excavation of the soil can also lead to landslides of the excavation slopes. Excavation reduces the overburden pressure, so that the soil or rock expands and its shear strength decreases.

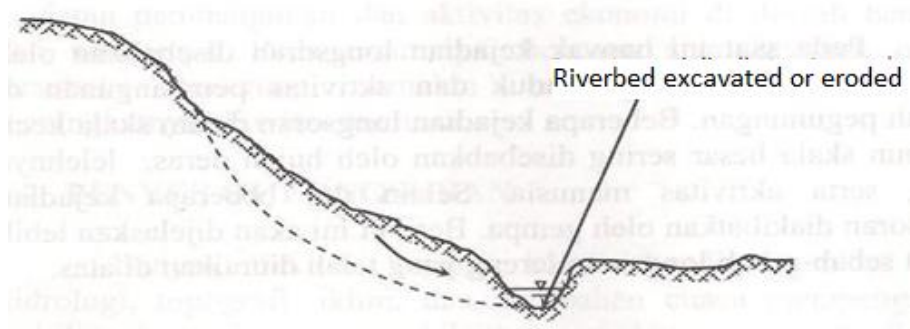


**Figure 3. 3 The Riverbed Deepens Due to Excavation or Erosion**

(Source: Hardiyatmo, 2012)

2. Rain and increase in pore water pressure

The shear strength of the soil in the field depends on its water content, that is, if the water content (pore water pressure) increases, the shear strength decreases. Most slope failures occur after or during heavy or prolonged rains. Water that infiltrates into the soil, in addition to reducing the shear strength of the soil, also adds to the weight of the slope-forming soil itself. The combination of the two is often the cause of slope failure.

The behavior of annual rainfall affects the frequency of landslides. The softening of the slope-forming material due to the increase in soil water content due to rain, as well as the increase in ground water level during the rainy season also affect the speed of soil mass movement. Rising ground water level causes a reduction in the shear strength of the soil. The increase in pore water pressure around the potential landslide area reduces the effective stress thereby reducing the shear strength.

3. Rapid Drawdown

Slope failure also often occurs when the water level of a pond, river or reservoir drops suddenly or in a short period of time, especially for silty or loamy soils. The loss of water pressure on the slopes that were previously submerged in water becomes not submerged, causing the weight of the soil above the potential landslide area to become heavier, so that the soil tends to move or sag downward. In addition, as the self-weight of the slope increases due to lowering of the water table, higher pore water pressures develop in the soil along the surface of the potential landslide plane. This reduces the shear resistance of the soil along the potential landslide plane.

4. Earthquake

Landslides can be caused by earthquakes, or vibrations caused by pile driving or rock blasting. Vibrations due to earthquakes can cause liquefaction of fine, loose sand or silt that is submerged in groundwater. In addition, vibration can also cause reduced shear strength in some sensitive clays.

In soils of fine, non-solid sand or silt that are below the water table, when

an earthquake occurs, in the pore cavities of the soil it will develop into high pore water pressure. This will drastically reduce the effective stress and shear strength of the soil. When the pore water pressure in the soil pores is equal to or greater than the overburden pressure, the material has a liquid-like property. In such conditions, the soil is called liquefaction. When there is an earthquake and the ground liquefied, the soil becomes like a viscous liquid consisting of a mixture of silt particles and air, and this viscous liquid can flow at high speeds.

### 3.2.2 Slope Stability Analysis

On a non-horizontal soil surface, the component of gravity tends to move the soil downward. If the component of gravity is such that the resistance to shear that can be exerted by the soil on the slip plane is exceeded, the sloping soil surface is called a slope stability analysis. There are many factors influencing the analysis of slope stability, for example, the condition of the soil in layers, the anisotropic shear strength of the soil, the flow of water seepage in the soil and others.

### 3.2.3 Theory of Slope Stability Analysis

Based on Hardiyatmo (2010) the purpose of the stability analysis is to determine the safety factor of the potential landslide area. In the analysis of slope stability, several ideas were made, which are as follows.

1. Slope failure occurs along the surface of a certain landslide plane and can be considered as a 2-dimensional plane problem.
2. The landslide mass is considered a massive object.
3. The soil shear of the soil mass at each point along the landslide plane is independent of the orientation of the landslide surface, or in other words the shear strength of the soil is considered isotropic.
4. The safety factor is defined by showing the average shear stress along the potential landslide area, and the average soil shear strength along the landslide surface.

The safety factor is defined as the ratio between the resisting force and the

driving force, which can be seen in Equation 3.1.

$$F = \frac{c}{c_d} \quad (3.1)$$

Knowing:

$\tau$  = The shear resistance that the soil can exert (kN/m<sup>2</sup>),

$r_d$  = Shear stress that occurs due to gravity of the soil that will slide (kN/m<sup>2</sup>),

F = Safety Factor

According to the Mohr-Coulomb theory, the shear resistance ( $r$ ) that can be exerted by the soil, along its landslide plane, can be expressed in Equation 3.2.

$$\tau = c + \sigma \operatorname{tg} \phi \quad (3.2)$$

Knowing:

$r$  = Shear Stress (kN/m<sup>2</sup>)

$c$  = Cohesion (kN/m<sup>2</sup>)

$\phi$  = friction angle in the soil (degrees)

$\sigma$  = Normal Stress (kN/m<sup>2</sup>)

In the same way, the equation for the shear stress that occurs ( $\tau_d$ ) due to soil loads and other loads on the landslide surface can be written as in Equation 3.3.

$$\tau_d = c_d + \sigma \operatorname{tg} \phi_d \quad (3.3)$$

Knowing:

$\tau_d$  = Shear Stress (kN/m<sup>2</sup>),

$c_d$  = Cohesion (kN/m<sup>2</sup>),

$\phi_d$  = Friction angle in the soil (degree),

$\sigma$  = Normal Stress (kN/m<sup>2</sup>)

Substituting from Equation 3.18 and Equation 3.19 to Equation 3.4, we get Equation 3.20

$$F = \frac{c + \sigma \operatorname{tg} \phi}{c_d + \sigma \operatorname{tg} \phi_d}$$

$$c_d + \sigma \operatorname{tg} \phi_d = \frac{c}{F} + \frac{\operatorname{tg} \phi}{F} \quad (3.4)$$

For the purpose of providing a factor of safety for each component of the shear strength, the factor of safety can be expressed in Equations 3.5 and 3.6.

$$F_c = \frac{c}{c_d} \quad (3.5)$$

$$F_\phi = \frac{\text{tg}\phi}{\text{tg}\phi_d} \quad (3.6)$$

Knowing:

$F_c$  = Safety factor on the cohesion component,

$F_\phi$  = Safety factor on the friction component

#### 3.2.4 Circle Landslide Field

Curved or circular landslides occur in slope landslides from homogeneous cohesive soils. Slope failure of the cohesive soil type occurs due to the increase in soil water content. The cause of landslides is due to the unavailability of sufficient soil strength to withstand the downward movement of the landslide in the landslide area.

The curvature of the landslide field can be circular (cylindrical), logarithmic spiral or a combination of both. In practice, a landslide is often encountered with a landslide area that is not in the form of a continuous curve, due to the intersection of the landslide plane with a hard soil layer or a very soft layer. The assumed form of the landslide field in the form of a circle is intended to make it easier to calculate the stability analysis of the landslide field that often occurs in nature. Errors in slope stability analysis are not caused by the assumed shape of the landslide field, but by errors in determining soil properties and determining the location of the critical landslide area (Bowles, 1984 in Hardiyatmo, 2006).

#### 3.2.4 Slice Method

The wedge method is used on inhomogeneous soils and the seepage flow in the soil is erratic. The normal force acting at a point in the circle of the landslide

area is affected by the weight of the soil above that point. In the wedge method, the landslide mass is divided into several vertical slices. Figure 3.4 shows the forces acting on the wedge. These forces consist of the shear force ( $X_r$  and  $X_l$ ) and the effective normal force ( $E_r$  and  $E_l$ ) along the sides of the wedge, as well as the resultant effective shear force ( $T_i$ ) and the resultant effective normal force ( $N_i$ ) acting along the base of the wedge. . In the section, the pore water pressures  $u_l$  and  $u_r$  and act on both sides, and the pore water pressures  $U_i$  act basically.

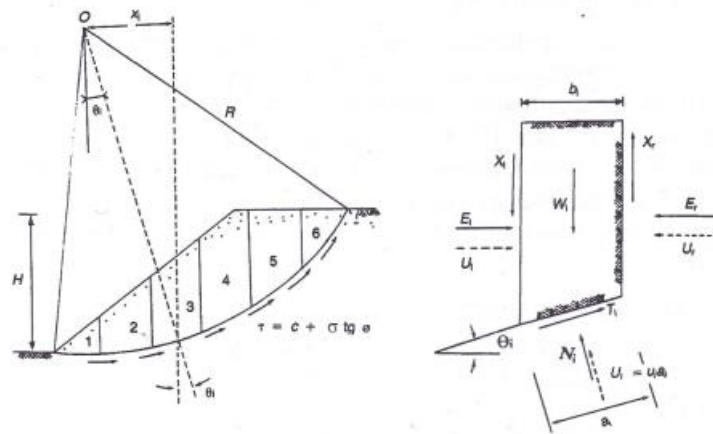


**Figure 3. 4 The force that Acting on the Slice**

(Source: Hardiyatmo 2006)

### 3.3 Geotextile

The collapse or slide that occurs is not due to the pull or pressure between the soil grains, but is caused by the overturning or slipping of the soil particles. By knowing the type of failure that occurred, soil reinforcement can be applied to the landslide area by placing soil reinforcement material, anchoring (soil nailing) and so on.

In this final project using geotextile reinforcement, where geotextile is a waterproof material or factory-made textile material made from synthetic materials, such as: polypropylene, polyester, polyethylene, nylon, polyvinyl chloride and a mixture of these materials. All of these materials are thermoplastic. (Hardiyatmo 2008). Based on the method of manufacture, geotextiles are divided into two types, namely;



1. Woven geotextile

Plaiting is the method used to create woven geotextiles, and because of their relatively high tensile strength, they are typically employed in the field as dividing layers and reinforcement layers. As reinforcement, woven geotextiles serve as reinforcement in the soil. Meanwhile, as a separator, woven geotextile functions to separate soft soil from hard soil.

2. Non woven geotextile

Plaiting is not used to create non-woven geotextiles; instead, ties or adhesives are used to join the generated tissue or fibers.

- 3.3.1. Geotextile Mechanical Properties

Mechanical properties of geotextile are as follows;

1. Tensile Strength

Depending on the use, the geotextile must be able to support loads and be deformed. The load will cause deformation and this deformation will mobilize the tensile strength of the geotextile. The tensile strength of geotextiles is an important property required. Various kinds of geotextile tensile strength are used depending on the main function under consideration, namely for reinforcement, separation, drainage or filtration. Tensile strength values can be obtained from tensile tests carried out until the geotextile fails.

2. Gab Tensile Strength

Geotextiles generally have low compressibility, especially for non-woven geotextiles. The higher the normal stress acting on the geotextile surface, the lower the thickness. The compressibility or compressibility of geotextiles expresses the change in thickness caused by normal stresses acting on the surface of the geotextile.

3. Fatigue Strength

Fatigue strength is defined as the geotextile's ability to withstand repeated (cyclic) loads before failure. In the laboratory, this cyclic load test is carried out until the test load fails. The test object is pulled and stretched

lengthwise at a constant speed at a predetermined length.

### 3.3.2 Geotextile Function

When you want to design using geosynthetics, the geosynthetic function that will be applied must be determined first, then the appropriate type of material is selected. Geotextile functions include;

#### 1. Separator Function

Installation of geotextile which is a flexible synthetic material as a separator between two different materials will maintain the integrity of both, so that the two materials remain intact materials, and as a result, the geosynthetic inserted system becomes stronger. Koerner (2005) in Hardianto (2008) illustrates the difference in grain movement mechanisms due to the use of geotextiles on soft subgrade which functions as a separator, as shown in Figure 3.5.

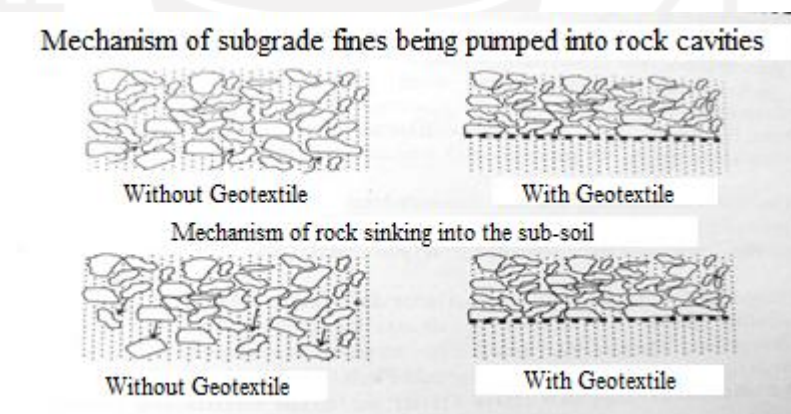


**Figure 3. 5 Differences in grain movement mechanism due to the use of geotextiles on soft-subgrade soils that function as separators**

(Source: Koerner, 2005 on Hardiyatmo, 2008)

#### 2. Filtration Function

Geotextile in its function as a filter must provide the possibility of fluid movement through it, namely the flow perpendicular to the plane of the sheet. At the same time, the geotextile must also be able to hold the soil upstream so that the soil particles do not go along with the flow. The factor

that must be given simultaneously is a sufficiently large permeability (requires the size of the geotextile pore openings). Then the ability of the geotextile to hold the soil grains so that the soil does not participate in the flow (requires a tight arrangement of threads) and prevents the movement of soil grains through the geotextile.

### 3. Reinforcement Function

Reinforcement layer, in general, soil is not able to withstand tensile stress. If these conditions are found, a geotechnical construction will be made which is usually quite expensive. For example on a steep slope, if the slope is made naturally with a high cohesion value it may still be safe, but if it is made of backfill it is usually reinforced with a retaining wall. A retaining wall made of masonry will require relatively large dimensions so that it requires a large enough area, if it is made of reinforced concrete it takes a long time and is expensive. With the ability of geotextiles that are able to withstand tension and are able to withstand shear (due to soil friction), geotextiles can be used as reinforcement in soil.

#### 3.3.3 Soil-Geotextile Interaction

The principle of reinforced soil is that the mechanical properties of the soil are improved by reinforcement placed parallel to the direction of the main strain in order to compensate for the weakness of the soil in resisting tensile forces. Soil properties become strong to withstand this tension as a result of the interaction between soil and reinforcement. Cooperation between soil and reinforcement in supporting the load will occur when there is friction between the two. With this friction, the soil transfers the forces acting on it to the reinforcement.

Geotextiles resist tensile stresses transmitted to the soil by friction between the geotextile and the soil. The stress-strain response between geotextiles and soils is usually different, and depends on the applied stress level. (Hardiyatmo, 2008)

## 3.4 Plaxis

Technological developments give rise to various complex structures so that in

such a complex analysis, exact methods will be difficult to use. As a better solution, develop various numerical methods which are a method of approaching the exact solution as accurately as possible. Numerical method is a mathematical engineering that transforms expressions of continuous mechanics (forms of calculus and differential equations) into discrete mechanics (forms of matrices). One of the numerical methods that has been developed in numerical analysis is the Finite Element Method.

In this final project, for slope stability analysis, Plaxis version 8.6 application program will be used. Plaxis is a finite element program that has been specially developed for the analysis of deformation and stability in geotechnical engineering. In the Plaxis program, a triangular element with six nodes is used and a triangular element with fifteen nodes as a finite element (Figure 3.6). The fifteen-node triangular element is a very accurate element for producing high levels of stress quality in difficult problems. The use of this element requires large memory and the calculation is relatively slow. Therefore, the use of simpler elements can be an option. The triangular element with six nodes is a fairly accurate element that gives good results in standard deformation (Brinkgreve, 2007).

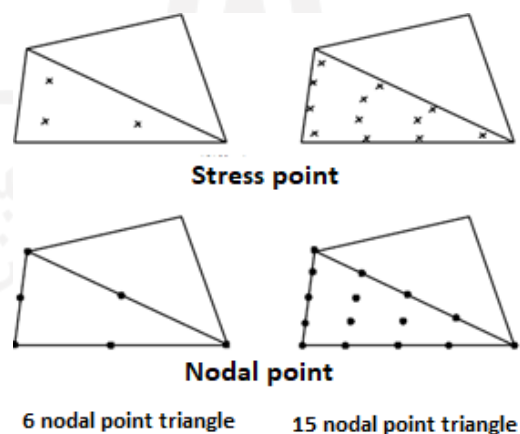


**Figure 3.6 Position of Nodal Point and Stress Point on Earth**

(Source: Brinkgreve, 2007)

In geotextile elements which are line elements with two degrees of freedom at each node ( $u_x$  and  $u_y$ ), the number of nodes will adjust to the triangular element used. The use of a triangular element with six nodes defines three nodes in the geotextile element and five nodes in the use of a triangular element with fifteen nodes.



**Figure 3.7 Position of Nodal Points and Stress Points on Geotextile Elements**

(Source: Brinkgreve, 2007)

When adding a soil element, such as geotextile, the interface element is used to simulate the interaction between the soil and the geotextile. When a triangular ground element with fifteen nodes is used, the interface element relationship is limited by five pairs of nodes. If a triangular element with six nodes is used, then the interface element relationship is limited by three pairs of nodes (Figure 3.8). The interface element is a finite thickness, but in the finite element formulation, the coordinates of each pair of nodes are the same, which means that the interface element has no thickness.

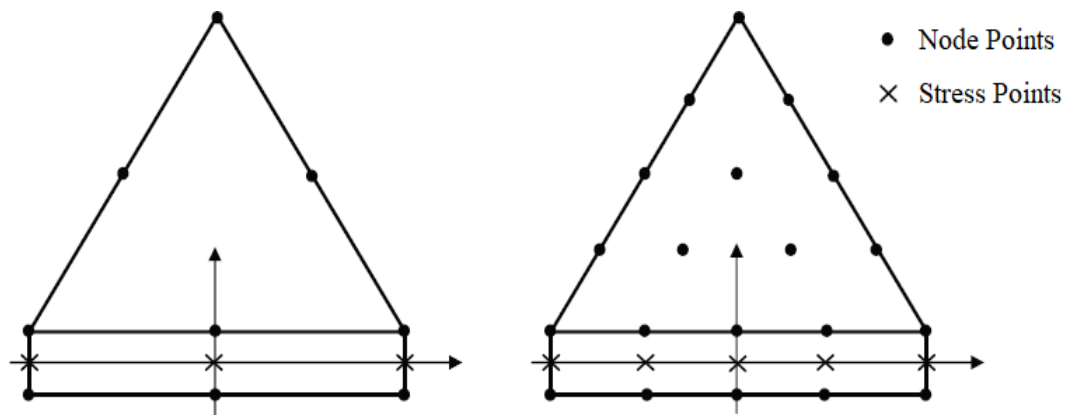


**Figure 3.6 Distribution of Nodal Points and Stress Points in Interfacial Elements**

(Source: Brinkgreve, 2007)

In the Plaxis program there are five material models, namely Mohr-Coulomb model (MC), Jointed Rock model (JR), Hardening Soil model (HS), Soft Soil Creep model (SSC) and Soft Soil model (SS). This final project uses the assumption of the Mohr-Coulomb model as a method that can complete the initial analysis to describe the behavior of the soil. The Mohr-Coulomb model is an elastic-plastic model with five parameters:  $T$  as the dilatation angle,  $E$  and  $\nu$  for the soil elasticity model, and  $\nu$  for the soil plasticity model. The Mohr-Coulomb model is a first-order approximation of soil or rock behavior. It is advised to utilize this model when conducting a preliminary analysis of the issue at hand. Every layer is represented with an average stiffness value that is constant. Calculations frequently happen quickly as a result of the constant stiffness qualities, and it is possible to get a rough idea of the model's deformation shape. The initial stress condition of the soil has a significant impact in nearly all soil deformation issues in addition to the five model components. The initial stress of the soil must be determined by determining the proper 0 procedure.

Plasticity has a relationship with the formation of strain that cannot be returned to its original state. To evaluate whether plasticity has occurred in the

calculations, a yield function (*yield function*,  $f$ ), is used as a function of stress and strain. A yield function can generally be expressed as a plane in the principal stress space.





## **CHAPTER IV**

### **RESEARCH METHOD**

#### **4.1 General Review**

The Cibitung - Cilincing Toll Road Development Project Sta 3+550 was the subject of this final project's research. This study aims to find the safety value before and after retrofitting using geosynthetics with variations in ground water level. To analyze this research, Plaxis 8.6 program was used. Plaxis program is a geotechnical application program that can be used to analyze slope stability. From this analysis, it is hoped that it can be determined which conditions produce the best safety factor, so that the slope stability strength planning can be used as a reference for the recommended soil conditions.

#### **4.2 Research Data**

The data of this research is secondary data of the Cibitung – Cilincing Toll Road Project. Secondary data required include:

1. Field test soil data and laboratory test soil data are both examples of soil data. Data from the SPT (Standard Penetration Test) test results, specifically data from field test soil data presented as tables and graphs.

Data from laboratory testing on soil include the following:

- a. Soil volume weight ( $\gamma$ )
  - b. Cohesion ( $c$ ), and
  - c. Inner sliding angle ( $\phi$ ).
2. Soil Layer Data.

3. Earthquake Data.
4. Slope Data.

### **4.3 Data Analysis Method**

This slope reinforcement analysis and slope design uses the Plaxis 8.6 application. To find the safety value of the existing slope using the slope method.

### **4.4 Research Stage**

The research data used in the analysis of this Final Project are as follows.

1. Searching and studying literature related to the research topic,
2. Collect data and references needed to support research,
3. Formulate existing problems for slope stability,
4. Determine the parameters that affect the slope stability analysis,
5. Analyzing the stability of the original unreinforced slope with the Plaxis 8.6 application,
6. Design slope reinforcement with geotextiles,
7. Analyzing slope stability with geotextile reinforcement and groundwater level variations with the Plaxis version 8.6 application,
8. Discussion on slope stability analysis, and,
9. Conclusion and suggestion.

### **4.5 Loading**

#### **4.5.1 Vehicle Loading**

According to Wikipedia, provincial roads are collector roads in the primary road network system that connects provincial capitals with district/city capitals, or between district/city capitals, and provincial strategic roads. Then the live load is obtained from the vehicle load. The pavement load used is 10 kN/m<sup>2</sup> from secondary data, while the traffic load is 15 kN/m<sup>2</sup>, presented in Table 4.1 as follows.

**Table 4.1 Traffic Load Parameter Data**

<b>Function</b>	<b>System Network</b>	<b>Annual Average Daily Traffic (LHR)</b>	<b>Traffic load (kN/m<sup>2</sup>)</b>
Primary	Arteries	All	15
	Collector	> 10.000	15
		< 10.000	12
Secondary	Arteries	> 20.000	15
		< 20.000	12
	Secondary	> 6.000	12
		< 6.000	10
	Local	> 500	10
		< 500	10

Source: public Works Department (2009)

#### 4.5.2 Earthquake Load

The earthquake load used in the slope stability analysis is a dynamic earthquake load. The Bekasi area has a peak earthquake acceleration (PGA) between 0.3 - 0.4 g. The data that corresponds to the duration of the earthquake is data from American Canyon California friends in late 2014 which had an earthquake peak acceleration of 0.3938 g. For the time interval, 3.2 seconds is used, this time is considered to have passed the peak acceleration of the earthquake. Zoning maps and graphs of the relationship between earthquake acceleration and earthquake time Figures 4.1 below show this.

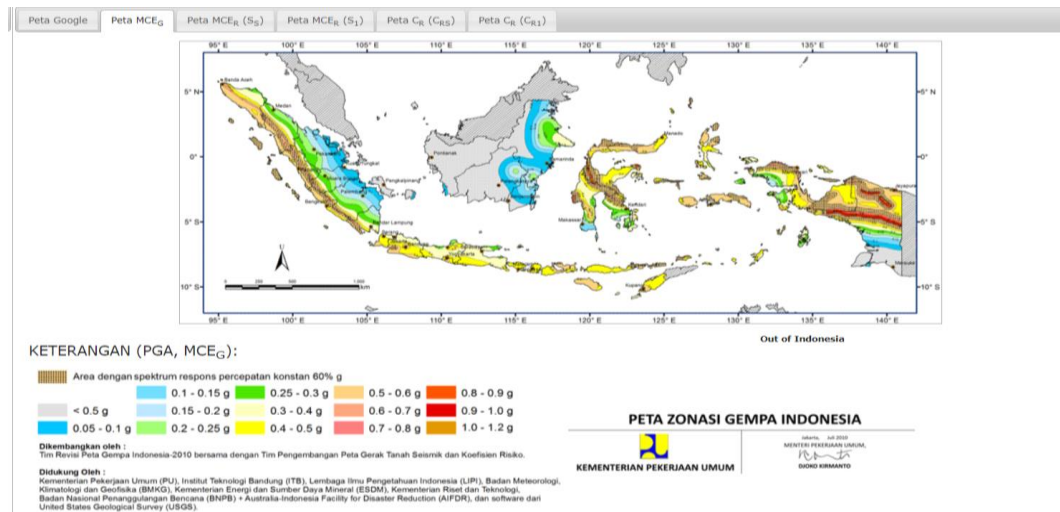


**Figure 4. 1 Earthquake Zoning Map**

(Source: puskim.pu.go.id, 2018)

## 4.6 Plaxis Modeling

### 4.6.1 Soil Parameter

In slope stability analysis, soil parameters are a very important input, soil parameters are obtained based on secondary data from the Geotechnical Analysis Report for the Cibtiung – Cilincing Toll Road Project. The input soil parameters can be seen in Table 4.2 below.

**Table 4.2 Parameter of Data Soil Construction Period**

Name	Unit	Silty Clay	Sandy Silt	Sandy Silt	Clayey Sand
Model	-	MC	MC	MC	MC
Type	-	DRAINED	DRAINED	DRAINED	DRAINED
$\gamma_{unsat}$	kN/m <sup>3</sup>	14	18	20	16
$\gamma_{sat}$	kN/m <sup>3</sup>	16	20	22	19
$K_x$	m/day	4.500E-03	4.300E-05	4.300E-05	0.1
$K_y$	m/day	4.500E-03	4.300E-05	4.300E-05	0.1
$E$	kN/m <sup>3</sup>	4000	20000	24000	11000
$\nu$	-	0.25	0.3	0.334	0.3

Cohesion (C)	kN/m <sup>3</sup>	10.1043	79.37	85	10
Shear angle (φ)	°	8	30	30	25
Dilated Angle (ψ)	°	0	0	0	0

Source: PT. Carina Griya Mandiri (2017)

**Table 4.3 Parameter Data of Soil Post Construction**

Name	Unit	<i>Silty Clay</i>	<i>Sandy Silt</i>	<i>Sandy Silt</i>	<i>Clayey Sand</i>
Model	-	<i>MC</i>	<i>MC</i>	<i>MC</i>	<i>MC</i>
Type	-	<i>DRAINED</i>	<i>DRAINED</i>	<i>DRAINED</i>	<i>UNDRAINED</i>
$\gamma_{unsat}$	kN/m <sup>3</sup>	14	18	20	16
$\gamma_{sat}$	kN/m <sup>3</sup>	16	20	22	19
$K_x$	m/day	4.500E-03	4.300E-05	4.300E-05	0.1
$K_y$	m/hari	4.500E-03	4.300E-05	4.300E-05	0.1
$E$	kN/m <sup>3</sup>	4000	20000	24000	11000
$\nu$	-	0.25	0.3	0.334	0.3
Cohesion (C)	kN/m <sup>3</sup>	10.1043	79.37	85	10
Shear angle (φ)	°	8	30	30	25
Dilated Angle (ψ)	°	0	0	0	0

Source: PT. Carina Griya Mandiri (2017)

#### 4.6.2 Geotextile

The normal stiffness (EA) value for the geotextile that is used as input for the Plaxis software can be determined using Equation 4.1 below.

$$EA = \frac{Fg}{\Delta l/l} \quad (4.1)$$

Description:

$F_g$  = The allowable tensile strength of the geotextile (kN/m), and  
 $\Delta l/l$  = Strain in geotextiles

The geotextile used is the production of PT. Tekindo Geosystems. The geotextile used is a type of woven or woven geotextile. The geotextile data can be seen in Table 4.2 below.

**Table 4.4 Parameter Data Woven Geotextile UW-250**

Parameter	Notation	Value	Unit
allowable tensile Strength	Ta	52	kN/m
Strain	E	20	%
Normal Rigidity	EA	260	kN/m

Source: PT. Tekindo Geosistem (2020)

#### 4.7 Plaxis Program Operation

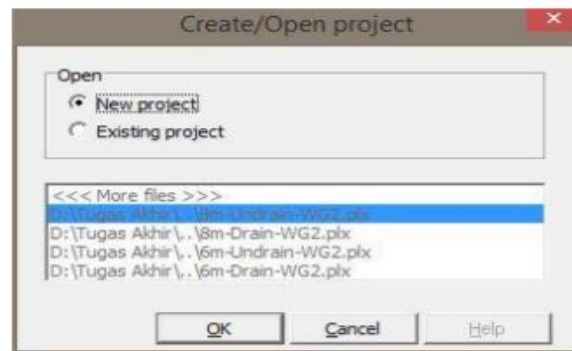
How to operate Plaxis version 8.6 through 3 stages, that are Plaxis input, Plaxis Calculation, and Plaxis Output.

##### 4.7.1 Plaxis Input

The steps carried out in the analysis using the Plaxis 8.6 program are as follows.

##### 1. Open Plaxis Program

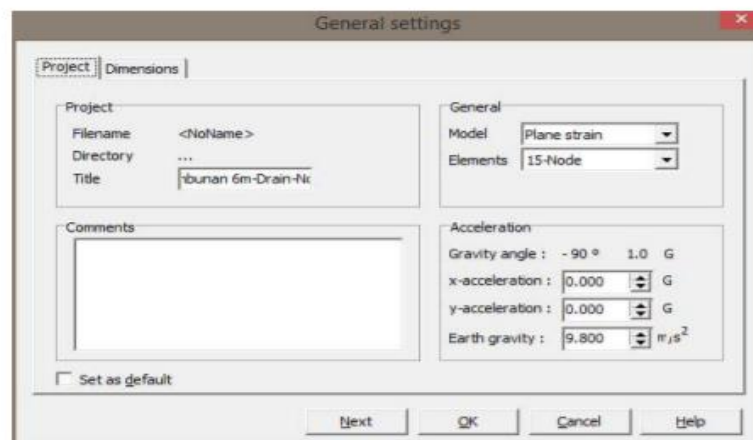
Double-clicking the Plaxis input software icon will open the Plaxis application. Then, as shown in Figure 4.2 below, a popup with the option to create/open a project will appear; pick new project and then click OK to create a new job..



**Figure 4. 2 Square Box of Create/Open Project**

## 2. General Setting

there are two dialog tabs uin general setting, that are the project and dimensions tab. Choose or click the sheet of project tab, Type the project's name there to be modeled in the title dialog box. Choose the plane strain model analysis in the general box, select the 15-Node basic element type for analysis to produce accurate stress and collapse loads.

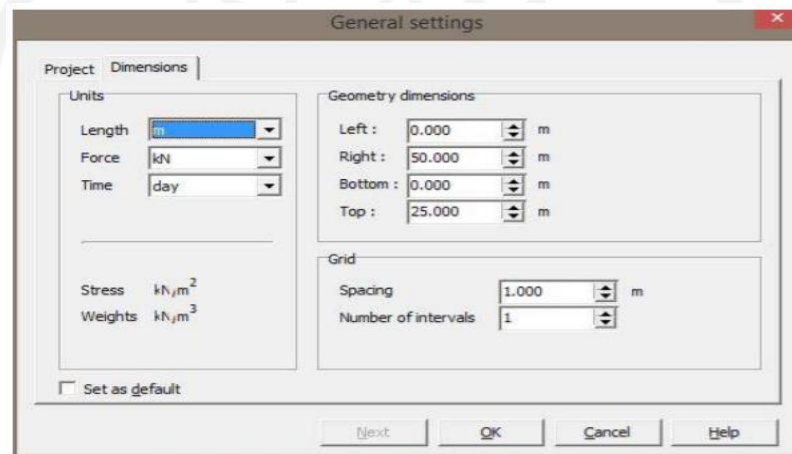


**Figure 4. 3 Tab Project from the General Setting Window**

In the geometry dimensions tab options, use the pre-selected units in the units box (Length = m, Force = kN, Time = day). In the geometry dimensions box, the size of the drawing area is entry required, when entering the top and bottom coordinates of the geometry to be made. Plaxis will add a small margin so the geometry will be






on the drawing plane. After that input 0.0; 50.0; 0.0; 25.0 each in the left, right, bottom, and top fields in the dialog box. The Grid box includes the values for setting the grid spacing. This grid will form a dotted matrix that is used to enter the exact description of the existing grid during modeling. The distance between the points is determined by the space value. Then for spacing enter a value of 1.0 and 1 for the number of intervals.



**Figure 4. 4 Tab Dimension from General Setting Window**

### 3. Geometry Modeling

The depiction of the geometric model is carried out with the following stages.

- a.  Choose the Geometry line option (already activated)  
Position the cursor at the center of the coordinates. Place the cursor at coordinates 0,0; 0.0 is the starting point in the depiction of geometry, after which the geometry is drawn according to the specified coordinates.
- b.  Click the standard fixities button on toolbar.
- c.  Click the Distributed load-load system A on toolbar.  
Then click on the start point and end point on the geometry receiving the load, then right click the mouse to end the evenly distributed load input.

Enter rated load evenly ( $10\text{kN/m}^2$ ).

#### 4. Parameter Material Input

For this program's material data entry, it can be done by using the material sets button on the toolbar or through the options available in the materials menu.

Select the Material Sets button on the toolbar.

- a. Click the option (new) at the bottom of the material sets window. A dialog box will appear with three tab-sheets, namely general, parameters, interface (See Figure 4.5 and Figure 4.6).
- b. In the Material Sets dialog box in the general tabs sheet, type "Silty Firm" in the identification box.
- c. Then select Mohr-Coulomb on the combo box material model and drained on the combo box material type.
- d. Enter the value to be input in the general properties and in the permeability box according to the nature of the material used.
- e. Click on the parameters tab of the four tab-sheet menu and enter values according to the properties of the material used. Since the geometry model does not use an interface, the third tab sheet can be skipped and then click OK to save the material.
- f. Click and drag the data set from the material sets window to the soil cluster in the drawing plane and drop it above it. Then the material is entered in the image field when the image field changes color.
- g. Then click the OK button on the Material Sets window to close the database.

The image shows a software dialog box titled "Mohr-Coulomb - Silty Firm". It has three tabs: "General", "Parameters", and "Interfaces". The "General" tab is selected. The dialog is divided into several sections:

- Material Set:**
  - Identification:
  - Material model:
  - Material type:
- General properties:**
  - $\gamma_{unsat}$ :   $\text{kN/m}^3$
  - $\gamma_{sat}$ :   $\text{kN/m}^3$
- Permeability:**
  - $k_x$ :   $\text{m/day}$
  - $k_y$ :   $\text{m/day}$
- Comments:**

At the bottom of the dialog, there are four buttons: "Next", "Ok", "Cancel", and "Help".

**Figure 4. 5 Tab General Sheet from  
Material Sets Window**

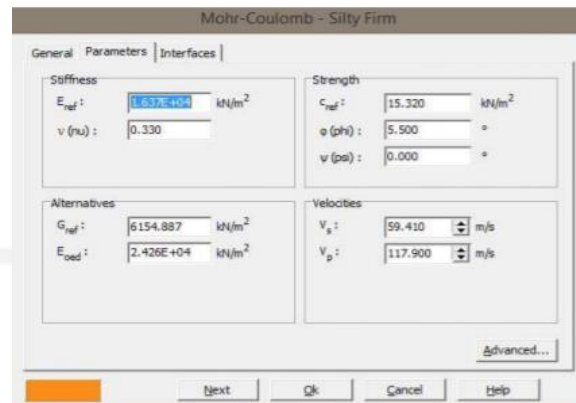


**Figure 4. 6 Tab Parameters from Material Sets Window**

5. Mesh Generation


Click the Generate Mesh option on the toolbar or select an array from the mesh menu. After the arrangement of the element network, after that a new window will open where the finite element network is shown as shown in Figure 4.7. Then click the <update> button to return to enter geometry mode.

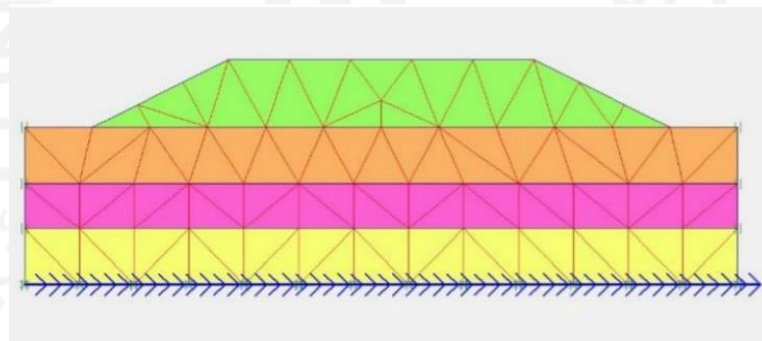



**Figure 4. 7 Finite Element Network (Meshing)**

6. Initial Condition

- a. Click the initial conditions on toolbar.

- b.  Since this project does not include water pressure, then proceed to the initial geometry configuration mode by clicking the button to the right of the “switch”. The phreatic line will automatically lie at the

bottom of the geometry.

- c.  Click the General initial stresses option on the toolbar. The Co-procedure dialog box will appear, select OK as shown in Figure 4.8 below.

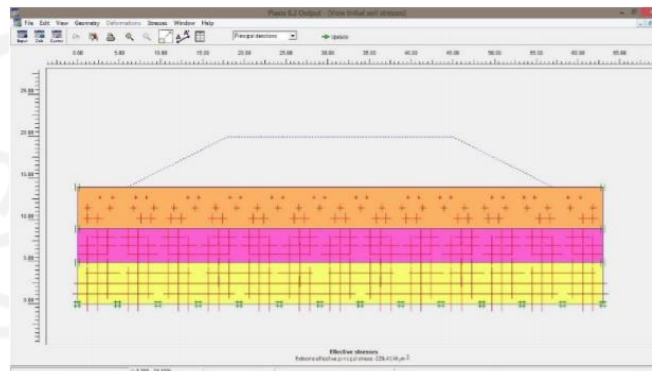


**Figure 4. 8 First Stress on Geometry**

- d.  Then click the Calculate.

#### 4.7.2 Plaxis Calculation

In calculation section (Figure 4.8) there are 4 tab sheets, namely generate, parameters, multipliers and preview. In the general tab sheet, in the calculation type, plastic analysis is selected which is used to determine the magnitude of the displacement from the conditions under review, phi/c reduction is selected to determine the effect of the earthquake, while in the parameters tab sheet, staged construction is selected for loading input.

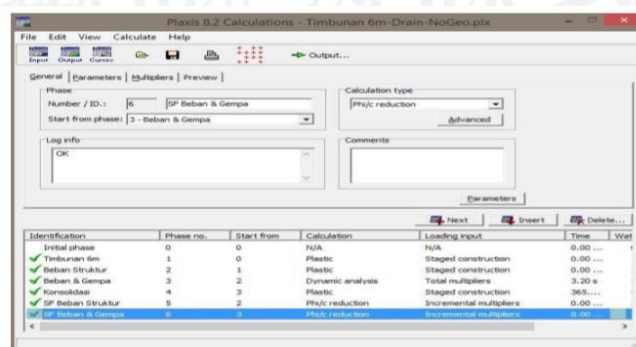


**Figure 4. 9 Calculations Window with Tab General Sheet**

The following step is to ascertain the point to be reviewed to describe in a curve view by clicking the select point for curve button as shown in Figure 4.10 below.

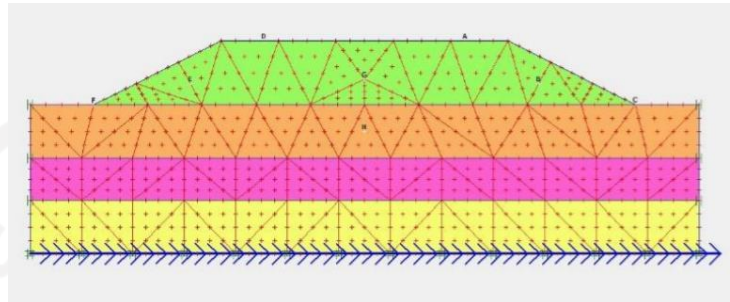


**Figure 4. 10 Selection of Curve Points Under Review**

#### 4.7.3 Plaxis Output

After the calculation and analysis stages are finished, then click the calculation button and to display the results of the calculation phase that has been carried out.

#### 4.8 Research Flowchart

Figures 4.11 below show the research flowchart or research flowchart and the slope modeling flowchart.

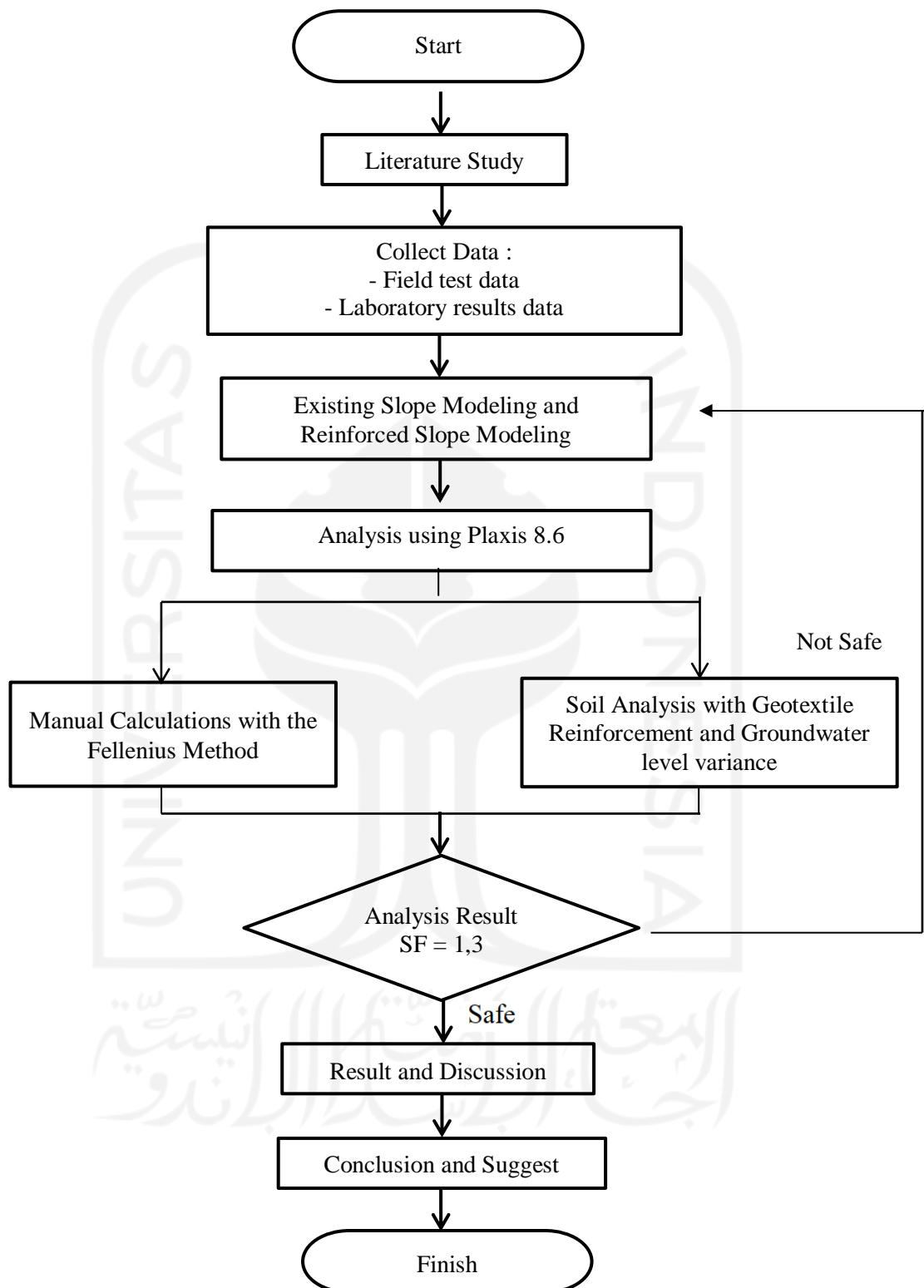


**Figure 4. 11 Flowchart of Final Project**

## **CHAPTER V**

### **ANALYSIS AND DISCUSSION**

#### **5.1 Analysis Overview**

The condition of the embankment slopes on the Cibitung – Cilincing toll road project at Sta 3+550 is the place for the case study to be conducted in this research. The site's soil is primarily made up of clay and silt, and the soil used is up to the third layer, which is located at a depth of 16 meters. Whereas compacted sandy loam is the soil used to build embankments. This analysis is done to assess whether there is a landslide on the slope at a specific embankment height. The embankment soil's inability to bear the forces generated by the load when the embankment is being built or used may be the reason for the collapse that results.

Varied embankment heights were analyzed to determine each layer of embankment that was safe against the loads that would occur. The state of the embankment will be evaluated in two conditions during construction and post-construction with different load parameters.

The structural load of the road surface during construction and the traffic load after construction are the load characteristics that are used. Additional geotextiles will be used for reinforcing on embankment slopes with safe numbers that don't fulfill safety standards. In order to determine whether extra geotextiles can survive potential landslides and improve the safety of road slope embankments, it is required to examine the use of reinforcement on risky embankment slopes.

The program used for slope modeling is Plaxis software 8.6. The output obtained from the modeling is knowing how much force may occur on the slope,



knowing the value of the slope safety number and how the slope is able to withstand the load.

## 5.2 Existing Embankment

### 5.2.1. Condition of Existing Embankment

Piles and land data that have been obtained can be illustrated into image forms. The existing conditions of the pile and the original soil type of each layer can be seen in Figure 5.1 below.

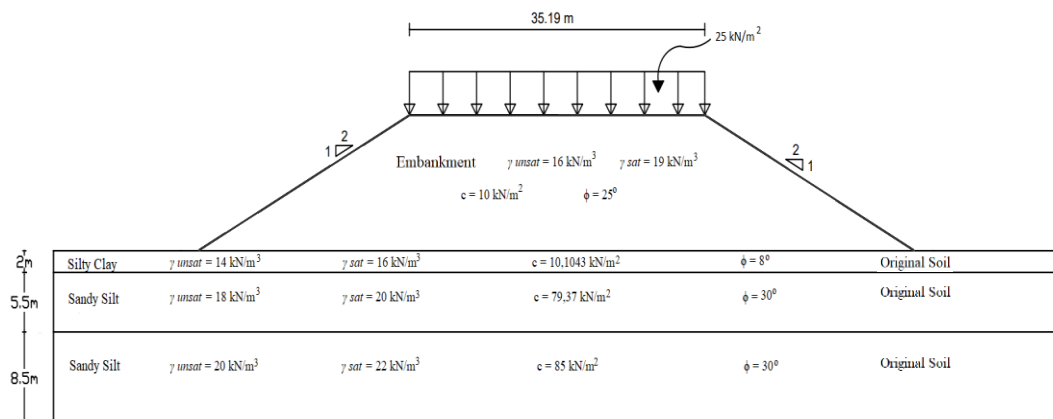


**Figure 5. 1 Geometry of the Existing Condition of the Initial Soil Slope.**

### 5.2.2. Analysis Using Plaxis Program

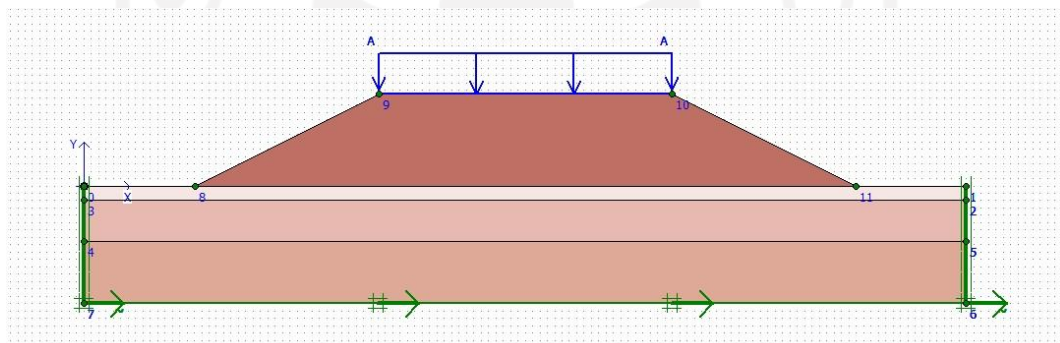
The embankment slopes with a height of 12.5m are the analysis output from the Plaxis 8.6 program that will be displayed in this analysis. The original soil, which consists of three layers of soil and is 16 meters deep, is above the embankment.

#### 1. Initial Slope Modelling

Slope modeling uses the original soil at the project site, as well as modeling dynamic earthquake loads and uniform loads. The width of the slope is 89.87 meters which will function as the Cibitung – Cilincing Sta. 3+550. The coordinate points that will be input into Plaxis 8.6 are presented in Table 5.1 and for slope modeling can be seen in Figure 5.2.

**Table 5.1 Existing Embankment Coordinates**

No.	X (m)	Y (m)	No.	X (m)	Y (m)
1	0	0	10	0	-7.5
2	120	0	11	15	0
3	120	-2	12	29.804	7.369
4	0	-2	13	31.804	7.369
5	0	-7,5	14	42.404	12.549
6	120	-7,5	15	77.596	12.549
7	120	-2	16	88.196	7.369
8	120	-16	17	90.196	7.369
9	0	-16	18	104.934	0

**Figure 5. 2 Modelling of Existing Embankment on Plaxis 8.6**

## 2. Analysis of Existing Embankment and Calculation

The original soil slope analysis in Plaxis 8.6 was carried out in 2 dimensions using traffic load. Figure 5.3 below shows the results of the finite element network (meshing) on the embankment slope.

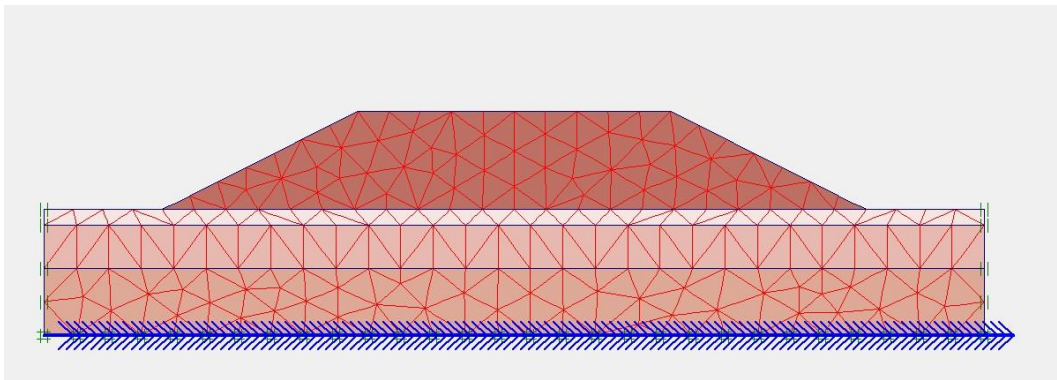


**Figure 5. 3 Meshing on Existing Embankment**

After the meshing is complete, it will continue with the initial conditions. In the project data obtained that the groundwater level is at a depth of 5 m from the original ground surface, then the process of generating water pressures is carried out according to the groundwater level. then move immediately to the computation of general initial stresses after finishing the initial geometric configuration.. The results of generating water pressures and initial soil stresses can be seen in Figure 5.4 below.

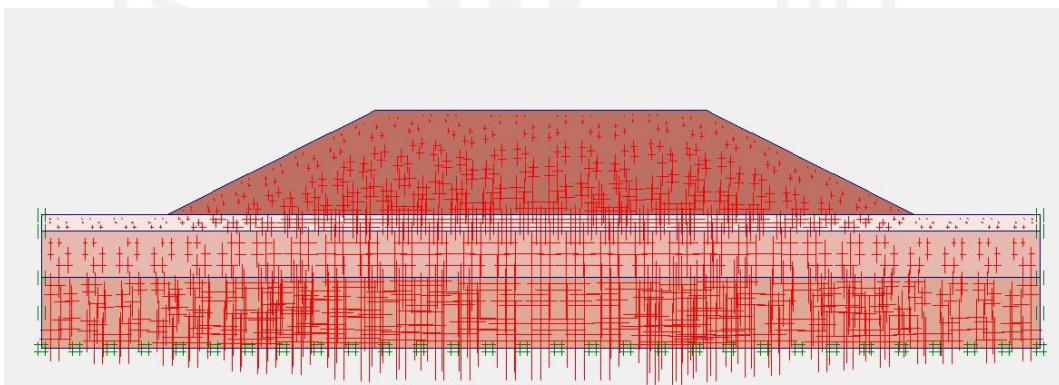


**Figure 5. 4 Initial Stresses on Existing Embankments**

To the next step, it enters the analysis calculation stage of the 12.5 m embankment slope. The first phase is an analysis of the calculation due to being given a 12.5m soil pile. The second stage is an analysis of the calculation due to being given a structural load on the surface of the embankment slope. The third stage is the calculation due to the existing earthquake load. The fourth stage is the calculation of the safe value due to structural loads, and the fifth stage is the calculation of the

safe number value due to loads and earthquakes. Then the sixth stage is the calculation of the consolidation of the decline. Figures 5.5 and 5.6 below show the outcomes of the distorted mesh on the 12.5m embankment.

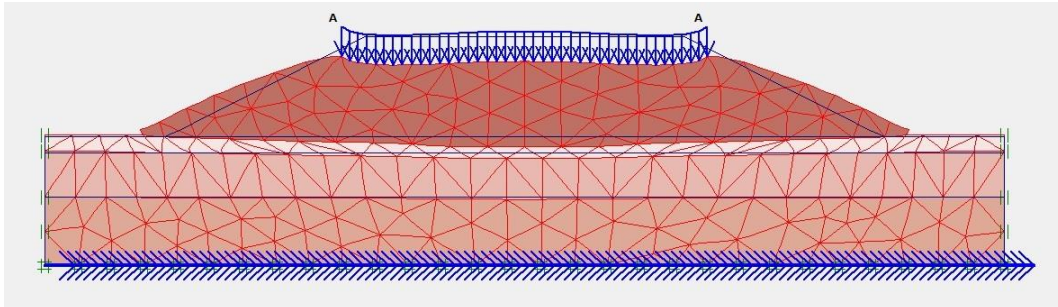


**Figure 5. 5 Deformed Mesh of Existing Embankment Due to Traffic Structure Load**

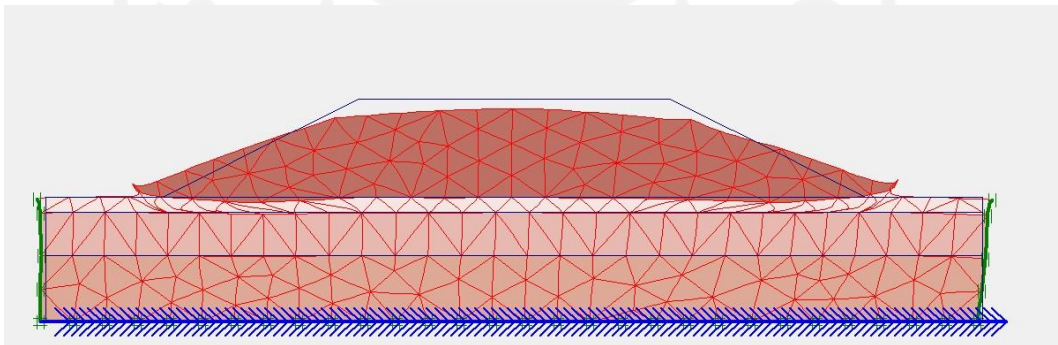


**Figure 5. 6 Deformed Mesh of Existing Embankment Due to Traffic and Earthquake Load**

Then for the total value of displacement on the original soil slope embankment 12.5 m due to traffic pavement loads has a value of  $71.66 \times 10^{-3}$  m, while the overall amount owed structural loads and earthquakes is obtained a value of  $117.17 \times 10^{-3}$  m. The displacement in total is depicted in Figures 5.7 and 5.8 below.



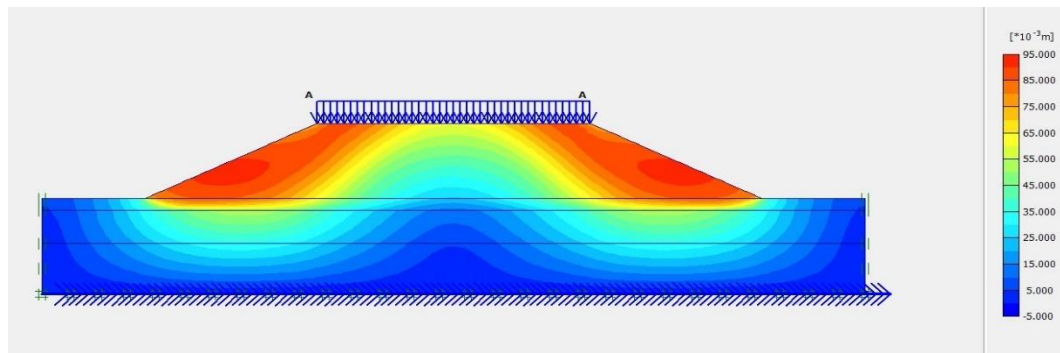


**Figure 5. 7 Total Displacement of Existing Embankment Due to Traffic Structure Load Total Displacement**

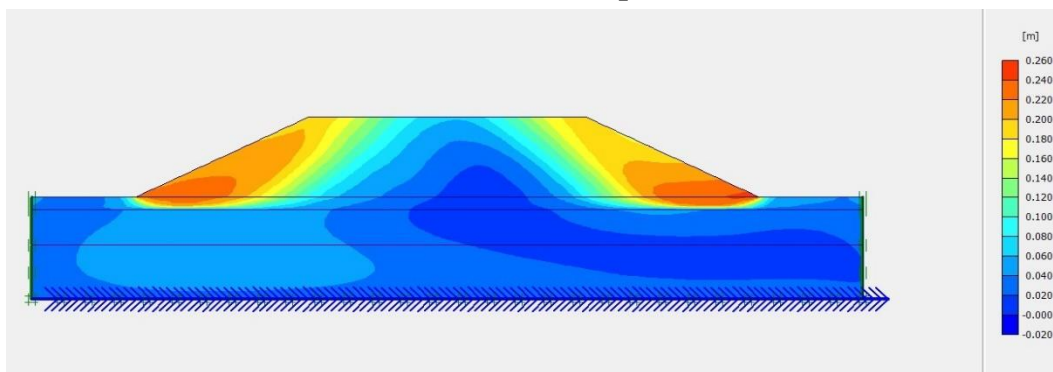


**Figure 5. 8 Total Displacement of Existing Embankment Due to Traffic and Earthquake Load**

Then for the direction of the original soil embankment when the traffic structure and earthquake loads are given. The direction of movement in embankment slope can be seen in the figures 5.9 and 5.10.

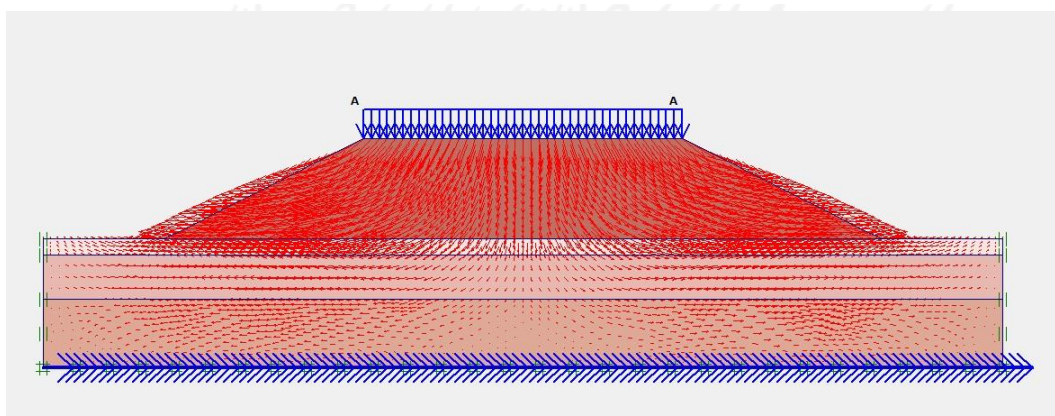


**Figure 5. 9 Direction Movement of Embankment Due to Traffic Structure Load**

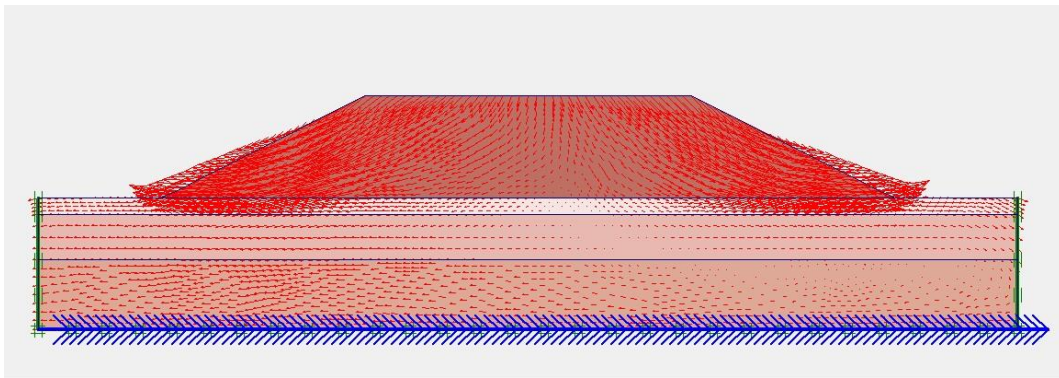


**Figure 5. 10 Direction Movement of Embankment Due to Traffic and Earthquake Load**

Figure 5.11 and 5.12 below show the possibility for a landslide on the initial soil slope embankment of 12.5 meter.

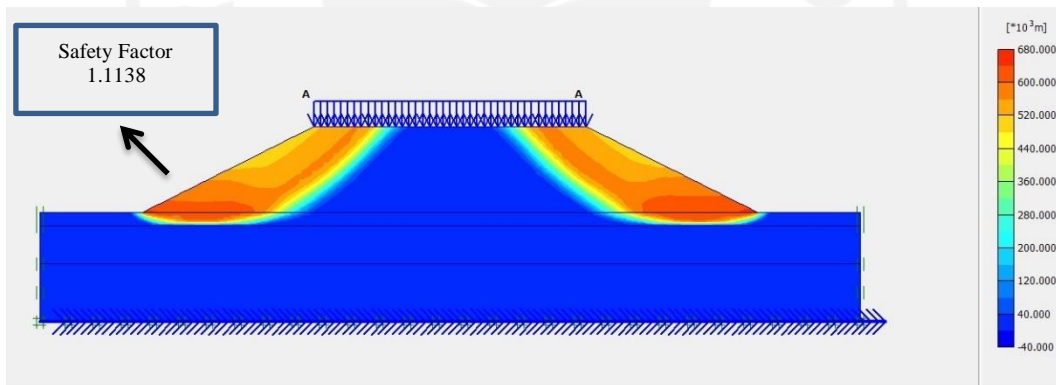


**Figure 5. 11 Potential Landslides of Embankment Due to Traffic Structure Load**

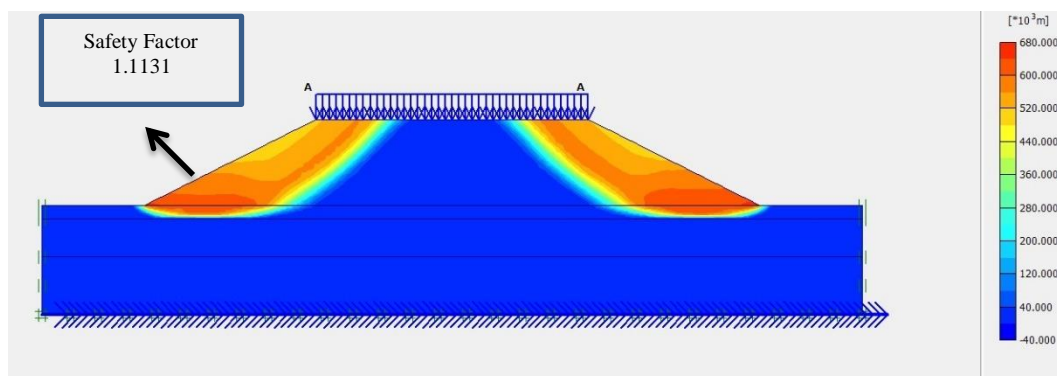


**Figure 5. 12 Potential Landslide of Embankment Due to Traffic Load and Earthquake Load**

Then for the value of effective stresses on the original soil slope embankment 12.5 m due to traffic structure loads has a value of  $-520.26 \text{ kN/m}^2$ , while due to traffic structure loads and earthquake loads it has a value of  $-522.74 \text{ kN/m}^2$ . Figure 5.13 and Figure 5.14 below show these outcomes.

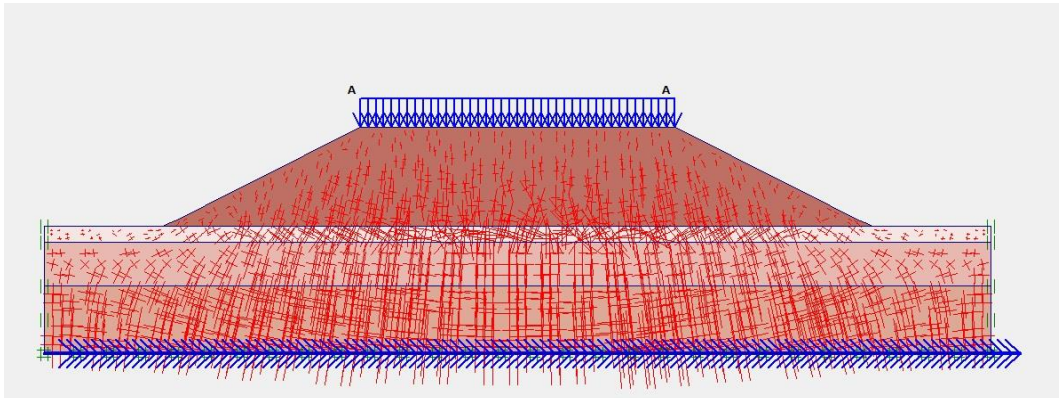


**Figure 5. 13 Effective Stresses of Existing Slope Embankment Due to Traffic Structure Load**

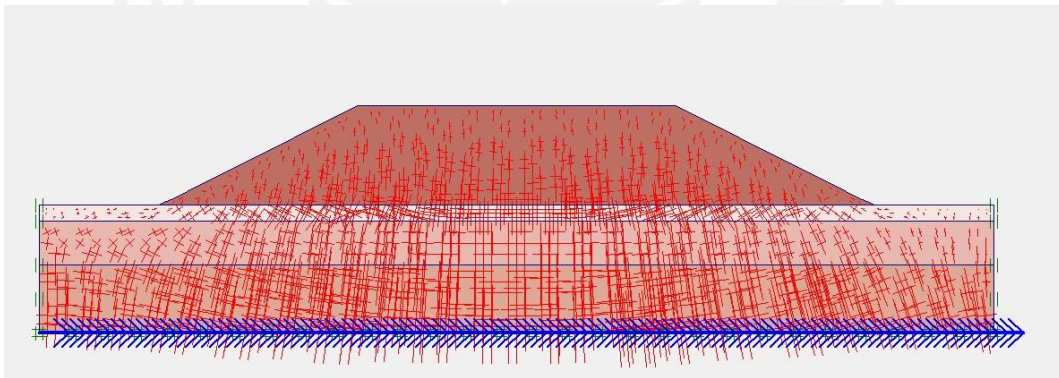


**Figure 5. 14 Effective Stresses of Existing Embankment Due to Traffic and Earthquake Load**

For the value of the safe number (SF) on the original soil slope embankment of 12.5 m without reinforcement due to traffic loads it has a value of 1.1138, while due to traffic loads and earthquake loads it has a value of 1.1131. The following Figure 5.15 shows the outcomes of the safe number values.





In the calculation using the Fellenius method, the landslide area is created from 11 slices. The total of whole length from the landslide plane (horizontal direction) = 31.89 m, then each slice will have a width of  $31.89/11 = 2.9$  m. The following is the calculation of slope stability using the Fellenius method.

1. Measuring the length of the landslide area that occurs in each pias (L)
2. Calculating the soil slice weight

$$W_i = \gamma \times A_i$$

The weight of the wedge that has a load on it can be calculated by the following formula.

$$W_i = (\gamma \times A_i) + (q \times L)$$

Where the magnitude of the road load ( $\text{kN/m}^2$ ) is the value of  $q$  and the width of the slice exposed to the load is the value of  $L$  (m).

An example of how to calculate the weight of the soil wedge from the initial slice and the final wedge for an unreinforced road can be seen in the calculation below. The results of the calculation of the weight of the slices from the beginning to the end can be seen in table 5.2 below.

$$W_1 = \gamma \times A_1 = ((16 \times 2,103) + (14 \times 0,815)) = 45,058 \text{ kN}$$

$$W_{11} = (\gamma \times A_1) + (q \times L) = (16 \times 7,484) + (25 \times 3,4) = 204,744 \text{ kN}$$

3. Below is a calculation to determine the size of the angle ( $\alpha$ ) and radians at each slice in the landslide plane. The recapitulation can be seen in the following table 5.2.

$$\begin{aligned} \text{Rad}_1 &= \alpha \times \frac{\pi}{180} \\ &= -10 \times \frac{\pi}{180} \\ &= -0.17453 \end{aligned}$$

$$\begin{aligned} \text{Rad}_{11} &= \alpha \times \frac{\pi}{180} \\ &= 50 \times \frac{\pi}{180} \\ &= 0.87266 \end{aligned}$$

4. For each pias it is necessary to calculate the value of  $W \sin \alpha$ . The recapitulation of the calculation results of  $W \sin \alpha$  for each pias can be seen in Table 5.2 below.

$$\begin{aligned}
 \text{Pias 1} &= W \times \sin \alpha \\
 &= 45.058 \times \sin (-10) \\
 &= -7.824 \text{ kN/m} \\
 \text{Pias 11} &= W \times \sin \alpha \\
 &= 204.744 \times \sin (50) \\
 &= 156.843 \text{ kN/m}
 \end{aligned}$$

5. For each pias it is necessary to calculate the value of  $W \cos \alpha$ . The recapitulation of the calculation results of  $W \cos \alpha$  for each pias can be seen in Table 5.2 below.

$$\begin{aligned}
 \text{Pias 1} &= W \times \cos \alpha \\
 &= 45.058 \times \cos (-10) \\
 &= 44.373 \text{ kN/m} \\
 \text{Pias 11} &= W \times \cos \alpha \\
 &= 204.744 \times \cos (50) \\
 &= 131.607 \text{ kN/m}
 \end{aligned}$$

The length of the curved line on layer 1 (A-B) is 22.72 meters, and the length of the curved line on layer 2 (B-C) is 13.71 meters, according to the measurements of the existing embankment geometry. Following the determination of the curved line's length, the following formula is used to determine the amount of sliding resistance used by the cohesion component.

$$\begin{aligned}
 \sum ciai &= (10 \times 22,72) + (10.1043 \times 13.71) \\
 &= 365.72995 \text{ kN}
 \end{aligned}$$

The value of the avalanche resistance by the friction component in the two layers is as follows.

$$\begin{aligned}
 W_i \cos \theta - U_i \times \tan \varphi &= (1471.4125 \times \tan(25)) + (812.36326 \times \tan(8)) \\
 &= 800.3012 \text{ kN}
 \end{aligned}$$

On the slopes of the road embankment there is a uniform load resulting from traffic loads and pavement loads of  $25 \text{ kN/m}^2$ . Then the moment resulting from the

uniform load is calculated as the moment that moves the soil. The calculation of the moment is as follows.

$$\begin{aligned} M_q &= (q \times A) \\ &= (25 \times 11,392) \\ &= 284.8 \text{ kN} \end{aligned}$$

The recapitulation of the results of manual calculations without groundwater values using the Fellenius method can be seen in Table 5.2 below.



**Table 5.2 Recapitulation of Calculations Using the Fellenius Method**

<b>Slice no</b>	<b>Soil Layer</b>	<b>A (<math>m^2</math>)</b>	<b>Weight <math>W_i</math> (kN)</b>	<b><math>\theta</math> (<math>^\circ</math>)</b>	<b>Radian</b>	<b><math>W_i \cos \theta_i</math> (kN)</b>	<b><math>W_i \sin \theta_i</math> (kN)</b>	<b><math>W_i \cos \theta - U_i = u_i \cdot a_i</math> (kN)</b>
1	1	2.103	29.442	-10	-0.17453	43.442	-7.6599	43.4428
	2	0.815	14.67					
2	1	6.305	88.27	-5	-0.08727	121.825	-10.658	121.8246
	2	1.89	34.02					
3	1	10.507	168.112	1	0.01745	198.238	3.4602	198.2378
	2	2.154	30.156					
4	1	14.709	235.344	6	0.10472	256.513	26.961	256.5131
	2	1.613	22.582					
5	1	11.922	190.752	11	0.19198	192.346	37.388	192.3459
	2	0.371	5.194					
6	1	19.748	315.968	16	0.27925	303.728	87.093	303.7279
7	1	18.726	299.616	21	0.36652	279.716	107.373	279.7156
8	1	19.078	305.248	27	0.47124	271.978	138.5796	271.9779
9	1	18.303	292.848	34	0.59341	242.782	163.758	242.7819
10	1	18.211	291.376	41	0.71558	241.602	210.021	241.6021
11	1	7.484	119.744	50	0.87266	131.607	156.843	131.6069
TOTAL						2283.775	913.159	

## 6. Calculations to determine the value of the safety factor (SF) at Sta. 3+550

The value of the safety factor or the number of safety on the original embankment slope by manual calculation using the Fellenius method is as follows.

$$\begin{aligned} \text{SF} &= \frac{(\sum ciai) + ((Wi \cos \theta - Ui) \times \tan \varphi)}{(Wi \sin \alpha) + (\text{Beban} \times \text{Luas})} \\ &= \frac{(365.7299 + 800.3012)}{(913.159001 + 284.8)} \\ &= 1.0147 \end{aligned}$$

The value of the safety factor generated by the unreinforced road using the Fellenius method manually calculated, which does not take into account the influence of the earthquake load, which is 1.0147. These results are not much different from the results of the analysis of the road without reinforcement and without earthquake loads using the Plaxis 8.6 program, which is 1.118.

### 5.4 Slope Reinforcement With Geotextile

According to Hardiyatmo (2008), geotextiles are sheet materials made of polymeric textile materials and are water-permeable, which can be in the form of non-woven, woven materials, which are used in contact with soil, rock or other geotechnical materials in Civil Engineering applications.

Geotextiles are generally made from the polymer polypropylene (some are made from polyester or polyethylene), which is made in the form of fibers or yarns, and finally used to make sheets of woven or non-woven fabrics. When this textile fabric is placed in the ground, it is called a geotextile.

In this final project, The used geotextile is of type UW-250 woven geotextile, which is produced by PT. Teknindo Superior Geosystems. The tensile strength value of the geotextile used is 52 kN/m and the strain value used is 20%.

#### 5.4.1 Geotextile Calculation Data

##### 1. Embankment Soil Parameter

- a. Soil volume weight ( $\gamma_b$ ) = 16 kN/m<sup>3</sup>
- b. Cohesion (c) = 10 kN/m<sup>3</sup>

- c. Inner friction angle ( $\phi$ ) = 25°
2. Geotextile
- a. Geotextile Type = UW-250 woven geotextile
- b. Ultimate Tensile Strength (Tu) = 52 kN/m
- c. Permit Tensile Strength (Ta) = 26 kN/m
3. Soil bearing capacity coefficient

The coefficient of soil bearing capacity can be seen in Table 5.3 below.

**Table 5.3 Coefficient of Soil Bearing Capacity**

$\phi$	$N_c$	$N_q$	$N_\gamma$	$\phi$	$N_c$	$N_q$	$N_\gamma$
10	8.85	2.47	1.22	26	22.25	11.85	12.54
11	8.80	2.71	1.44	27	23.94	13.20	14.47
12	9.28	2.97	1.69	28	25.80	14.72	16.72
13	9.81	3.26	1.97	29	27.86	16.44	19.34
14	10.37	3.59	2.29	30	30.14	18.40	22.40
15	10.98	3.94	2.65	31	32.67	20.63	25.90
16	11.63	4.34	3.06	32	35.49	23.18	30.22
17	12.34	4.77	3.53	33	38.64	26.09	35.19
18	13.10	5.26	4.07	34	42.16	29.44	41.06
19	13.93	5.80	4.68	35	46.12	33.30	48.03
20	14.83	6.40	5.39	36	50.59	37.75	56.31
21	15.82	7.07	6.20	37	55.63	42.92	66.19
22	16.88	7.82	7.13	38	61.35	48.93	78.03
23	18.05	8.66	8.20	39	67.87	55.96	92.25
24	19.32	9.60	9.44	40	75.31	64.20	109.41
25	20.72	10.66	10.8	41	83.86	73.90	130.22

Source: Ministry of Public Works (2009)

#### 5.4.2 External Stability

The slope must be stable against the effect of both internal and external



pressures while designing the embankment of the slope with geotextile reinforcement. External stability and internal stability will both be examined. The minimum vertical distance of the geotextile layer (SV) and the minimum length of the geotextile will both be determined using the external stability calculation (L).

The uniform load entered is 25 kN/m<sup>2</sup>, which is the maximum load under post-construction conditions. When determining the quantity of geotextile needed, the safety factor (SF) value to use as a guide is 1.5. In Figure 5.17 below, the forces that will affect the embankment slope are depicted.

1. Determine the minimum vertical distance between layers of geotextiles (SV)

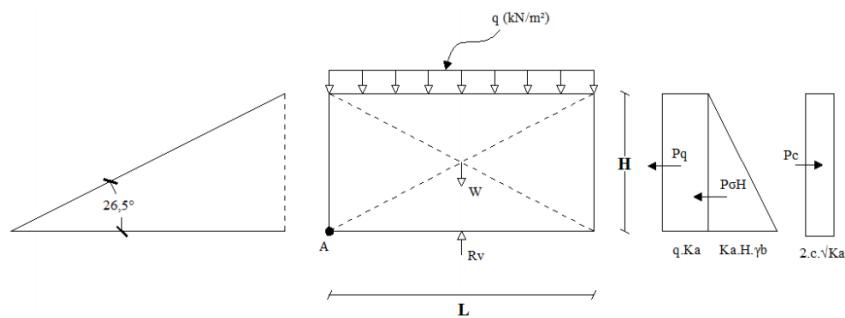


**Figure 5. 17 Forces Acting on Slope Pile**

Calculation of the active coefficient of the soil as follows.

$$K_a = \tan\left(45 - \frac{\varphi}{2}\right)$$

$$K_a = \tan\left(45 - \frac{25}{2}\right)$$

$$= 0,40586$$

- a. Minimum vertical distance of embankment geotextile (SV) layer 2m

$$\sigma_{hc} = (q \times K_a) + (K_a \times H \times \gamma_b) - (2 \times c \times \sqrt{K_a})$$

$$= (25 \times 0.40586) + (0.40586 \times 2 \times 16) - (2 \times 10 \times \sqrt{0.40586})$$

$$= 10.3925 \text{ kN/m}^2$$

$$SV = \frac{T_{all}}{\sigma_{hc} \times SF}$$

$$= \frac{26}{10.3925 \times 1.5}$$

$$= 1.668 \text{ m}$$

Field installed SV = 1 m (minimum)

Many layers of geotextile = 2m / 1m = 2 layers

- b. Minimum vertical direction distance of embankment geotextile (SV) layer 4m

$$\begin{aligned}\sigma_{hc} &= (q \times K_a) + (K_a \times H \times \gamma_b) - (2 \times c \times \sqrt{K_a}) \\ &= (25 \times 0.40586) + (0.40586 \times 4 \times 16) - (2 \times 10 \times \sqrt{0.40586}) \\ &= 23.38 \text{ kN/m}^2\end{aligned}$$

$$\begin{aligned}SV &= \frac{T_{all}}{\sigma_{hc} \times SF} \\ &= \frac{26}{23,38 \times 1,5} \\ &= 0.741 \text{ m}\end{aligned}$$

Field installed SV = 0.5 m (minimum)

Many layers of geotextile = 4m / 0.5m = 8 layers

- c. Minimum vertical distance of embankment geotextile (SV) layer 6m

$$\begin{aligned}\sigma_{hc} &= (q \times K_a) + (K_a \times H \times \gamma_b) - (2 \times c \times \sqrt{K_a}) \\ &= (25 \times 0.40586) + (0.40586 \times 6 \times 16) - (2 \times 10 \times \sqrt{0.40586}) \\ &= 36.3675 \text{ kN/m}^2\end{aligned}$$

$$\begin{aligned}SV &= \frac{T_{all}}{\sigma_{hc} \times SF} \\ &= \frac{26}{36.3675 \times 1.5} \\ &= 0.477 \text{ m}\end{aligned}$$

Field installed SV = 0.5 m (minimum)

Many layers of geotextile = 6m / 0.5m = 12 layers

- d. Minimum vertical distance of embankment geotextile layer (SV) 8m

$$\begin{aligned}\sigma_{hc} &= (q \times K_a) + (K_a \times H \times \gamma_b) - (2 \times c \times \sqrt{K_a}) \\ &= (25 \times 0.40586) + (0.40586 \times 8 \times 16) - (2 \times 10 \times \sqrt{0.40586})\end{aligned}$$

$$\begin{aligned}
 &= 49.355 \text{ kN/m}^2 \\
 SV &= \frac{T_{all}}{\sigma_{hc} \times SF} \\
 &= \frac{26}{49.355 \times 1.5} \\
 &= 0.351 \text{ m}
 \end{aligned}$$

Field installed SV = 0.5 m (minimum)

Many layers of geotextile = 8m / 0.5m = 16 layers

Minimum vertical distance of embankment geotextile (SV) layer  
10m

$$\begin{aligned}
 \sigma_{hc} &= (q \times K_a) + (K_a \times H \times \gamma_b) - (2 \times c \times \sqrt{K_a}) \\
 &= (25 \times 0.40586) + (0.40586 \times 10 \times 16) - (2 \times 10 \times \sqrt{0.40586}) \\
 &= 62.342 \text{ kN/m}^2
 \end{aligned}$$

$$\begin{aligned}
 SV &= \frac{T_{all}}{\sigma_{hc} \times SF} \\
 &= \frac{26}{62,342 \times 1,5} \\
 &= 0.278 \text{ m}
 \end{aligned}$$

Field installed SV = 0.5 m (minimum)

Many layers of geotextile = 10m / 0.5m = 20 layers

- e. Minimum vertical direction distance of embankment geotextile (SV)  
layer 12.5m

$$\begin{aligned}
 \sigma_{hc} &= (q \times K_a) + (K_a \times H \times \gamma_b) - (2 \times c \times \sqrt{K_a}) \\
 &= (25 \times 0.40586) + (0.40586 \times 12,5 \times 16) - (2 \times 10 \times \sqrt{0.40586}) \\
 &= 78.577 \text{ kN/m}^2
 \end{aligned}$$

$$\begin{aligned}
 SV &= \frac{T_{all}}{\sigma_{hc} \times SF} \\
 &= \frac{26}{78,577 \times 1,5} \\
 &= 0.221 \text{ m}
 \end{aligned}$$

Field installed SV = 0.5 m (minimum)

Many layers of geotextile =  $12.5\text{m} / 0.5\text{m} = 25$  layers

## 2. Determining the length of the geotextile

### a. Stability against rolling

$$SF = \frac{\sum MR}{\sum MD} = \frac{\text{Holding Moment}}{\text{Rolling Moment}} \geq 1,5$$

$$\begin{aligned} \sum MD &= \left( q \times Ka \times \frac{1}{2} \times H^2 \right) + \left( \frac{1}{2} \times Ka \times \gamma b \times H^2 \times \frac{1}{3} \times H \right) \\ &\quad - \left( 2 \times c \times \sqrt{Ka} \times \frac{1}{2} \times H^2 \right) \end{aligned}$$

$$\sum MR = \left( \frac{1}{2} \times q \times L^2 \right) + \left( \frac{1}{2} \times \gamma b \times H \times L^2 \right)$$

$$SF = \frac{\left( \frac{1}{2} \times 25 \times L^2 \right) + \left( \frac{1}{2} \times 16 \times 12,5 \times L^2 \right)}{(25 \times 0,4058 \times 12,5^2) + \left( \frac{1}{2} \times 0,4058 \times 16 \times 12,5^2 \times \frac{1}{3} \times 12,5 \right) - (2 \times 10 \times \sqrt{0,4058} \times \frac{1}{2} \times 12,5^2)}$$

$$SF = \left( \frac{112,5 \times L^2}{1911,12} \right)$$

$$L^2 = \frac{1911,12 \times 1,5}{112,4\sqrt{5}} = 25.4816 \text{ m}$$

$$L = 5.04793 \text{ m}$$

The length of the geotextile to resist overturning on the soil heap taken is 5 m.

### b. Stability over the shear

$$SF = \frac{(q \times \tan \delta \times L) + (H \times \gamma b \times \tan \delta \times L)}{(q \times Ka \times H) + (0,5 \times Ka \times \gamma b \times H^2) - (2 \times c \times \sqrt{Ka} \times H)}$$

Shear resistance at the base of the reinforcement ( $\delta = 2/3 \times 25 = 16.667$ )

$$SF = \frac{(25 \times \tan(16,667) \times L) + (12,5 \times 16 \times \tan(16,667) \times L)}{(25 \times 0,4058 \times 12,5) + (0,5 \times 0,4058 \times 16 \times 12,5^2) - (2 \times 10 \times \sqrt{0,4058} \times 12,5)}$$

$$SF = \frac{67,3606 \times L}{474,886}$$

$$L = \frac{474,886 \times 1,5}{67,3606} = 10.5749 \text{ m}$$

The length of the geotextile to resist shear in the soil embankment is taken as long as 11 m.

- c. Stability over the eccentricity

$$\frac{1}{6} x L \geq e$$

$$E = \frac{\sum MD}{Rv} = \frac{(q x Ka x \frac{1}{2} x H^2) + (\frac{1}{2} x Ka x \gamma b x H^2 x \frac{1}{3} x H) - (2 x c x \sqrt{Ka} x \frac{1}{2} x H^2)}{(H x \gamma b x L) + (q x L)}$$

$$\frac{L}{6} \geq \frac{1911,12}{(12,5 x 16 x L) + (25 x L)}$$

$$\frac{L}{6} \geq \frac{1911,12}{225 x L}$$

$$L^2 = 50.9631 \text{ m}$$

$$L = 7.13885 \text{ m}$$

The length of the geotextile to resist eccentricity in the soil embankment is taken as long as 7 m.

- d. Stability to bearing capacity of soil

$$Nc = 20,72$$

$$N\gamma = 10,8$$

$$L \leq \frac{\sigma_{ult}}{(H x \gamma b) + q}$$

$$\sigma_{ult} = [(c x Nc) + (0,5 x L x \gamma b x N\gamma)] x SF$$

$$\sigma_{ult} = [(10 x 20,72) + (0,5 x L x 16 x 10 x 10,8)] x 1,5$$

$$\sigma_{ult} = 310,8 + (129,6 x L)$$

$$L \leq \frac{310,8 + (129,6 x L)}{(12,5 x 16) + 25}$$

$$225,8 L \leq 310,8 + (129,6 x L)$$

$$L = \frac{310,8}{225,8 - 129,6}$$

$$L = 3.23077 \text{ m}$$

The length of the geotextile to withstand the bearing capacity of the soil on the soil embankment is taken as long as 3 m.

Of the four types of soil slope stability parameters above, the maximum length of the geotextile used is 11 m. The length of

geotextile requirements for slopes with other embankment heights can be seen in Table 5.4 below.

**Table 5.4 Recapitulation of Geotextile Length Requirements**

Embankment Height (H)	Stability of Roll	Stability of Shear	Stability of Eccentricity	Bearing Capacity Stability	Minimum length (L)
2 m	0.427	0.685	0.604	-4.28	1
4 m	1.278	2.340	1.808	-7.655	3
6 m	2.153	4.195	3.045	-36.1	5
8 m	3.039	6.125	4.298	13.282	7
10 m	3.930	8.091	5.558	5.610	9
12.5 m	5.047	10.57	7.138	3.230	11

### 5.4.3 Internal Stability

#### 1. Geotextile overlapping length

##### a. 2m embankment

$$L_o = \frac{\sigma_{hc} \times SV \times SF}{2 \times \gamma b \times H \times \tan \varphi}$$

$$L_o = \frac{10,393 \times 1 \times 1,5}{2 \times 16 \times 2 \times \tan 25} = 0.522 \text{ m}$$

Because the minimum overlapping length is 1 meter, the length taken is 1 m.

##### b. 4m embankment

$$L_o = \frac{\sigma_{hc} \times SV \times SF}{2 \times \gamma b \times H \times \tan \varphi}$$

$$L_o = \frac{10,393 \times 0,5 \times 1,5}{2 \times 16 \times 4 \times \tan 25} = 0.293 \text{ m}$$

Because the minimum overlapping length is 1 meter, the length taken is 1 m.

##### c. 6m embankment

$$L_o = \frac{\sigma_{hc} \times SV \times SF}{2 \times \gamma b \times H \times \tan \varphi}$$

$$L_o = \frac{10,393 \times 0,5 \times 1,5}{2 \times 16 \times 6 \times \tan 25} = 0.3046 \text{ m}$$

Because the minimum overlapping length is 1 meter, the length taken is 1 m.

d. 8m embankment

$$L_o = \frac{\sigma_{hc} \times SV \times SF}{2 \times \gamma b \times H \times \tan \varphi}$$

$$L_o = \frac{10,393 \times 0,5 \times 1,5}{2 \times 16 \times 8 \times \tan 25} = 0.3100 \text{ m}$$

Because the minimum overlapping length is 1 meter, the length taken is 1 m.

e. 10m embankment

$$L_o = \frac{\sigma_{hc} \times SV \times SF}{2 \times \gamma b \times H \times \tan \varphi}$$

$$L_o = \frac{10,393 \times 0,5 \times 1,5}{2 \times 16 \times 10 \times \tan 25} = 0.3133 \text{ m}$$

Because the minimum overlapping length is 1 meter, the length taken is 1 m.

f. 12,5m embankment

$$L_o = \frac{\sigma_{hc} \times SV \times SF}{2 \times \gamma b \times H \times \tan \varphi}$$

$$L_o = \frac{10,393 \times 0,5 \times 1,5}{2 \times 16 \times 12,5 \times \tan 25} = 0.3160 \text{ m}$$

Because the minimum overlapping length is 1 meter, the length taken is 1 m.

2. The Effectiveness Length of Geotextile

a. 2m embankment

$$L_e = \frac{SF \times SV \times K_a \times \gamma b \times H}{2 \times \gamma b \times H \times \tan \varphi}$$

$$L_e = \frac{1,5 \times 1 \times 0,4058 \times 16 \times 2}{2 \times 16 \times 2 \times \tan 25} = 0.6 \text{ m}$$

The effective length that used is 0,5 m.

b. 4m embankment

$$L_e = \frac{SF \times SV \times K_a \times \gamma b \times H}{2 \times \gamma b \times H \times \tan \varphi}$$

$$Le = \frac{1,5 \times 1 \times 0,4058 \times 16 \times 2}{2 \times 16 \times 4 \times \tan 25} = 0,33 \text{ m}$$

The effective length that used is 0,5 m.

c. 6m embankment

$$Le = \frac{SF \times SV \times Ka \times \gamma b \times H}{2 \times \gamma b \times H \times \tan \varphi}$$

$$Le = \frac{1,5 \times 1 \times 0,4058 \times 16 \times 2}{2 \times 16 \times 6 \times \tan 25} = 0,33 \text{ m}$$

The effective length that used is 0,5 m.

d. 8m embankment

$$Le = \frac{SF \times SV \times Ka \times \gamma b \times H}{2 \times \gamma b \times H \times \tan \varphi}$$

$$Le = \frac{1,5 \times 1 \times 0,4058 \times 16 \times 2}{2 \times 16 \times 8 \times \tan 25} = 0,33 \text{ m}$$

The effective length that used is 0,5 m.

e. 10m embankment

$$Le = \frac{SF \times SV \times Ka \times \gamma b \times H}{2 \times \gamma b \times H \times \tan \varphi}$$

$$Le = \frac{1,5 \times 1 \times 0,4058 \times 16 \times 2}{2 \times 16 \times 10 \times \tan 25} = 0,33 \text{ m}$$

The effective length that used is 0,5 m.

f. 12,5m embankment

$$Le = \frac{SF \times SV \times Ka \times \gamma b \times H}{2 \times \gamma b \times H \times \tan \varphi}$$

$$Le = \frac{1,5 \times 1 \times 0,4058 \times 16 \times 2}{2 \times 16 \times 12,5 \times \tan 25} = 0,33 \text{ m}$$

The effective length that used is 0,5 m.

#### 5.4.4 Soil-Geotextile Tensile Force Check

The working shear stress is calculated to see if the chosen geotextile can sustain the tensile tension that results from an SV value of 0.5 m. Figure 5.18 below shows the friction transmission between soil and geotextile.



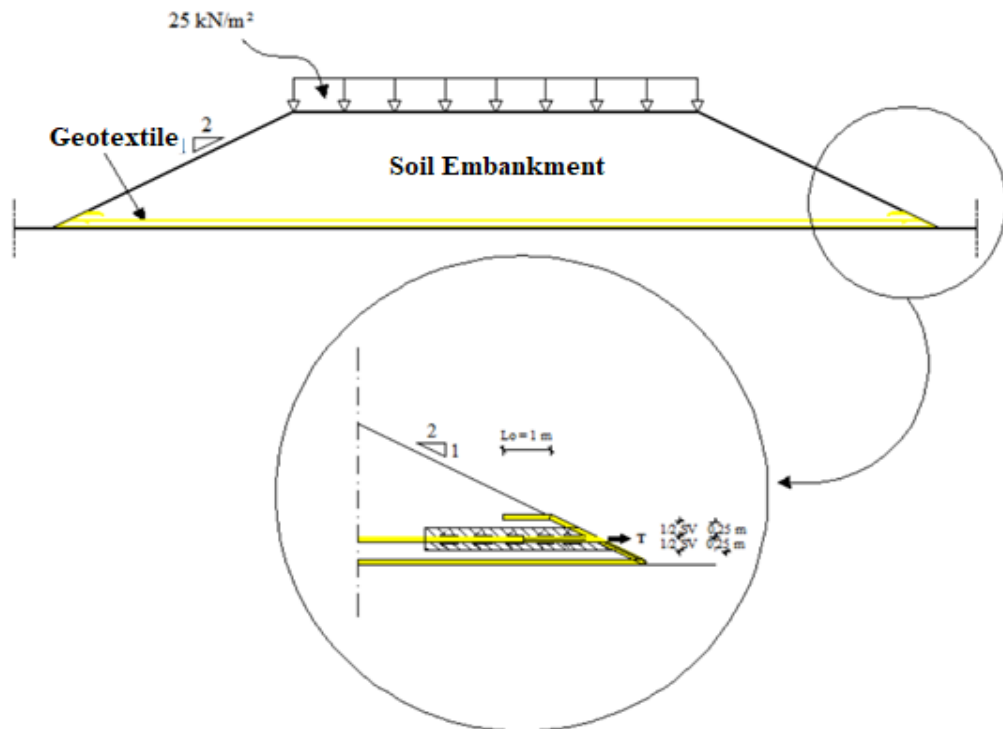


**Figure 5. 18 Soil-Geotextile Friction Transfer**

The geotextile will stiffen and transfer the stress to the passive area when it gets a load from above (soil). Therefore, the geotextile needs to be strong enough to resist the tensile forces exerted on it. Consequently, it is essential to check the tensile force and design a geotextile type that can withstand the tensile force. The following equation can be used to calculate the tensile force exerted on the geotextile.

$$\begin{aligned}
 T &= \tan \varphi \times 2 \times \sigma_n \times b \times L \\
 &= \tan(25) \times 2 \times \left( \frac{1}{2} \times 0,5 \times 16 \right) \times 1 \times 11 \\
 &= 41.035 \text{ kN}
 \end{aligned}$$

Given that the type of geotextile utilized has a tensile strength of 52 kN/m, the tensile force exerted above on the geotextile is calculated to be 41.035 kN. Since  $52 \text{ kN/m} > 41.035 \text{ kN}$ , the geotextile's strength is sufficient to withstand the tensile forces at work (safe).

## 5.5 Slope Modelling with Geotextile Reinforcement

Analysis modeling of natural soil slope embankment with additional geotextile reinforcement is carried out by analyzing the same geometric conditions and in accordance with the calculation of needs

### 1. Initial slope modeling

preliminary modeling of the same geometry original soil embankment slopes on an unreinforced 12.5m embankment. Laying down geotextiles horizontally with an SV of 0.5 meters and a 1 meter overlap. Assuming that the length has achieved the minimum total length of the geotextile requirement calculation, the total length of the geotextile is used along the slope at the bottom. Table 5.5 lists the coordinate points entered into Plaxis 8.6, and Figure 5.19 below shows the slope modeling coordinate points.

**Table 5.5 Slope Coordinates**

No.	X (m)	Y (m)	No.	X (m)	Y (m)
1	0	0	11	0	-7.5
2	120	0	12	15	0
3	120	-2	13	29.804	7.369
4	0	-2	14	31.804	7.369
5	0	-7,5	15	42.404	12.549
6	120	-7,5	16	77.596	12.549
7	120	-2	17	88.196	7.369
8	120	-16	18	90.196	7.369
9	0	-16	19	104.20	0
10	15	0	20	102.20	0.5
11	16	0.5	21	103.20	0.5
12	17	0.5	22	104.20	0

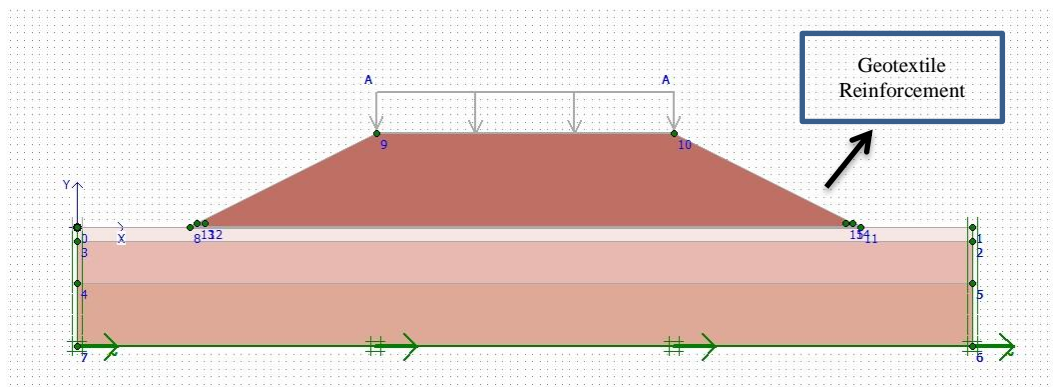


**Figure 5. 19 Modeling of Reinforced 12.5m Soil Embankment Slope**

2. Calculation Analysis of Reinforced Soil Embankment Slope

The soil slope analysis in Plaxis 8.6 was carried out in 2 dimensions using traffic load. Figure 5.20 below shows the results of the finite element network (meshing) on the embankment slope.

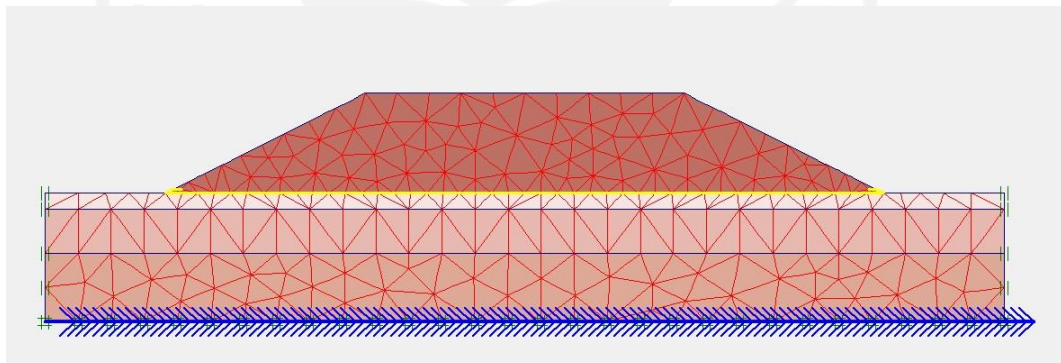


**Figure 5. 20 Meshing on Reinforced 12.5m Soil Embankment Slope**

The process of the initial soil stresses is carried out by generating again because the initial soil conditions for post-construction have been filled in as high as 12.5 m and the geotextile reinforcement has been completed. And actively installed. The results of the initial soil stresses process can be seen in Figure 5.21 below.

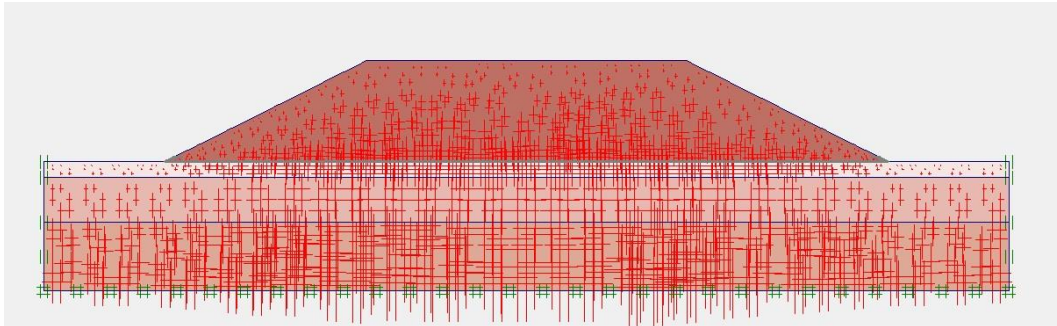


**Figure 5. 21 Initial Soil Stress On The Slope of 12.5m Embankment with Reinforcement.**

Then for the next analysis is an analysis of the original soil calculation with reinforcement. The results can be seen in Figure 5.22 and Figure 5.23 below.

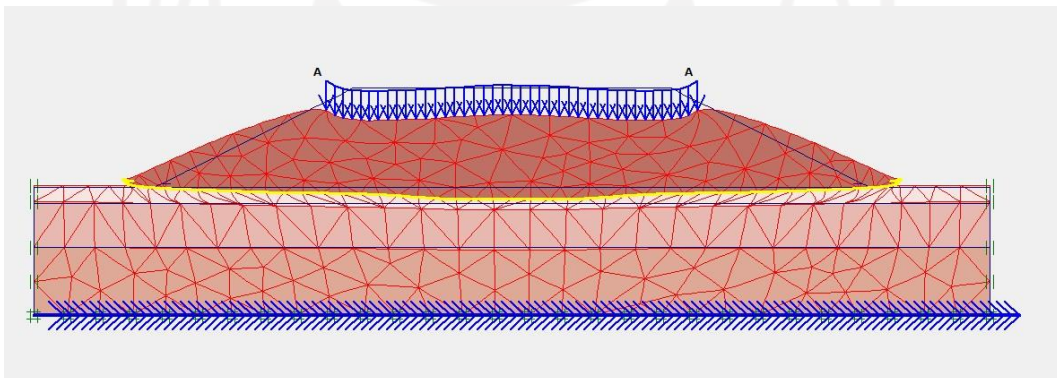


**Figure 5. 22 Deformed Mesh 12.5m Slope Embankment Due to Traffic Loads**

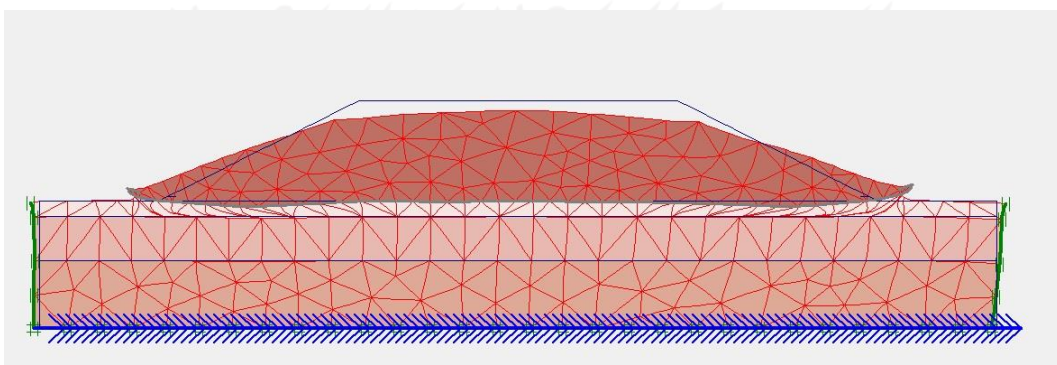


**Figure 5. 23 Deformed Mesh Slope 12.5m Embankment Due to Traffic and Earthquake Loads**

The results of the total displacement values that occur on slope embankments with a traffic load of  $83.25 \times 10^{-3}$  m, while on slope embankments with traffic loads and earthquakes are  $132.94 \times 10^{-3}$  m. The results of the complete displacement that took place are depicted in the following figures, 5.24 and 5.25.

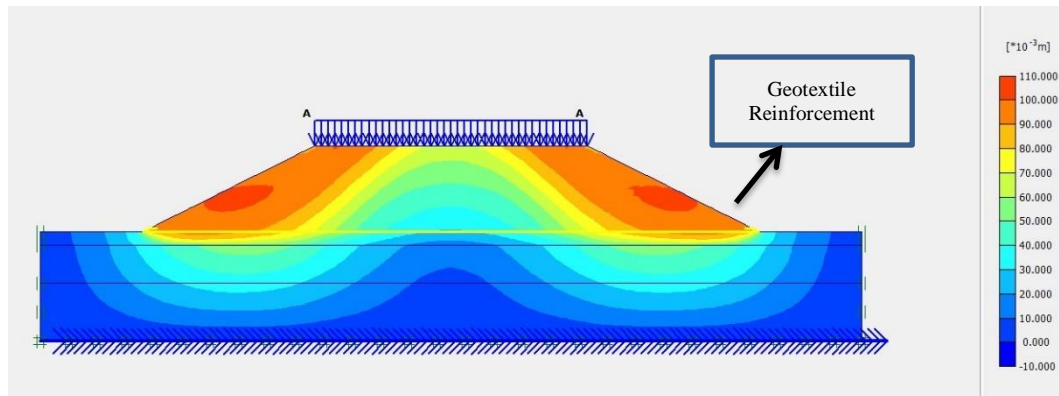


**Figure 5. 24 Total Displacement of 12.5m Embankment Slope Due to Traffic Load**

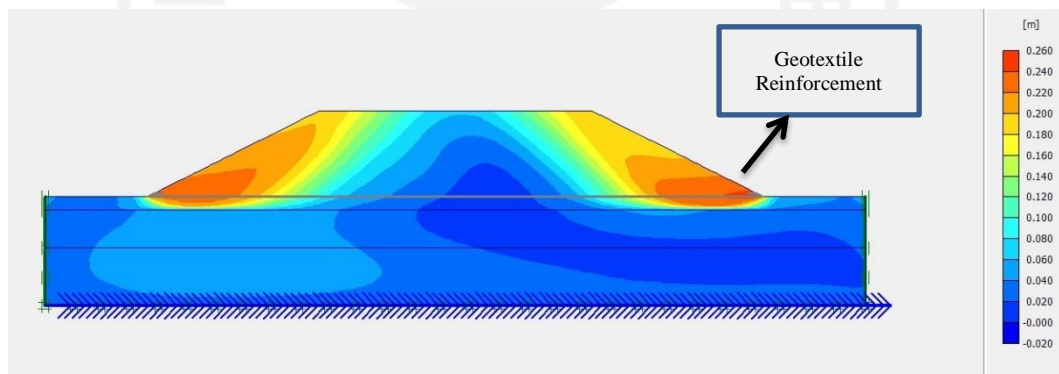


**Figure 5. 25 Total Displacement of 12.5m Embankment Slope Due to Traffic Load and Earthquake Load**

Figures 5.26 and 5.27 below show the direction of movement that takes place on the 12.5m slope embankment.



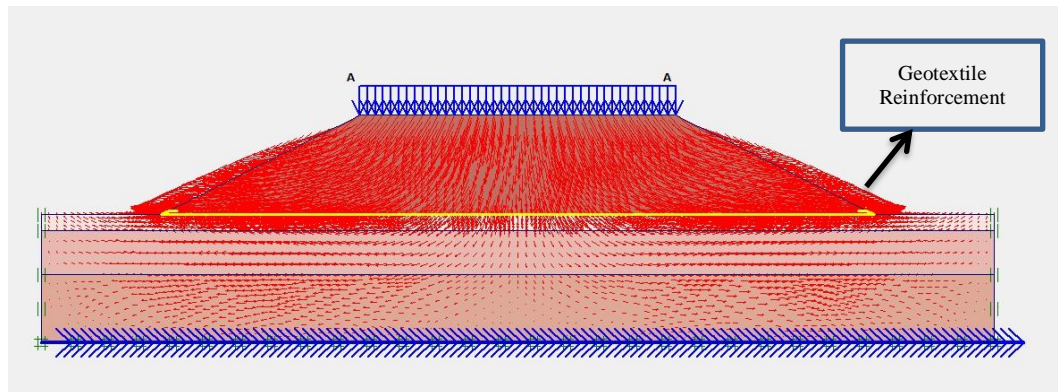


**Figure 5. 26 Direction of Movement of 12.5m Earth Piled Slope Due to Traffic Load**

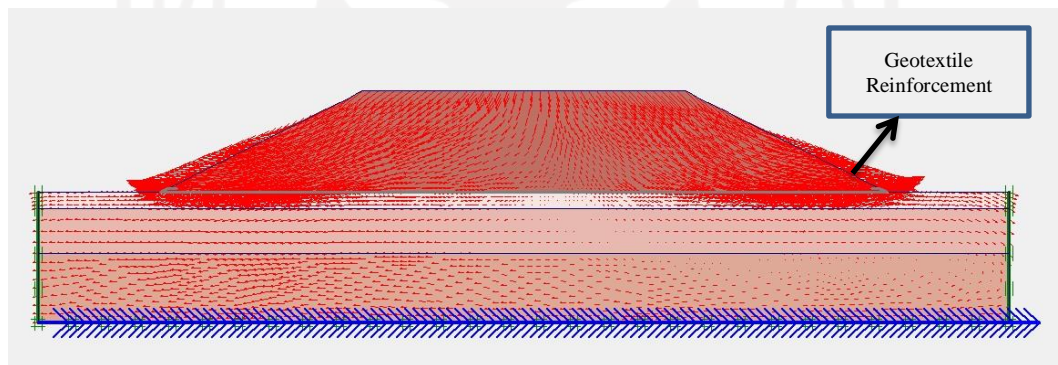


**Figure 5. 27 Direction of Movement of 12.5m Earth Piled Slope Due to Traffic and Earthquake Load**

Figures 5.28 and 5.29 below show the occurrence of landslides as a result of traffic loads and earthquake loads that occur.

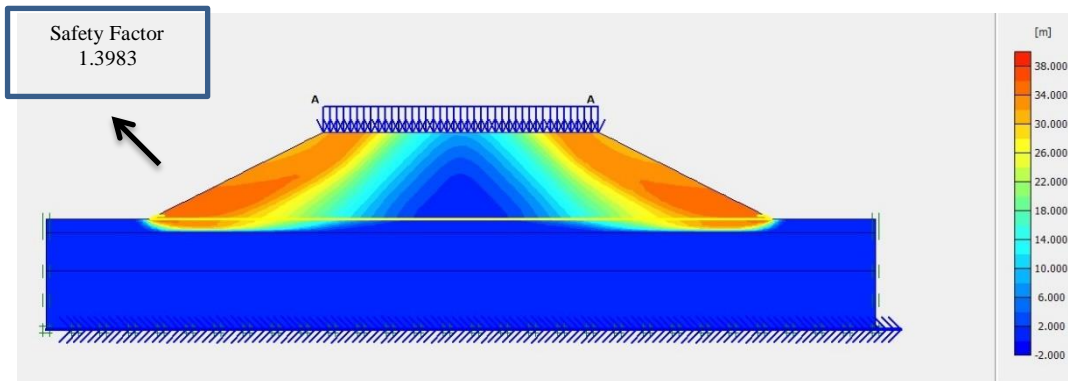


**Figure 5. 28 Potential for Landslide of 12.5m Embankment Slope Due to Traffic Load**

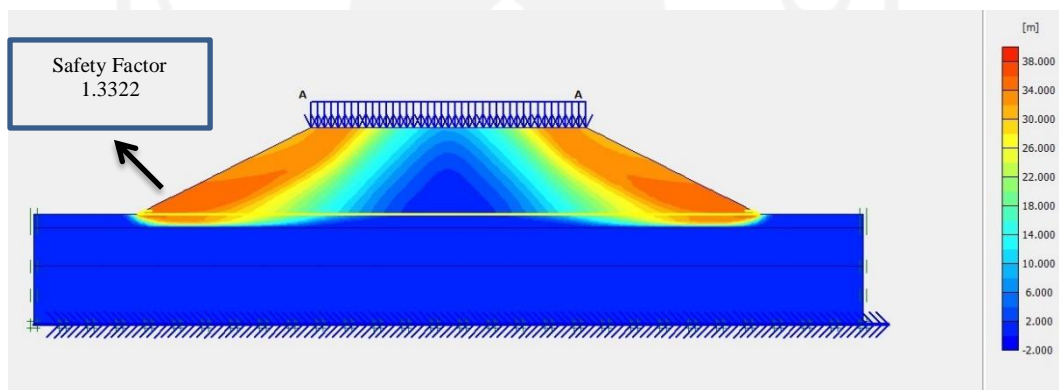


**Figure 5. 29 Potential for Landslide of 12.5m Embankment Slope Due to Traffic and Earthquake Load**

The effective stresses caused by traffic loads on the 12.5 m embankment slope are  $-515.53 \text{ kN/m}^2$ , whereas the effective stresses caused by loads and earthquakes are  $-515.93 \text{ kN/m}^2$ . These calculations' outcomes are depicted in the following Figures 5.30 and 5.31.



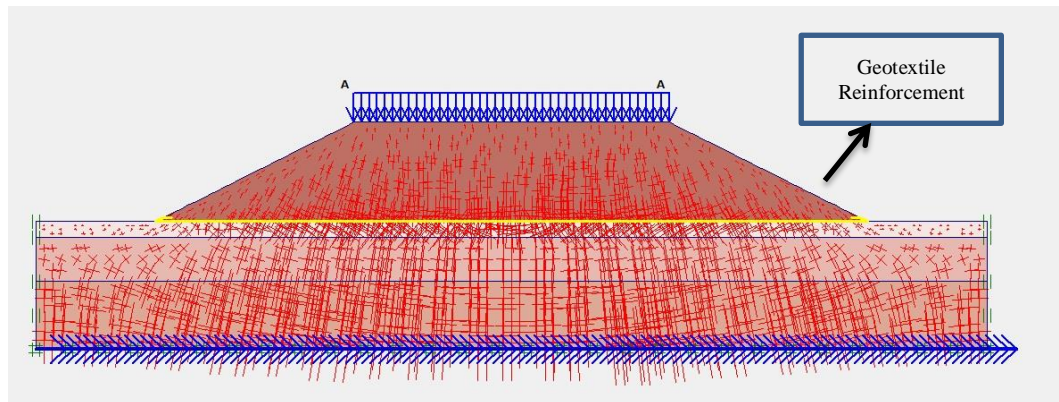


**Figure 5. 30 Effective Stresses 12.5m Embankment Slope Due to Traffic Loads**

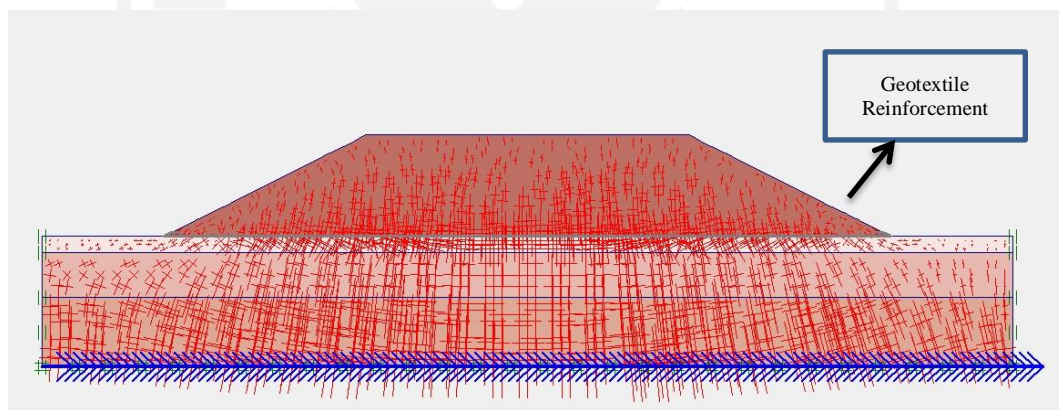


**Figure 5. 31 Effective Stresses 12.5m Embankment Slope Due to Traffic and Earthquake Loads**

The results of the safe number value of the 12.5m embankment slope were obtained from the results of the analysis due to traffic loads of 1.3983 while the safe number values due to traffic loads and earthquakes were 1.3322. The value of the safe number can be seen in the following curve in Figure 5.32.

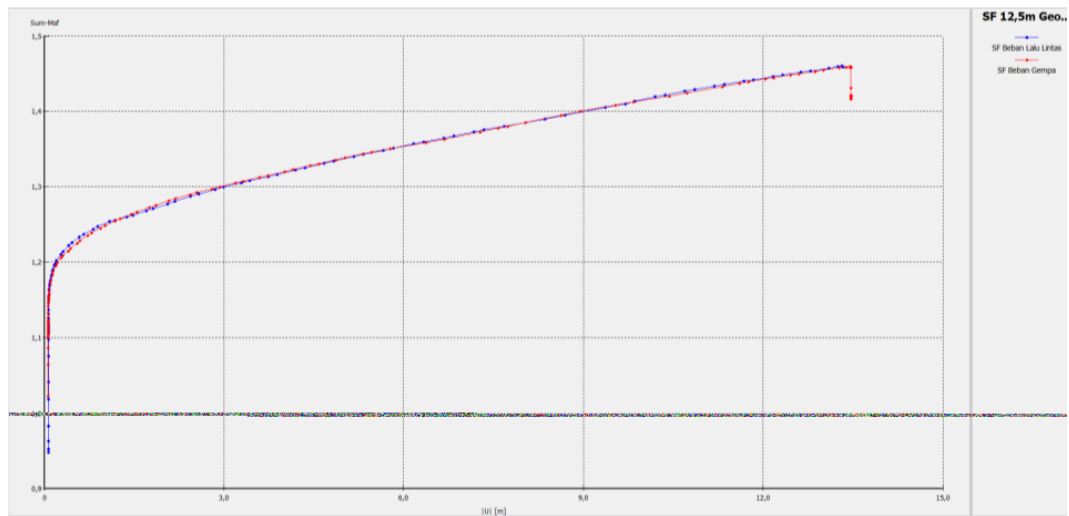


**Figure 5. 32 SF Curve Slope 12.5m Soil**

## **5.6 Results of Slope Modeling with Geotextile Reinforcement in Groundwater Level Variations**

The results of the modeling in Plaxis 8.6 on slopes with variations in groundwater level of 6 meters, 4 meters, 3 meters and 0 meters are as follows.

### **1. Groundwater level 6 meter**

For the deformation mesh results without vehicle loads and earthquakes, see Figure 5.33. The results of the deformation mesh with vehicle and earthquake loads are shown in Figure 5.34.

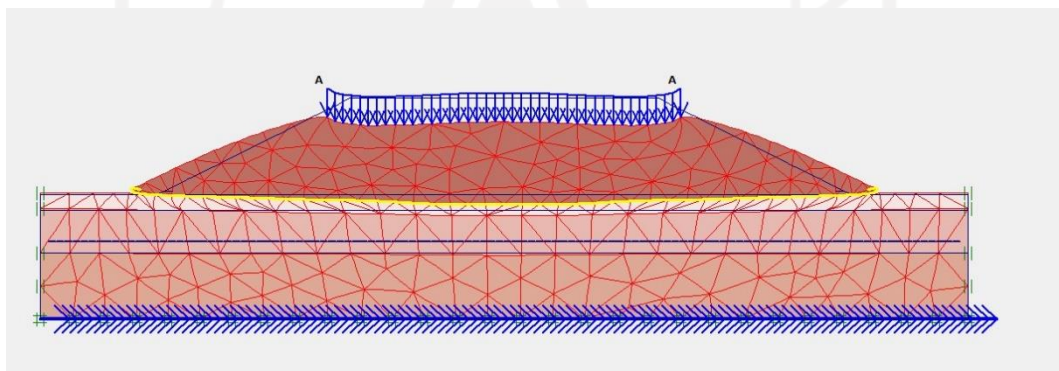


**Figure 5. 33 Deformed Mesh on Slopes with Geotextile Reinforcement Due Own Loaded at a Groundwater Level of 6 Meters**

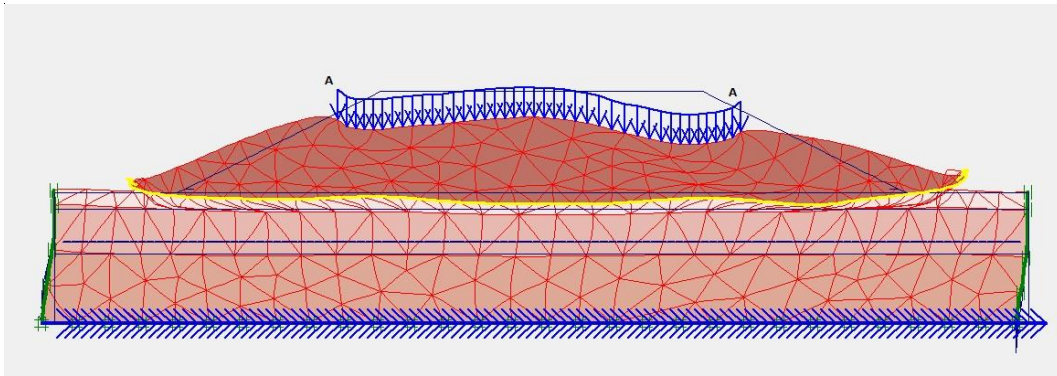


**Figure 5. 34 Deformed Mesh on Slopes with Geotextile Reinforcement Due Traffic and Earthquake Load at a Groundwater Level of 6 Meters**

The analysis results for slopes with percutaneous geotextiles at a groundwater level of 6 meters with self-loading show a safe value of 1.3487 as can be seen in Figure 5.35, due to vehicle loads and an earthquake of 1.3366 can be seen in Figure 5.36.

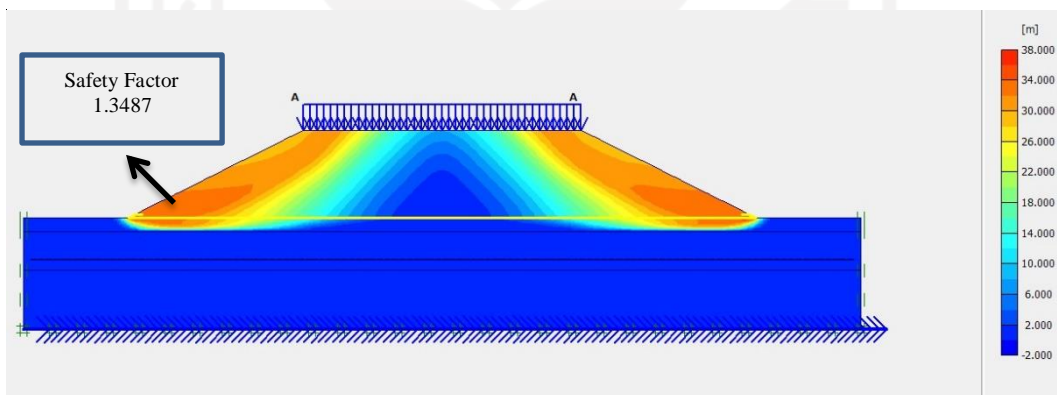


**Figure 5. 35 Landslide Potential Area on Own Loaded Geotextile at a Groundwater Level of 6 Meters**

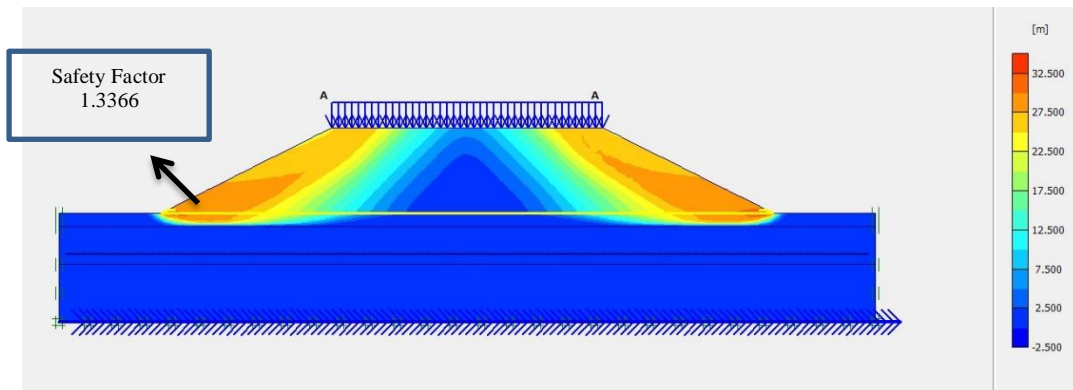


**Figure 5. 36 Landslide Potential Areas on Reinforced Geotextile Slopes with Vehicle and Earthquake Loads at a Groundwater Level of 6 Meters**

2. Groundwater level 4 meter

The deformation mesh without vehicle load and earthquake on a slope with a groundwater level of 4 meters can be seen in Figure 5.37, the deformation mesh with vehicle and earthquake loads can be seen in Figure 5.38.

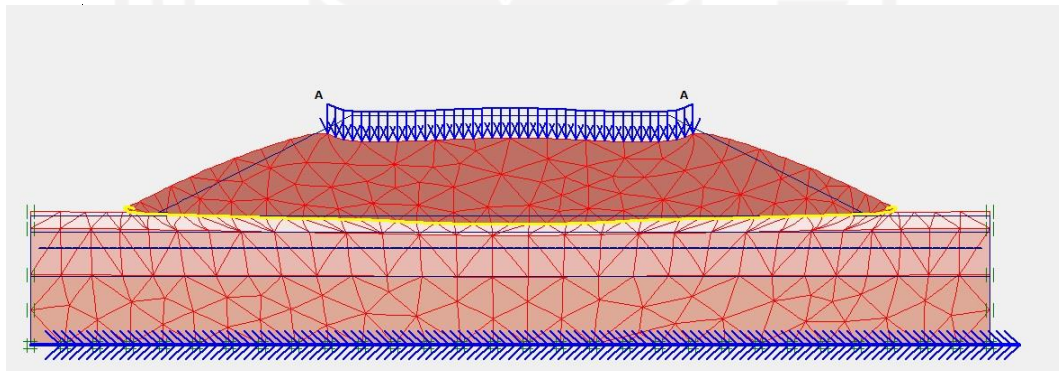


**Figure 5. 37 Deformed Mesh on Slopes with Geotextile Reinforcement Due Own Loaded at a Groundwater Level of 4 Meters**



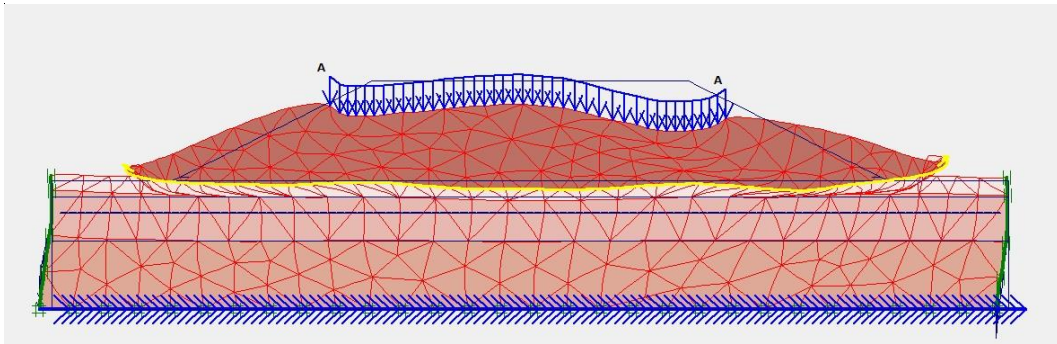


**Figure 5. 38 Deformed Mesh on Slopes with Geotextile Reinforcement Due to Traffic and Earthquake Load at a Groundwater Level of 4 Meters**

The magnitude of the safe value obtained from the analysis of the Plaxis 8.6 program on slopes with percutaneous geotextiles with a groundwater level of 4 meters with a self-load of 1.3474 can be seen in Figure 5.39, due to vehicle loads and an earthquake of 1.3260 can be seen in Figure 5.40.

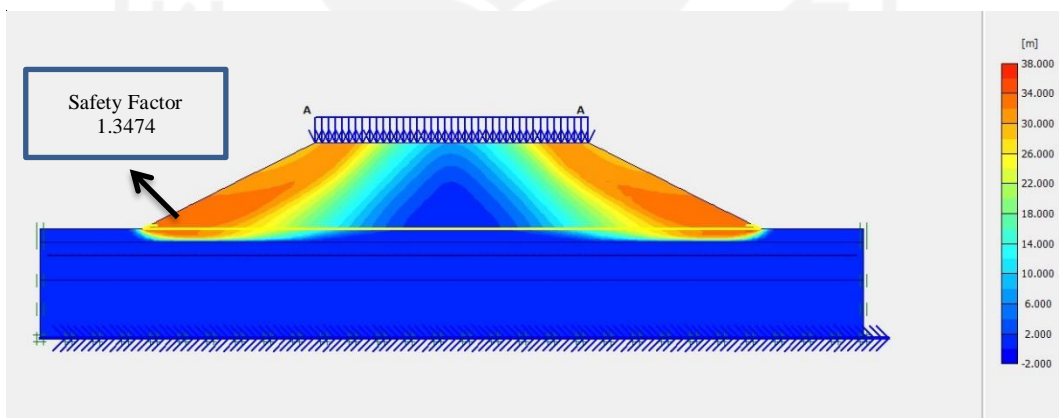


**Figure 5. 39 Landslide Potential Area on Own Loaded Geotextile at a Groundwater Level of 4 Meters**

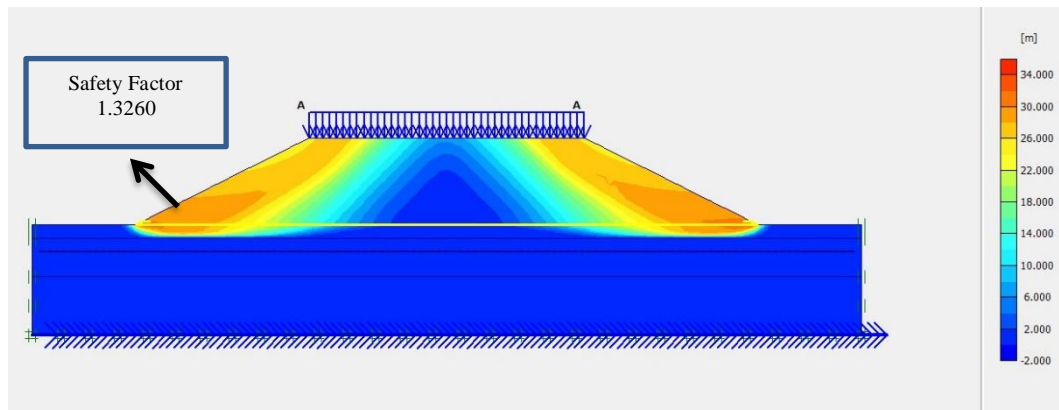


**Figure 5. 40 Landslide Potential Areas on Reinforced Geotextile Slopes with Vehicle and Earthquake Loads at a Groundwater Level of 4 Meters**

3. Groundwater level 3 meter

The deformation mesh without vehicle and earthquake loads is shown in Figure 5.41, for the results of the deformation mesh with vehicle and earthquake loads in Figure 5.42.

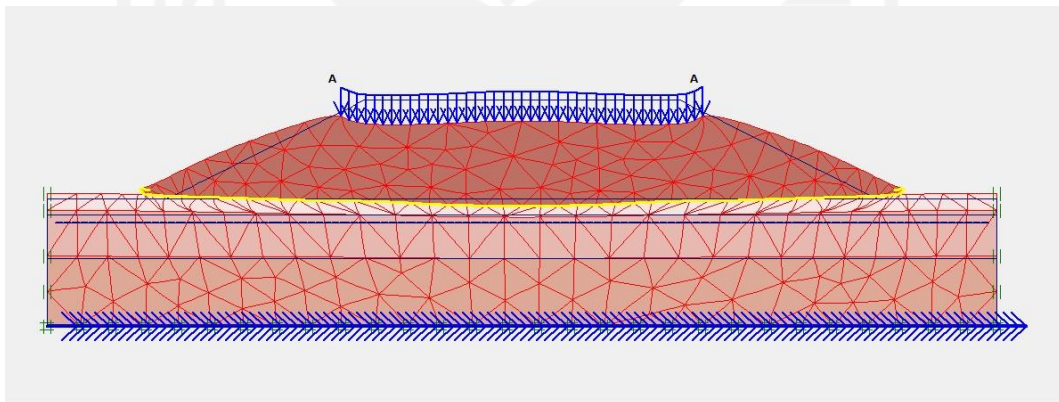


**Figure 5. 41 Deformed Mesh on Slopes with Geotextile Reinforcement Due to Own Loaded at a Groundwater Level of 3 Meters**

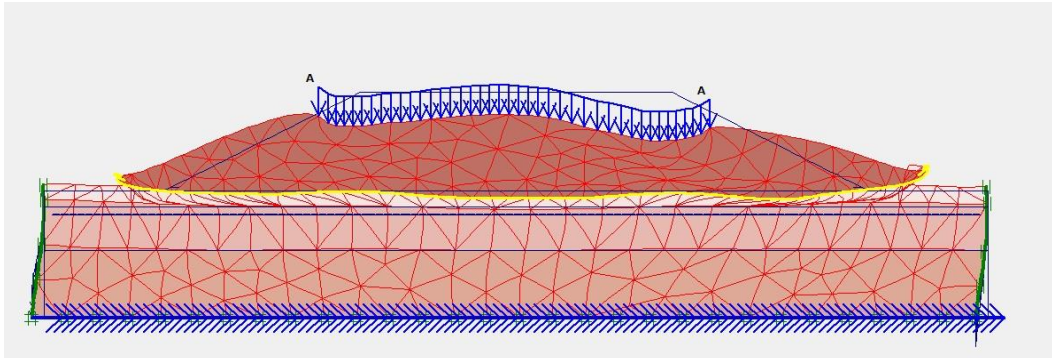


**Figure 5. 42 Deformed Mesh on Slopes with Geotextile Reinforcement Due to Traffic and Earthquake Load at a Groundwater Level of 3 Meters**

The magnitude of the safe value from the Plaxis 8.6 program analysis for percutaneous geotextile slopes at a groundwater level of 3 meters with an own load of 1.3323 can be seen in Figure 5.43, due to vehicle loads and an earthquake of 1.3103 can be seen in Figure 5.44.

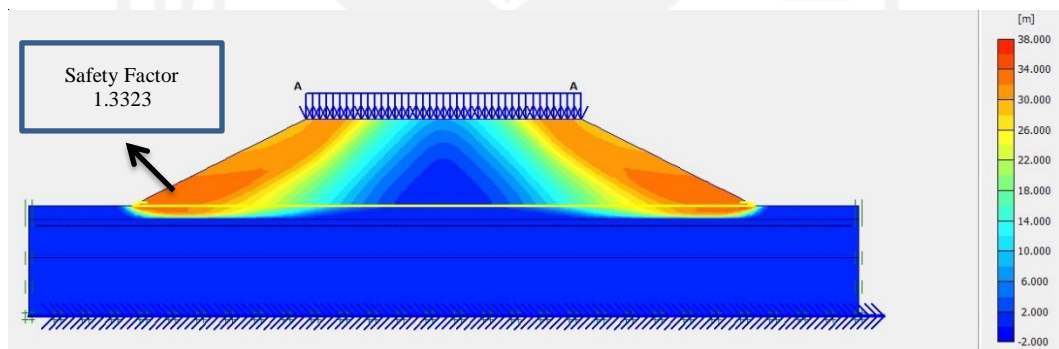


**Figure 5. 43 Landslide Potential Area on Own Loaded Geotextile at a Groundwater Level of 3 Meters**



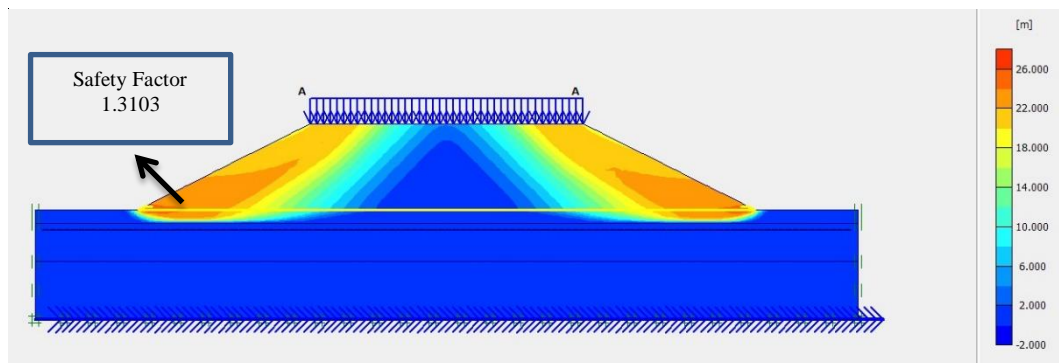


**Figure 5. 44 Landslide Potential Areas on Reinforced Geotextile Slopes with Vehicle and Earthquake Loads at a Groundwater Level of 3 Meters**

**4. Groundwater level 0 meter**

The deformation mesh without vehicle and earthquake loads is shown in Figure 5.45, for the results of the deformation mesh with vehicle and earthquake loads in Figure 5.46.

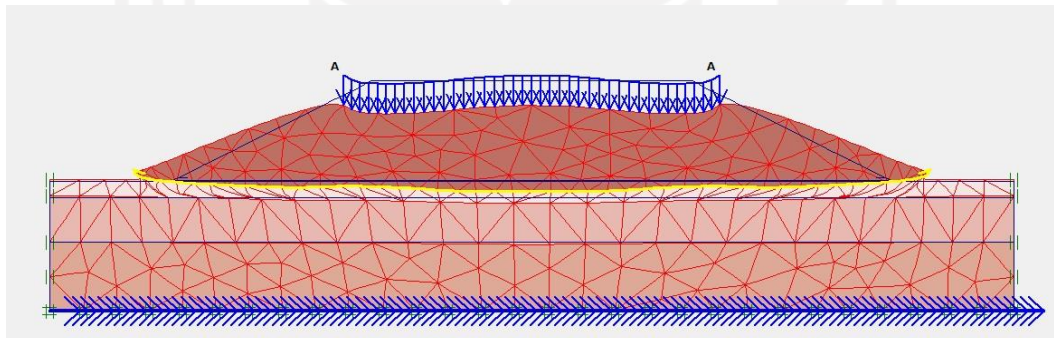


**Figure 5. 45 Deformed Mesh on Slopes with Geotextile Reinforcement Due to Own Loaded at a Groundwater Level of 0 Meters**

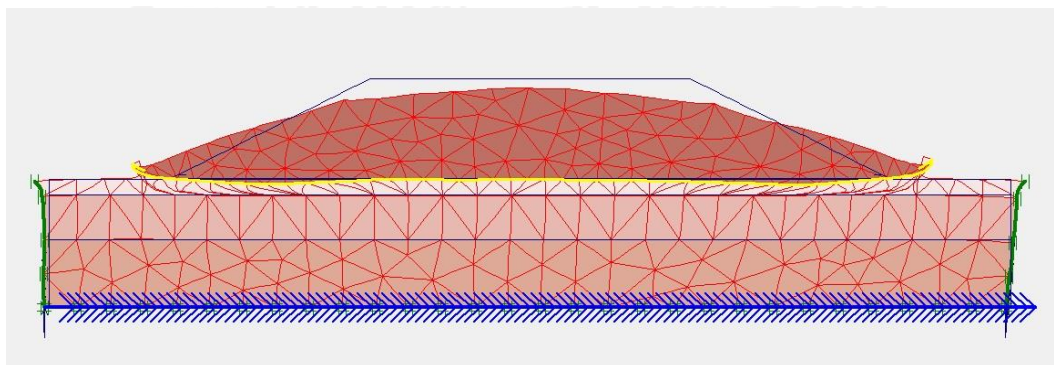


**Figure 5. 46 Deformed Mesh on Slopes with Geotextile Reinforcement Due to Traffic and Earthquake Load at a Groundwater Level of 0 Meters**

The magnitude of the safe value from the Plaxis 8.6 program analysis for percutaneous geotextile slopes at a groundwater level of 0 meters with an own load of 1.3278 can be seen in Figure 5.47, due to vehicle loads and an earthquake of 1.3050 can be seen in Figure 5.48

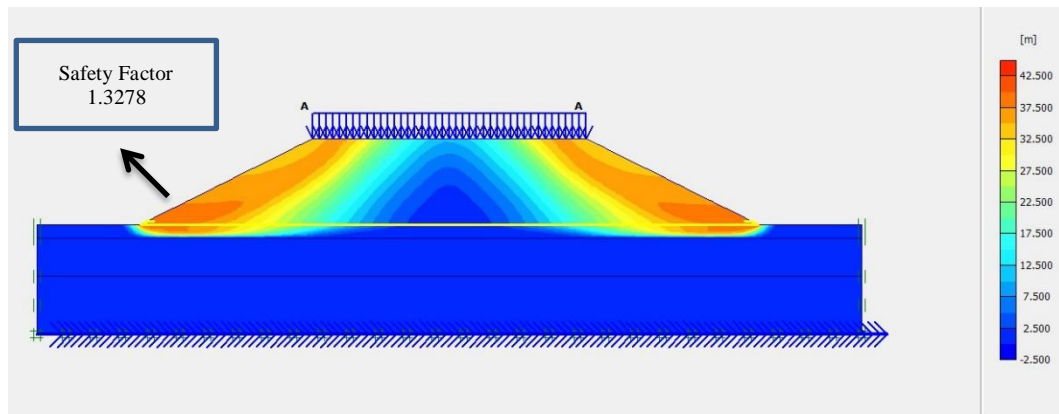


**Figure 5. 47 Landslide Potential Area on Own Loaded Geotextile at a Groundwater Level of 0 Meters**

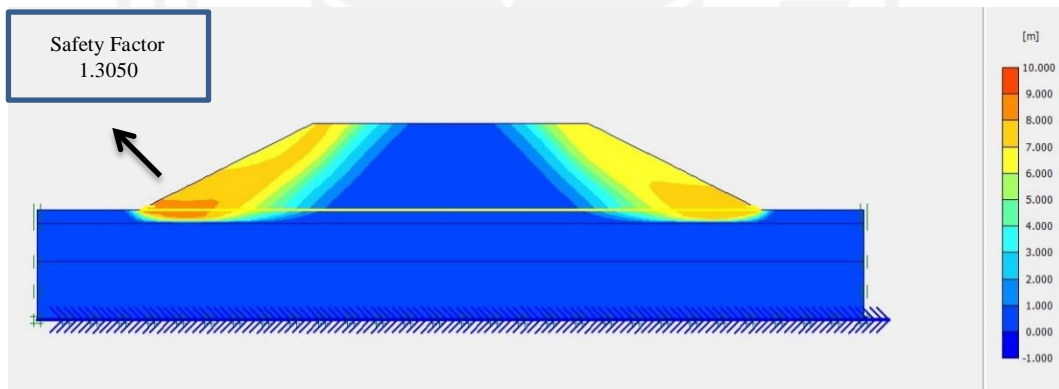


**Figure 5. 48 Landslide Potential Areas on Reinforced Geotextile Slopes with Vehicle and Earthquake Loads at a Groundwater Level of 0 Meters**

**Tabel 5.6 Recapitulation of Safety Factor Results Considering of Variations in the Groundwater Level**

Safety Factor (SF)	Load	6	4	3	0
	Own Load		1.3487	1.3474	1.3323
Vehicle and Earthquake Load		1.3366	1.3260	1.3103	1.3050

In the analysis using the Plaxis program with groundwater level variation, it shows that the safety factor is classified as safe, but the existing slope with self-loading shows that the safety factor value is not fullfil the criteria of safety factor for tollroad which is 1,3 with a value of 1.0147 when using the Slice Method calculation, this could be due to the less accurate calculation accuracy.

## 5.7 Discussion

The analysis carried out on the original slopes before being reinforced with geotextiles using the Plaxis 8.6 program did not meet the safety factor requirements for toll roads which were 1.3. After being analyzed with the Slice Method (Fellenius), the value of the safety factor on the slope without load is 1.118 which indicates that the slope condition is critical. This shows that the slope does not meet the requirements for a safe number of 1.3, so that the slope is unsafe and a slide occurs.

The next step is to analyze the slope with geotextile reinforcement. The result shown by Plaxis 8.6 is an increase in the value of the slope factor of safety with the result of SF Values are 1,3983 on the traffic load and 1,3322 on the traffic and earthquake load. The value of the safety factor at the 6 meter groundwater table under self-loading is 1.3487, with vehicle loads and earthquakes of 1.3366. The value of the safety factor at the 4-meter groundwater table under self-loading is 1.3474, with vehicle loads and earthquakes of 1.3260. The value of the safety factor at the 3-meter groundwater table under self-loading is 1.3323, with vehicle loads and earthquakes of 1.3103. The value of the safety factor at the 0-meter groundwater table under self-loading is 1.3278, with vehicle loads and earthquakes of 1.3050.

From the analysis in sub-chapter 5.6 above, the slope safety factor value tends to decrease when the groundwater level rises. This is because groundwater can reduce the physical and mechanical properties of the soil. The increase in the groundwater level also affects the level of pore pressure ( $\mu$ ), which means it reduces

the shear resistance of the slope mass, especially in the soil material (soil). An increase in the groundwater table can also increase groundwater discharge and increase subsurface erosion (piping or subaqueous erosion). As a result, more fine fraction (silt) of the soil mass will be washed away, so that the resistance of the soil mass will decrease (Bell in Zufaldi, 2009).

The decrease in the value of the slope safety factor in variations in groundwater level is due to the fact that the slope has been reinforced with geotextiles. The geotextile has the ability to hold soil particles and prevent migration (piping) of soil particles through the geotextile (Hardiatmo 2008).

The recapitulation result of analysis and calculation can be seen in table 5.7 below.

**Table 5.7 Safety Factor Recapitulation Result of Analysis and Calculation with Plaxis 8.6**

Embankment Slope Condition	SF Value of 12,5m Embankment					
	Without Geotextiles	With Geotextiles	With Groundwater Level Depth Variance			
			6m	4m	3m	0m
Traffic Load	1.1138	1.3983	1.3487	1.3474	1.3323	1.3278
Traffic & Earthquake Load	1.1131	1.3322	1.3366	1.3260	1.3103	1.3050

## **CHAPTER VI**

### **CONCLUSION AND SUGGESTION**

#### **6.1 Conclusion**

From the case studies and analysis that has been carried out on the Cibitung – Cilincing Sta 3+550 Toll Road, the following conclusions can be mention as follows..

1. The value of the safety factor of the existing slope without reinforcement is still below the specified conditions, namely  $> 1.3$ , which is 1.1138 for structure traffic load and 1.1131 for Traffic and Earthquake Load so reinforcement must be carried out.
2. Slopes that are reinforced with geotextiles, the safety value increases above the specified conditions which is for the Structure traffic load is 1,3983 and 1,3322 for Traffic and Earthquake Load.
3. Slopes that are reinforced with geotextiles with variations in the groundwater level, the higher the groundwater level, the value of the safety factor decreases but is still above the specified conditions which are for 6 meter level are 1.3487 for traffic load and 1.3366 for traffic and earthquake load, for 4 meter level are 1.3474 for traffic load and 1.3260 for traffic and earthquake load, for 3 meter level are 1.3323 for traffic load and 1.3103 for traffic and earthquake load, for 0 meter level are 1.3278 for traffic load and 1.3050 for traffic and earthquake load.

#### **6.2 Suggestion**

Based on the results of the analysis and conclusions above, the following suggestions can be taken.

1. Geotextile reinforcement can be used as an alternative in tackling landslides on Cibitung – Cilincing Sta 3+550 Toll Road.
2. In this study when conducting an analysis using only one reinforcement parameter using geotextile type reinforcement, for further research it can

be taken into account alongside a comparison when employing extra or substitute reinforcing characteristics like sheet pile, borepile, or bamboo crest.

3. For researchers who will carry out further research, apart from providing reinforcement for embankments, it is also possible to consider the use of alternative soil stability additives, for instance, chemical stability when soil from the original slope is combined with chemicals like lime, cement, and others.





## BIBLIOGRAPHY

- Arsy, Aisyah. 2018. Analisis Stabilitas Timbunan Pada Konstruksi Badan Jalan Dengan Perkuatan Geotekstil Menggunakan Metode Fellenius (Study Kasus: Proyek Jalan Tol Solo-Kertasono STA 4+175). *Tugas Akhir*. University of Islam Indonesia. Yogyakarta.
- Brinkgreve, R. B. J. 2007. *PLAXIS 2D-Versi 8*. Delft University of Technology and Plaxis. Netherland.
- Bowles, J.E. 1984. *Physical and Geotechnical Properties of Soils*. McGraw-Hill, Inc, USA.
- Departemen Pekerjaan Umum. 2009. *Standar Geometri Jalan Bebas Hambatan Untuk Jalan Tol*. Direktorat Jenderal Bina Marga. Jakarta.
- Du, Changbu., Liang, Lidong., Yi, Fu., Niu, Ben. 2021. *Effects of Geosynthetic Reinforcement on Tailings Accumulation Dams*. Liaoning Technical University. Fuxin.
- Hardiyatmo, H. C. 1992. *Mekanika Tanah I*. PT. Gramedia Pustaka Utama. Jakarta.
- Hardiyatmo, H.C. 1994. *Mekanika Tanah 2*. PT. Gramedia Pustaka Utama. Jakarta.
- Hardiyatmo, H.C. 2006. *Mekanika Tanah I Edisi keempat*. Gadjah Mada University Press. Yogyakarta.
- Hardiyatmo, H.C. 2008. *Geosintetik untuk Rekayasa Jalan Raya Aplikasi Dan Perancangan*. Gadjah Mada University Press. Yogyakarta.
- Hardiyatmo, H.C. 2010. *Mekanika Tanah Edisi V 2010*. Gadjah Mada University Press. Yogyakarta.
- Hardiyatmo, H.C. 2012. *Tanah Longsor dan Erosi*. Gajah Mada University Press. Yogyakarta.
- Hediyanto, Rizaldi. 2018. Analisis Stabilitas Lereng Dengan Perkuatan Dinding Kantilever dan Sheetpile Pada Bantaran Sungai Code. *Tugas Akhir*. University of Islam Indonesia. Yogyakarta.
- Hariyadi, S. 2016. Kajian Stabilitas Lereng Timbunan Pada PT. Kayan Kaltara Coal Job Site PT. Nata Energi Resources Kabupaten Bulungan Propinsi



- Kalimantan Utara. *Tugas Akhir*. Kutai Kartanegara University. Kutai.
- John, N.W.M. 1987. *Geotextiles*. Blackie. USA.
- Kafikanda, D.W. 2019. Analisis Stabilitas Lereng Menggunakan Geotekstil Dengan Program Geoslope Studi Kasus Jalan Tol Balikpapan-Samarinda, Pada Sta. 1+975. *Tugas Akhir*. University of Islam Indonesia. Yogyakarta.
- Niroumand, Hamed et al. 2014. *The Role of Geosynthetics in Slope Stability*. Teknologi Malaysia University. Kuala Lumpur.
- PT. Carina Griya Mandiri, (2017). Soil Data.
- PT. Teknindo Geosistem Unggul. (Without Year). Technical Spesification. Geotextile Woven. Surabaya.
- PUSKIM. 2018. *Peta Zonasi Gempa*. (<http://puskim.pu.go.id/peta-zonasigempa/>). Accesses on 5 December 2022.
- Wardana, IG.N. 2011. *Pengaruh Perubahan Muka Air Tanah dan Terasering Terhadap Perubahan Kestabilan Lereng*. Bali. Jurnal Teknik Sipil Vol.15, No.1, January 2011.
- Ogundare, Damilola., Familusi, Ayokunle., Osunkunle, A.B., Olusami, Joel. 2018. *Utilization Of Geotextile For Soil Stabilization*. 7. 224-231.
- Wibowo, D.A. (2016). Pengaruh Kondisi Ekstrim Terhadap Stabilitas Internal dan Eksternal Dinding Penahan Tanah Menggunakan program Plaxis 8.2. *Tugas Akhir*. Islam Indonesia University. Yogyakarta.

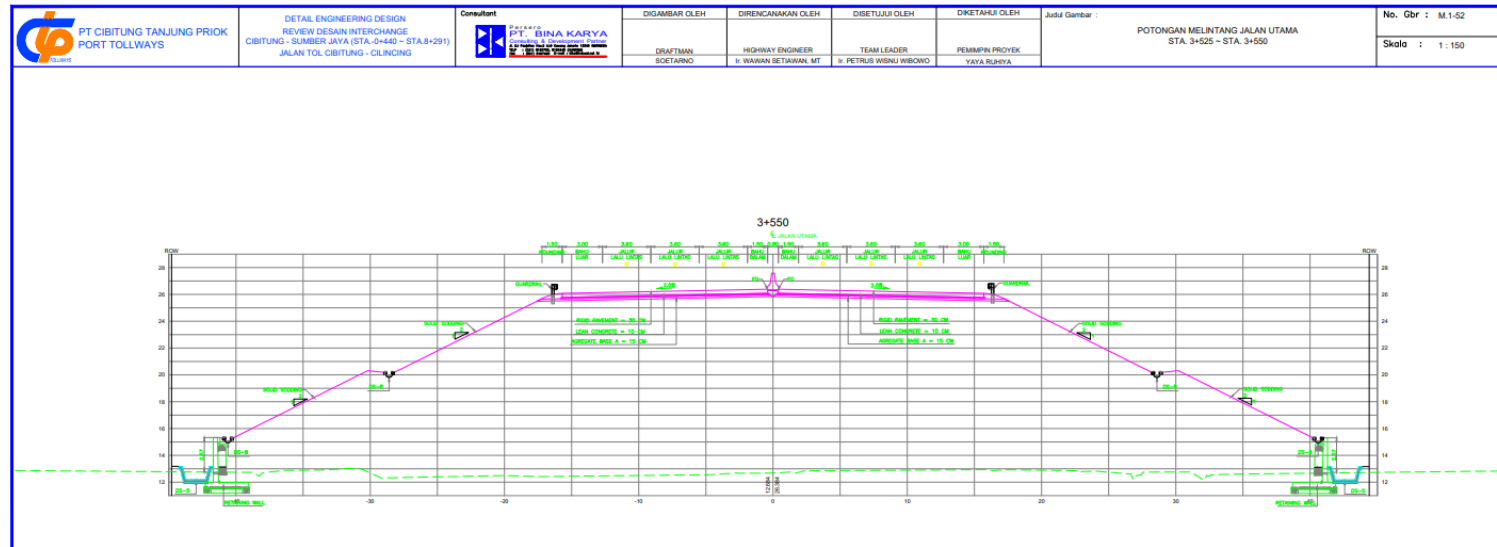




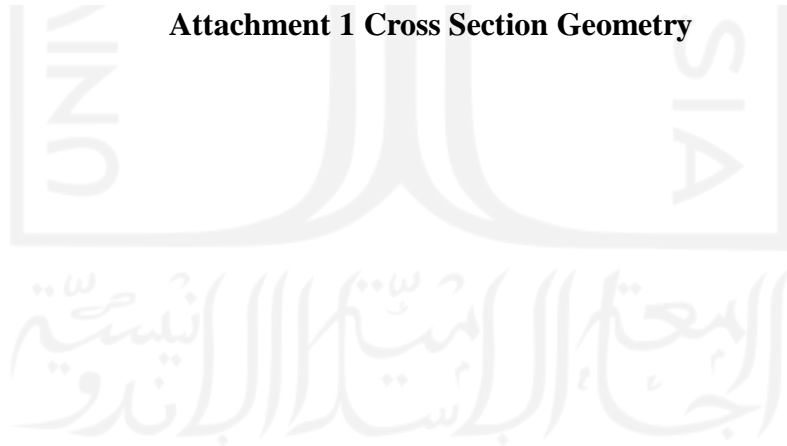
The logo of Universitas Islam Indonesia is a large, light gray watermark in the background. It features a central stylized emblem resembling a flame or a flower, with the word "ISLAM" above it and "UNIVERSITAS" on the left and "INDONESIA" on the right. Below the emblem is the university's name in Arabic calligraphy: "الجامعة الإسلامية في اندونيسيا".

# ATTACHMENT

### Attachment 1 Cross Section Geometry



Attachment 1 Cross Section Geometry



## Attachment 2 Soil Sample Lab Test Data

# DATA LABORATORIUM DAN QUARRY

PROYEK JALAN TOLL CIBITUNG – CILICING SEKSI 1



Persero  
**PT. BINA KARYA**  
Consulting & Development Partner  
Jl. D.I. Panjaitan Raya 2 Lt.3P Gading Serpong 12534G INDONESIA  
TELP : (021) 8190705, 8198445 (HUNTING)  
FAX : (021) 8197490 E-mail : bika@indosat.net.id

## DATA LABORATORIUM

No	Depth	STA	Borlog	LL	PL	PI	Clay	Activity	Ysat	c	φ
	m			%	%	%	%		kN/m3	kN/m2	degree
1	2	3+400	BH-27	81.72	31.62	50.1	49	1.022	16.71	21	15
2	2	3+550	BH-25	79.9	37.71	42.19	50	0.844	16.3	10.3	8
3	2	3+550	BH-26	80.5	31.94	48.56	52	0.934	16.36	10.9	8
4	2	7+500	BH-28	81.18	31.88	49.3	52	0.948	16.73	19.7	15
5	4	7+500	BH-28	81.54	31.9	49.64	50	0.993	16.81	21.9	16
6	6	7+500	BH-28	81.41	31.82	49.59	48	1.033	16.86	23.7	18



Persero  
**PT. BINA KARYA**  
Consulting & Development Partner  
Jl. D.I. Panjaitan Raya 2 Lt.3P Gading Serpong 12534G INDONESIA  
TELP : (021) 8190705, 8198445 (HUNTING)  
FAX : (021) 8197490 E-mail : bika@indosat.net.id

Attachment 2 Soil Sample Lab Test Dat

Attachment 3 SPT data at Sta 3+550



**PT. CARINA GRIYA MANDIRI**  
 ENGINEERING & MANAGEMENT CONSULTANT  
 Jl. Pahlawan Revolusi No. 2A Jakarta 13430, Telp.021-8613824, Mail : pt\_cg\_mandiri@yahoo.com

- ENGINEERING DESIGN
- SOIL INVESTIGATION
- SUPERVISION
- MINING EXPLORATION
- SURVEY / MAPPING

PROJECT : RENCANA PEMBANGUNAN JALAN TOL LINGKAR LUAR JAKARTA II, RUAS CIBITUNG - CILINCING		BORING NO : BH-25							
LOCATION : BUP WANAJAYA ( STA. 3+550 - TITIK 2 )		ELEVATION : 0,00 m (MTS) SHEET NO : 1							
DATE	DEPTH (m)	BORING PROFILE	STANDARD PENETRATION TEST				qu POCKET PENETRO METER	CORE RECOVERY %	LITHOLOGIC DESCRIPTION
			N = Number of Blows	P = Penetration (cm)					
			0 10 20 30 40 50 60	N/P	N/P	N/P			
15 Sept 17	± 0.00								Kordinat : X = 732127 Y = 9307817
	- 2.00			12 / 15	14 / 15	17 / 15	N = 31		Lempung lanauan, merah Contoh : 1 (- 1,50 ± - 2,00) m SPT : 1 (- 2,00 ± - 2,45) m Lanau pasiran membatu, coklat
				17 / 15	20 / 15	23 / 15	N = 43		SPT : 2 (- 4,00 ± - 4,45) m Lanau pasiran membatu, coklat
				19 / 15	23 / 15	26 / 15	N = 49		SPT : 3 (- 6,00 ± - 6,45) m Lanau pasiran membatu, coklat
	- 7.50			18 / 15	22 / 15	25 / 15	N = 47		SPT : 4 (- 8,00 ± - 8,45) m Lanau pasiran, abu-abu
				20 / 15	26 / 15	29 / 15	N = 55		SPT : 5 (- 10,00 ± - 10,45) m Lanau pasiran, abu-abu
				25 / 15	30 / 10	-	N > 60		SPT : 6 (- 12,00 ± - 12,25) m Lanau pasiran, abu-abu

Attachment 3 SPT Data at Sta 3+550

## Attachment 4 Data of Technical Specification Geotextile Woven

**UnggulTex**  
POLYPROPYLENE WOVEN GEOTEXTILES

**TECHNICAL SPESIFICATIONS**

PROPERTIES	UNIT	TEST METHOD	UW - 150	UW - 200	UW - 250
<b>Physical Properties</b>					
Mass	g/m <sup>2</sup>	ASTM D 5261-92	150	200	250
Thickness	mm	ASTM D 5199-91	0.5	0.6	0.7
Colour	-	-	Black	Black	Black
<b>Mechanical Properties</b>					
Stimp Tensile Strength (Wrab/Weft)	kN/m	ASTM D 4595-94	37/35	42/39	52/52
Elongation at Max. Load (Wrab/Weft)	%	ASTM D 4595-94	19/18	20/20	20/20
Grap Tensile Strength (Wrab/Weft)	N	ASTM D 4632-91	1210/1200	1600/1600	1750/1750
Elongation at Max. Load (Wrab/Weft)	%	ASTM D 4632-91	14/13	22/22	22/22
Trapezoidal Tear Strength (Wrab/Weft)	N	ASTM D 4533-91	615/615	700/700	800/800
<b>Hydraulic Properties</b>					
Pore Size O <sub>95</sub>	µm	ASTM D 4751-95	320	275	250
Water Permeability	l/m <sup>2</sup> /sec	100 mm water head	28	16	7.5
<b>Environmental Properties</b>					
Effect of soil Alkalinity	-	-	nil	nil	nil
Effect of soil Acidity	-	-	nil	nil	nil
Effect of Bacteria	-	-	nil	nil	nil
Effect of U.V. Light	-	-	Stabilized	Stabilized	Stabilized
<b>Packaging</b>					
Roll Length	m	-	150 - 200	150 - 200	150 - 200
Roll Width	m	-	3 - 4	3 - 4	3 - 4
Roll Area	m <sup>2</sup>	-	640 - 760	640 - 760	640 - 760
Roll Diameter (Approx)	m	-	0.4 - 0.5	0.4 - 0.5	0.4 - 0.5
Roll Weight (Approx)	kg	-	96 - 114	128 - 152	160 - 190

All information, illustration and specification are based on the latest product information available at the time of printing.  
The right is reserved to make changes at any time without notice.

## Attachment 4 Data of Technical Specification Geotextile Woven